LATERAL FORCES ON VERTICAL FACES FROM SAND BACKFILL SUBJECTED TO FALLING WEIGHTS

By

Chiu Ching A. Tsang

Submitted in Partial Fulfillment of the Requirements
for the Degree of
Master of Science in Engineering
in the
Civil Engineering Program

Adviser 2-23-79
Date

Dean of the Graduate School 4-17-79
Date

YOUNGSTOWN STATE UNIVERSITY

February, 1979

ABSTRACT

LATERAL FORCES ON VERTICAL FACES FROM SAND BACKFILL SUBJECTED TO FALLING WEIGHTS

Chiu Ching A. Tsang
Master of Science in Engineering
Youngstown State University, 1979

This project was undertaken to investigate the lateral pressures on the vertical face of a wall exerted by dynamic loadings. More specifically, it was the purpose of this thesis to investigate the pressure distribution and resulting lateral forces induced by sand backfill subjected to falling weights.

Briefly, a steel tank was filled with soil of known gradation and water content, filled to within nine (9) inches from the top. Two weights, one 32.5 lbs. and the other 65 lbs., were dropped from a height of 12' 9" above the surface of the soil. This was repeated twelve times. The load effects were picked up by BA-4 bridge amplifier and were recorded by a 447 oscillograph. The deflection on the recording paper was interpolated into pressure from calibration curves. Finally, the pressure at different levels, at different time intervals, were plotted for the final analysis.

The findings indicate that maximum stress was located at about three-fifths of the distance from the bottom, and decreased to nearly zero at about one-third of the distance from the bottom.

ACKNOWLEDGMENTS

The soil experimentation was performed at the William Rayen School of Engineering, Youngstown State University. The testing apparatus and steel tank was originally designed and built by William Baker, Charles Donaldson and Stephen Jordan, as their senior thesis in Civil Engineering.

Dr. John N. Cernica, Professor of Civil Engineering Department, served as thesis advisor. He offered constructive criticism throughout the project and also suggested various ways of improving the apparatus and the procedure of the experiment.

I would like to thank Mr. Lane Galey, Mr. Mike Repetski and Mr. Joseph Wolfe for their help in this project. They helped with the instrumentation; particularly the bridge amplifier and oscillograph, to build the bucket, and during the experimentation.

During the long term of procedure the author of the thesis consulted with Dr. John N. Cernica, Dr. Paul X. Bellini, Dr. Jack D. Bakos, Dr. Michael K. Householder and several other professors from other departments. The author appreciates their help and co-operation.

TABLE OF CONTENTS

PAGE

ABSTRACT ii

ACKNOWLEDGEMENTS iii

TABLE OF CONTENTS iv

LIST OF SYMBOLS v

LIST OF FIGURES vi

LIST OF TABLES vii

CHAPTER . . . .

I. INTRODUCTION 1

II. PROCEDURE 8

Apparatus 8

Filling the Tank 8

Calibration 9

Instrumentation 10

Testing Operation 13

Results of Testing 14

III. DISCUSSION 23

IV. CONCLUSION 36

V. RECOMMENDATIONS 38

APPENDIX A. Sieve Analysis and Tests of Soil Parameters . . . 40

APPENDIX B. Records of Experiment 50

APPENDIX C. Calibration Curves 53

APPENDIX D. Tables of Tabulation of Results 64

APPENDIX E. Charts of Experimental Results 86

LIST OF SYMBOLS

SYMBOL	DEFINITION	UNITS OR REFERENCE
i	$\sqrt{-1}$	
G	modulus of shear deformation or shear modulus	(lb/in^2)
N	wave number ($N + 2\pi/L$)	
t	time	(sec)
u	displacement in x-direction	(ft)
x	horizontal distance	(ft)
z	displacement in the vertical direction, positive downward	(in)
α	parameter relating shear-wave velocity to compression-wave velocity	
γ	unit weight of soil	(lb/ft^3)
$\bar{\varepsilon}$	cubic dilatation or volumetric strain of elastic body	
λ	Lame's constants ($\lambda = \frac{2\nu G}{1-2\nu}$)	(lb/in^2)
ν	Poisson's ratio	
π	3.13159...	
ρ	mass density ($\rho = \gamma/g$)	($lb\text{-}sec^2/ft^4$)
Φ	potential function	
Ψ	potential function	
$\bar{\omega}$	circular frequency	(rad/sec)
∇^2	Laplacian operator ($\nabla^2 = \partial^2/\partial x^2 + \partial^2/\partial z^2$ for Cartesian coordinates)	
σ_x	stress in one direction	(kip/sq in)
V_p	velocity of compression wave	(ft/sec)
E	modulus of linear deformation	(lb/in^2)
μ	modulus of rigidity	
V_c	velocity of wave propagation	(ft/sec)
G	shear modulus $G = \frac{E}{2(1+\nu)}$	(lb/in^2)
ω	angular velocity	(rad/sec)
L	wave length	(ft)
K	ratio between the velocity of the surface wave and the velocity of the shear wave	

LIST OF FIGURES

FIGURE		PAGE
1-4	Testing Apparatus	15
5-8	Results of Testing	90
9-10	Results of Sieve Analyses	43
11-12	Comparison of Results of Experiments With Richart's Mathematical Approach	46
13-14	Results of Direct Shear Test	49
15-16	Records of Experimental Results	51
17-26	Calibration Curves	53
27-67	Pressure vs Height	87

LIST OF TABLES

TABLE		PAGE
1	Test of Water Content	41
2-3	Sieve Analysis	42
4-10	Results of Experiments: 9th Dropping	65
11-14	Results of Experiments: 10th Dropping	72
15-19	Results of Experiments: 11th Dropping	76
20-24	Results of Experiments: 12th Dropping	81

CHAPTER I

INTRODUCTION

The problems associated with the design of retaining structures to resist dynamic loadings, either from falling weights or from other external sources, still require special solutions dictated by local soil conditions and environment. The retaining structure must satisfy both the criteria for static loadings, as well as for resisting the dynamic conditions.

Designing to resist dynamic loading requires the knowledge of (1) failure of the chosen design function and the numerical limits on the failure criteria, (2) the relationships between the applied loads and the quantities which are significant in the failure criteria, (3) methods to identify and evaluate these significant quantities, and (4) the factor of safety to apply in the design process. Some valuable information is provided in various sources but particularly by Rausch[1*] (1943), Lorenz[2] (1960), Barkan[3] (1962), Harris and Crede[4] (1961).

The design to resist static loading is covered in the field of soil mechanics with the experimental and theoretical aspects of lateral earth pressure exerted by soil on a vertical surface. Jacob Field, R.B. Peck, George B. Sowers, P.R.N. Stroyer, and Professor Karl Terzaghi have contributed the semi-empirical formulas for this purpose. J.C. Meem at the first of the century, H.G. Moulton in 1920, Karl Terzaghi, in Berlin in 1936 and P.R.N. Stroyer did some investigation of the actual pressure distribution on a vertical surface.

---

*Superscripted number indicates reference cited.

A large-scale earth pressure testing machine was built in 1932 under the direction of Terzaghi at the Massachusetts Institute of Technology to measure both the horizontal and the vertical pressure exerted on the flexible wall. All during this period the investigators were only dealing with static loading relating to soil mechanics.

The problems related to vibration of soils and retaining structures to resist dynamic conditions have required increased attention during the past two decades, and notable advances have been made during the past ten years. The late Professor K. Terzaghi directed the attention of F.E. Richart, Jr. towards soil dynamics in 1951 and subsequently provided many forms of assistance and encouragement. Several of the recent improvements in the analyses of soil dynamics problems are based on methods developed by Professor N.M. Newmark. Dr. T.Y. Sung and Professors B.C. Hardin, J. Lysmer, and V.P. Drnevich have also contributed ideas and methods in soil dynamics.

F.E. Richart, Jr., J.R. Hall, Jr., and R.D. Woods[6] in their book "Vibrations of Soils and Foundations" published in January 1969, and Dr. Wu of Ohio State University in his book "Soil Dynamics" have considered problems related to soil pressures from dynamic loads. Since most of them used a mathematical approach instead of an experimental approach, this project was undertaken as a supplement to the theoretical soil dynamics studies, especially stress on vertical wall due to falling weights.

A steel tank, a bridge amplifier, and an oscillograph were the basic components of the apparatus used for the experiment. Only the changes in pressure due to dropping weights were measured; those due to the static hydrostatic effects of the sand were neglected. These horizontal forces were measured via a calibrated arm which supports the pressure doors; stress bars or arms received the vibrating force from the falling weight and transferred it into strain signals recorded by the oscillograph. The oscillograph data were subsequently translated back to charts showing pressure versus height for the various time intervals, as shown in Figures 27 through 67. From these charts, one is able to obtain not only the magnitudes of pressures at various points along the retaining wall, but also the points of maximum pressures on the wall from the dropping weights.

During the instant in which the falling weight contacted the soil, only the soil contacted changed shape. Subsequently, a wave of pressure was formed at the point of contact and readily spread in every direction. Such phenomenon is termed as wave propagation -- similar to the propagation of sound and light in the atmosphere,etc. The phenomenon of reflection and refraction also occurs in the wave propagation of soil. This would cause the resulting curve of the experiment to have more than one maximum point. The wave propagation from the falling wieght was identified by F.E. Richart into a Rayleigh wave, a compression wave and a shear wave.

A longitudinal or dilatational wave, a lateral wave, a distortional wave and a Rayleigh wave spread out radially from the point of contact into the soil. The soil acts partially like a spring and partially like an absorber. The falling weight was bounced back, or rebounded by the reaction of the soil. Hence, both compressive stress and tensile stress were applied alternatively to the soil. It should be recognized that when a compressive stress was applied, both wave propagation velocity and particle velocity travel in the same direction. However, when tensile stress was applied, wave propagation velocity was opposite to particle velocity ($\dot{u}$) which depends on the stress ($\dot{u} = \frac{\sigma_x V_c}{E}$),[8] but wave-propagation velocity (V_c) was only a function of material properties ($V_c = \{(E + 4\mu/3)/\rho\}^{\frac{1}{2}}$).[8]

Since soil is a medium that could not sustain finite shear stress, a lateral wave would diminish in a very short distance from the point of contact.

The third type of wave was a distortional wave travelling with the velocity $V_s = G/\rho$[8] (G = shear modulus). The particle motion of distortional waves was perpendicular to the direction of propagation.

The fourth type of wave is a Rayleigh, or surface wave. The particle motion of Rayleigh surfacial waves was in the plane perpendicular to the surface along which the waves were travelling and parallel to the direction of propagation. The velocity of Rayleigh surfacial waves was equal to $\omega L/2\pi$; also $V_r = \sqrt{(1-2\nu)\ (KV_p)^2/(2-2\nu)}$.[8]

The soil is not a perfectly elastic material. There may be hysteresis in the load-unload cycle, or viscosity, resulting in a dissipation of energy. Stress waves with periods close to the relaxation time of such a medium were significantly attenuated in the medium.

Plastic waves are sometimes formed following the shock wave. Shock waves usually have a pulse of higher intensity which travel faster than the initial waves.

Since the tank was filled up in two layers, the lower layer was more compact than the upper layer. This was the case of a medium with a lower-velocity layer on top of a higher-velocity layer. Jones (1958)[7] showed that steady-state Love waves could be used to determine the shear wave velocity in the upper medium and the thickness of the upper layer. For a single surface layer the frequency equation for the Love wave is

$$\tan 2\pi H/L \ (V^2/V_{s1}^2 = 1)^{\frac{1}{2}} = G_2/G_1 \ \{(1-V^2/V_{s2}^2)/(V^2/V_{s2}^2-1)\}^{\frac{1}{2}}$$

L = wave length of vibrations,

V = phase velocity of the vibrations,

V_{s1} = phase velocity of shear waves in surface layer,

V_{s2} = phase velocity of shear waves in lower medium,

G_1 = shear modulus in the surface layer,

G_2 = shear modulus in the lower medium, and

H = thickness of the surface layer.

Elastic waves would be partially reflected at the interface between the two layers. Reflected waves returning to the surface of the layered half-space would encounter the interface between solid and void where it would be totally reflected. The Love wave as a horizontally polarized shear wave, generated by multiple total reflection, was trapped in the superficial layer.

At a free end, both compression wave and tension wave were reflected of the same magnitude and shape. Rayleigh waves would break into reflected Rayleigh wave, transmitted Rayleigh wave, reflected body wave and interface wave.

At the corner, the amount of energy carried away from the corner by each type of wave was a function of Poisson's ratio, angle of interface, and properties of the two quarter spaces.

The description of elastic waves was suitable for the low stress application. For high stress application, viscoelastic waves described the wave propagation with the elastic wave. What was viscoelastic wave was simply adding the retardation, time and attenuation factor into the elastic waves.

Damping would come to a maximum when the vibration was about equal to the retardation time and it fell off rapidly for any increase or decrease from this value. Velocity of viscoelastic wave increased significantly with frequency.

As the distance from the pulse increased, the initial jump in the stress decreased. Usually the time to reach the steady-state value increased for the viscoelastic material.

As for the elastic model the wave remained unchanged while the strain and particle velocity varied in the same manner with time.

Plastic waves only took place in the materials with nonlinear stress-strain relationships that were a long distance from the pulse.

In this experiment elastic waves took place first and might or might not be followed by the viscoelastic waves; plastic waves would not have happened in such a short distance.

Figure 27 through 69 show the results of stress versus time of complex constitution of waves propagation and the particle motion. The stress from static load is used as a reference point as zero point of stress. Negative stress denotes a decrease of static stress below the axis of reference.

The results of the experiment are applicable in the analysis of flexible retaining structure such as sheet piles, of the lateral supports, steel tanks, etc. Confinement effect is believed to be of low influence in the significant figures. For proper comparison, the condition of the backfill ought to be at the same water content, same gradation of soil and the same density used in the experiment. After repeated testing the gradation and the water content indicated rather low deviation due to rather dry aggregate used in the experiment. While the void ratio has changed, the significant effect was the change of the shear-wave velocities; this was due to the change of the void ratio and the confining pressure.

WILLIAM F. MAAG LIBRARY

CHAPTER II

PROCEDURE

Apparatus

The testing apparatus was a steel tank, forty-two inches square, and seven and a half feet high. The tank capacity was 91.9 cubic feet in volume constructed to hold approximately six tons of sand (Figure 1). The front of the tank had a movable wall which could be moved in and out by turning the one inch bolts threaded into fabricated steel lugs (Figure 2). The movable vertical wall contained fourteen windows, each four inches square. Window plates were fitted into the windows and attached to stress bars which were bolted to the outside of the movable wall (Figure 4). SR-4 strain gauges (Figure 4) were attached to the stress bars and measured the displacement produced by the lateral force of the soil. Plates 1, 2, and 3 are photographs of some of these components.

Filling the Tank

Before filling the tank, the soil was room dried and mixed to a uniform consistency. Therefore, the soil can be considered to be dried, of uniform density, and well mixed.

By using a concrete bucket and highlift, the sand was placed into a tank in layers and was not subject to any compaction.

Samples were taken on the top, meddle, and bottom of the tank to check the uniformity of the soil. The results indicate good uniformity. The density and the water content of the three samples were very close to each other. The results are given in Table 1.

During unloading trap doors were opened to let the soil flow out of the tank. Small buckets and a hand shovel were used in unloading.

Throughout the whole procedure of filling the tank, there were no readings taken, for the purpose of this project was to find the relating stress due to the dynamic (not static) load of the shock waves only.

Calibration

The strain gauges used were the original SR-4 strain gauges (gauge factor of 120) installed on the stress bars. In the past these gauges were used to measure static pressure only. In this project, however, they served to measure dynamic conditions. The results were reliable because SR-4 strain gauges were suitable for both static and dynamic responses.

Before the experiment and prior to the filling of the tank, the force on the stress bar and the deflection relationship were calibrated experimentally. The calibration experiment was a static response, while the falling weight experiment was a dynamic response. This, however, appears to be a common approach used by other investigators. The magnification factor of deflection of the stress bar is dynamic response is depended on the expression constituting of stiffness of the stress bar, duration time of the impusive force and the time. For this reason relative force is considered rather than the actual force. The dynamic response in such a low-force magnitude of 65 lbs.

The bridge amplifier and the oscillograph were adjusted to balanced conditions before calibration. No load readings of windows 1, 3, 4, 5, 6, 7, 8, 10, 11, and 12 were taken to establish relative data points on the recording paper used as the basis for the load readings.

The calibration was done by using a simple pulley system. Five static loads, ranging from 1.0 to 5.0 kips, were applied to window numbers 1, 3, 4, 5, 6, 7, 8, 10, 11, and 12. From these data final calibration curves were made. From these calibration curves, the difference in deflection between loading and no-loading readings could be converted into pressures acting on each window.

Instrumentation

The person making the measurements must not only be trained in dynamics, but must also understand the operation of electronic instruments.

In order to understand the behavior of basic elements in an electrical circuit one must make an analogy between electrical and mechanical components. Each electrical element has a corresponding mechanical element which responds in a mathematically identical manner.

The relationship of each electrical element with each mechanical element is shown as follows:

A resistor acts like a dashpot.

A capacitor acts like a physical element.

An inductor acts like a spring.

Analogous relationships between mechanical and electrical systems are shown as follows:

Force is analogous to current (I).

Velocity is analogous to voltage (E).

Displacement is analogous to E (dt).

Acceleration is analogous to (dE/dt).

Viscous-damping coefficient is analogous to 1/Resistance (R).

Spring constant is analogous to 1/Inductance.

Mass is analogous to capacitance.

The instruments used to pick up and record lateral forces on the vertical faces are the BA-4 amplifier and the 447 oscillograph.

Window and Stress Bar

The stress bar with a SR-4 strain gauge mounted on it was fixed on the movable wall with a four-inch square plate facing the window. The function of the stress bar was to carry the vibration from the soil pushing on the inside of the movable wall. The strain gauge attached to each stress bar was connected to the BA-4 bridge amplifier. The strain gauge changed the vibration response into an electrical signal which was picked up by the amplifier.

BA-4 Bridge Amplifier

The function of an amplifier was to increase the voltage or current amplitude of a weak signal. The ten-channel BA-4 bridge amplifier picked up the signals from ten different stress bars simultaneously. Unfortunately the BA-4 bridge amplifier sometimes indicated unstable readings. The unstable readings were caused by an improper gauge circuit rather than from the instrumentation. Electro-static noise was reduced by shielding and grounding and by bringing a compensating gauge near the active gauge. Electro-magnetic noise, such as that picked up in magnetic fields near motors, was difficult to reduce for it was impossible to move gauges and leads around.

Another possibility of instability and oscillation in the amplifier was accentuated by high gain settings, high impedance loads on the input and low impedance loads on the output. Different lengths of active and compensating gauge cables were also causes of instability and oscillation in the amplifier.

447 Oscillograph

The model 447 oscillographs were bench-mounted, direct writing, multiple channel, light beam oscillographs. Their functions were to record signals from the stress bars on eight-inch wide recording paper. Signals from individual channels were simultaneously recorded by the oscillograph but a seperate galvanometer was required for each channel.

In operation, light from a high intensity point source was collected on a curved mirror and focused on the galvonometers, illuminating the mirror of each galvanometer. The galvanometer mirrors reflected this intense light through the condensing lens to condensing mirror. Condensing mirror focused the light beams reflected by the galvanometer mirrors, into intense light spots on the recording paper. Thus, a trace was generated for each galvanometer element. When an external signal was introduced to a galvanometer, the galvanometer mirror deflected a distance proportional to the amplitude of the input signal, depending upon the sensitivity of the galvanometer and the input attenuation used. Timing lines and grid lines were provided in the recording paper so that amplitudes of recorded signals and the time periods could be quickly determined.

Testing Operation

After the tank was filled, the sand around the window plates was brushed away in order to be sure the window plates were free to move. The circuit between the strain gauges, the amplifier and the oscillograph was connected and checked. The oscillograph was warmed up for about fifteen minutes prior to testing. Meanwhile, the bridge amplifier and the oscillograph were adjusted to balanced conditions. The time interval of the oscillograph was set to 0.01 seconds and the speed of the oscillograph was set to 40 to 60 inch/second. The knobs of calibration and gain of the amplifier were turned to the operating condition. During the testing operation, the spots of light on the viewing screen of the oscillograph were adjusted to even-space and enough space to move. Weights of 32.5 and 65 lbs. were dropped from a height of 12'9" above the middle portion of the soil. Various investigators, including Deutschen Forschungsgesellschaft für Bodenmechanik (DEGEBO)[6] investigation during the early 1930's, Lysmer (1965), Fry (1963), Quinlan (1953), Reissner (1937) and Reissner and Sagoci (1944) and the analytical solutions presented by Arnold, Bycroft, and Warburton (1955) and by Bycroft (1956) their examples, found that the magnification factor for the exciting force due to vertical oscillation, torsional oscillation, horizontal oscillation and rocking oscillation, is depended on the mass ratio rather than the contact area. The mass ratio is depended on the mass of the vibration medium and its size and Poisson's ratio and mass moment of inertia of the vibration medium only. Control contact area is not necessary.

The same procedure was repeated twelve times but only the last four were considered in the analysis. The recording instrumentation was turned on while the weight dropped. The spots of light were adjusted and the window plates were brushed after each dropping. The traces representing the vibration of the window plates were checked before and after each dropping. After the experiment, the soil was removed from the tank. Water content and direct shear tests were performed for comparison of consistency. In addition, sieve analysis and relative density experiments were performed to check the void ratio.

Results of Testing

Refer to Figures 5 through 8. The results of testing from the first drop to the eighth drop were omitted due to the hystersis characteristics of the loose sand, the apparatus, and the surrounding influences mentioned in the instrumentation. The top line of the charts represents the top surface of the soil in the tank.

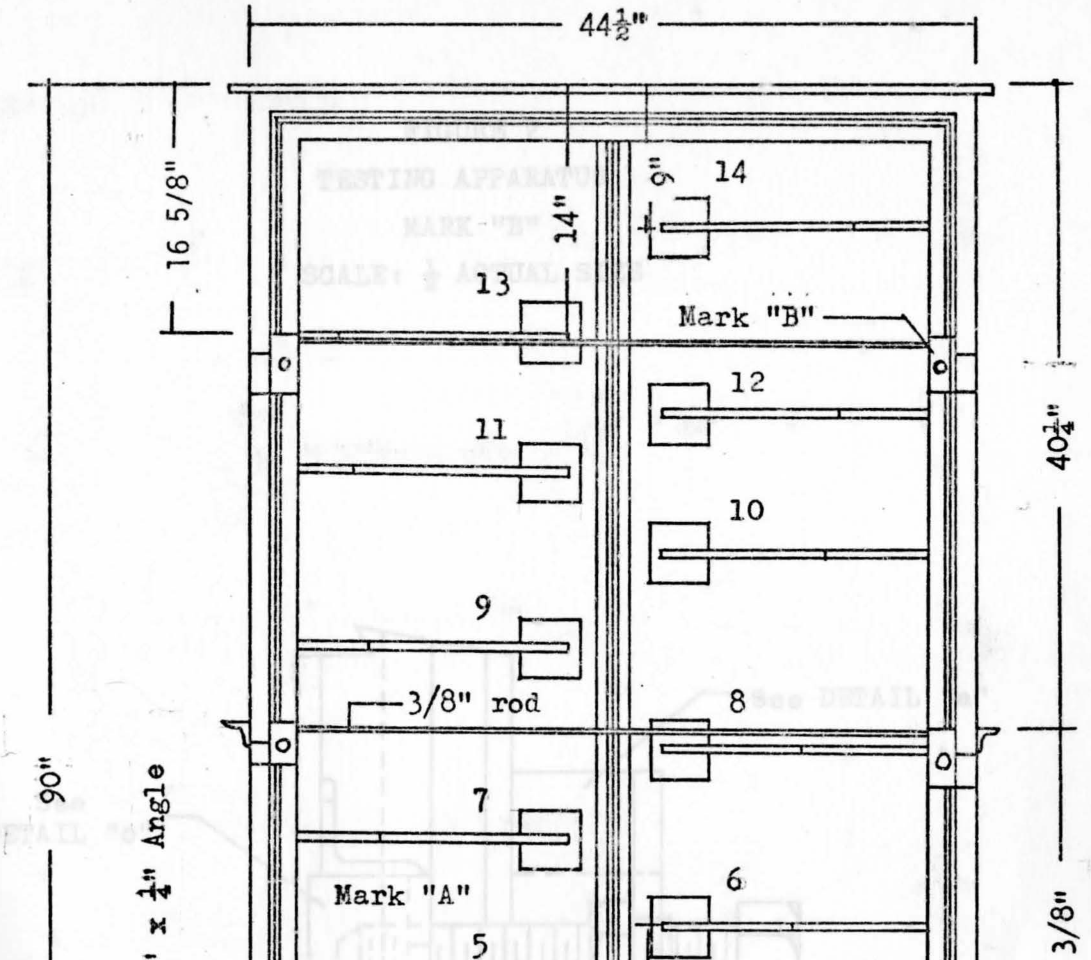
44½"
16 5/8"
14"
9"
14
13
Mark "B"
12
11
40¼"
10
9
3/8" rod
8
90"
7
2" x 1¼" x ¼" Angle
Mark "A"
6
5
27 3/8"
11"
4
3
2
22 3/8"
1
15"
10"
1¼"x1¼"x¼" Angle
1¼"x1¼"x¼"Angle

Fig. 1 TESTING APPARATUS

MOVABLE WALL - FRONT VIEW - SCALE: 1" = 12"

FIGURE 2
TESTING APPARATUS
MARK "B"
SCALE: $\frac{1}{2}$ ACTUAL SIZE

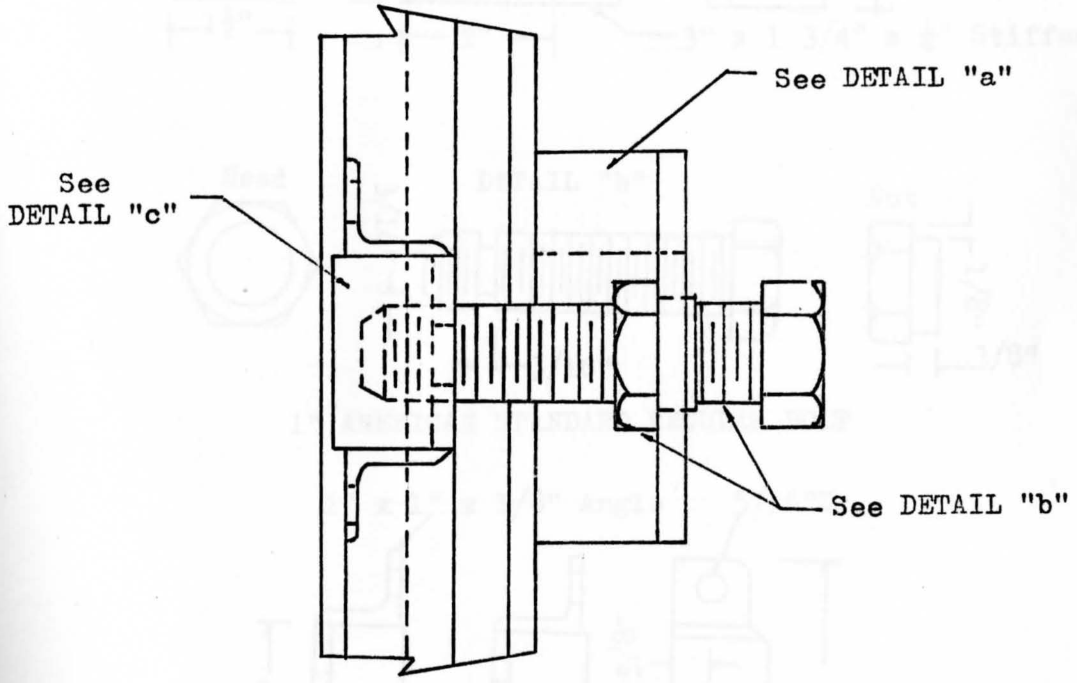
See DETAIL "a"
See DETAIL "c"
See DETAIL "b"

FIGURE 3
TESTING APPARATUS

DETAILS - SCALE: 1" = 2½"

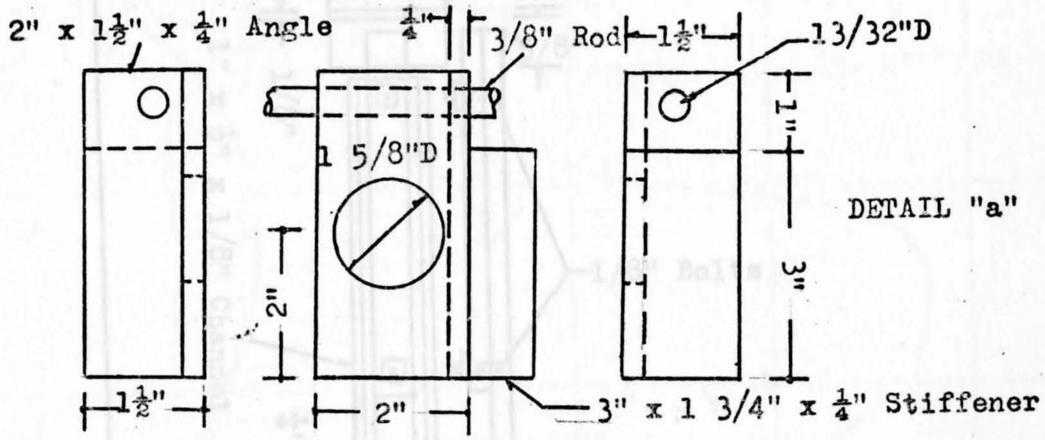
2" x 1½" x ¼" Angle
¼"
3/8" Rod
1½"
13/32"D
1 5/8"D
1"
DETAIL "a"
3"
2"
1½"
2"
3" x 1 3/4" x ¼" Stiffener

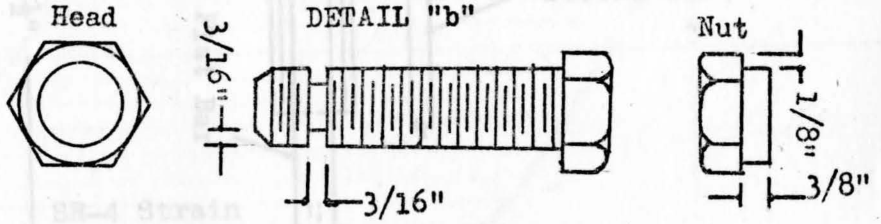
Head
DETAIL "b"
3/16"
3/16"
Nut
1/8"
3/8"

1" AMERICAN STANDARD REGULAR BOLT

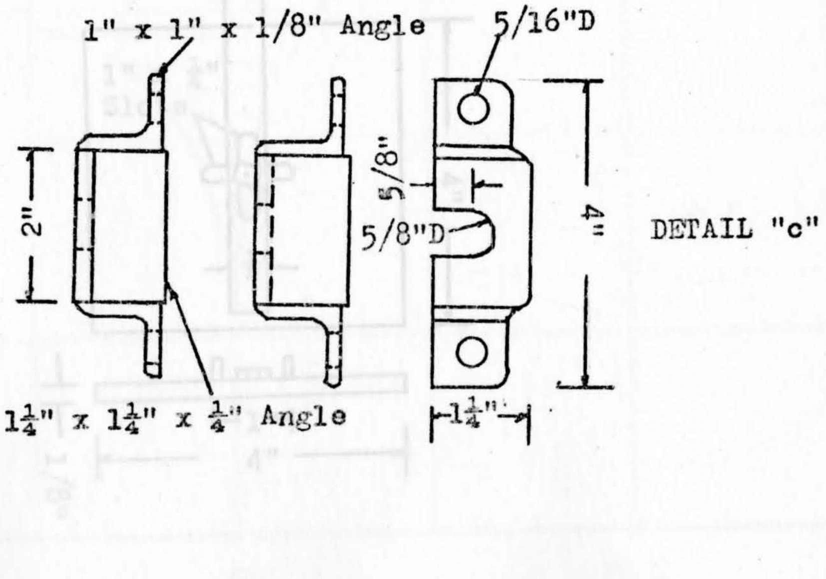
1" x 1" x 1/8" Angle
5/16"D
2"
5/8"
5/8"D
4"
DETAIL "c"
1¼" x 1¼" x ¼" Angle
1¼"

Fig. 4 TESTING APPARATUS

MARK "A" - DETAIL OF WINDOW & STRESS BAR

SCALE: 1" = 2½"

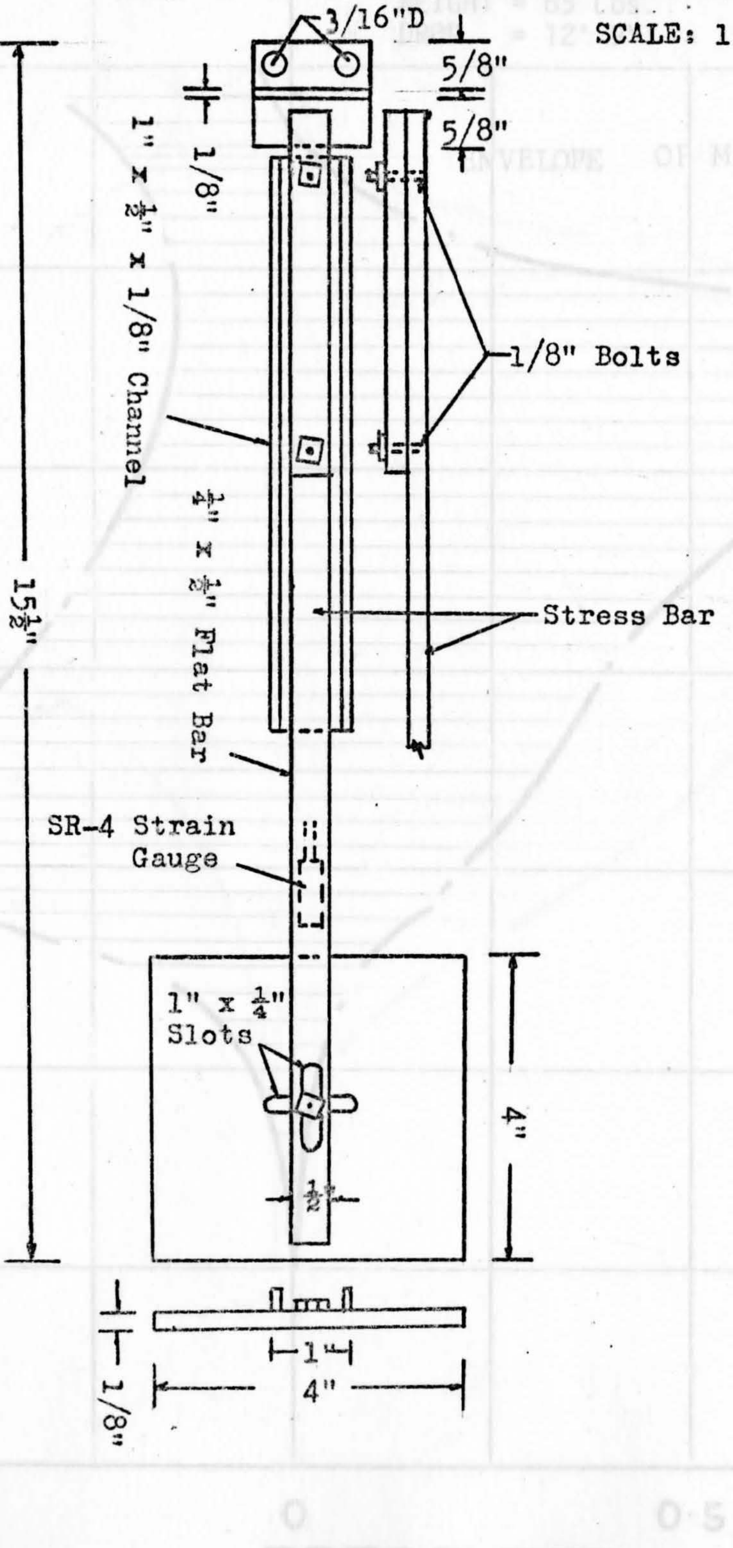
3/16"D
5/8"
5/8"
1/8"
1" x ½" x 1/8" Channel
¼" x ½" Flat Bar
1/8" Bolts
Stress Bar
15½"
SR-4 Strain Gauge
1" x ¼" Slots
½"
4"
1"
4"
1/8"

Fig. 5

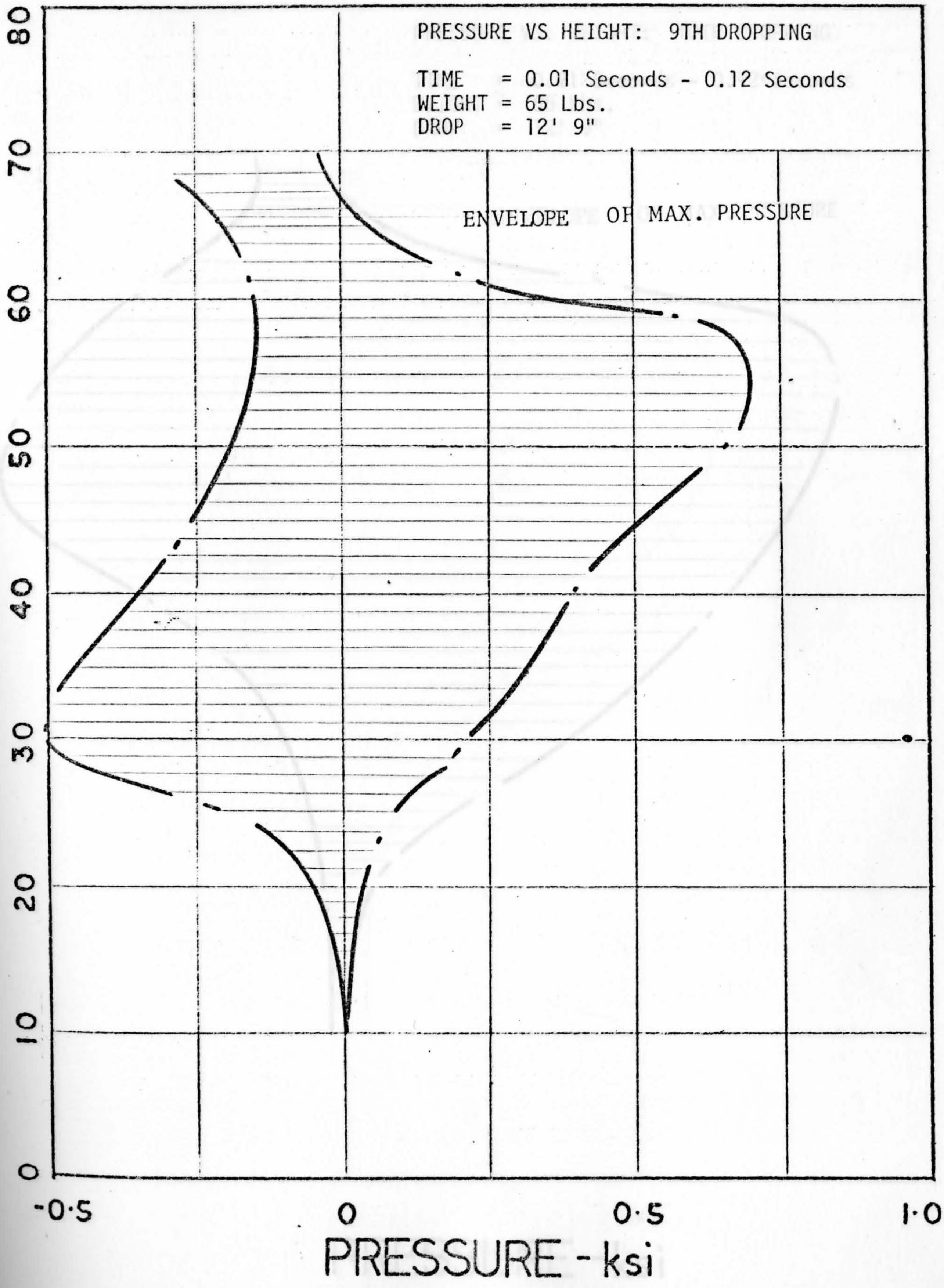
PRESSURE VS HEIGHT: 9TH DROPPING
TIME = 0.01 Seconds - 0.12 Seconds
WEIGHT = 65 Lbs.
DROP = 12' 9"
ENVELOPE OF MAX. PRESSURE
HEIGHT -in of the soil
0
10
20
30
40
50
60
70
80
-0·5
0
0·5
1·0
PRESSURE - ksi

Fig. 6

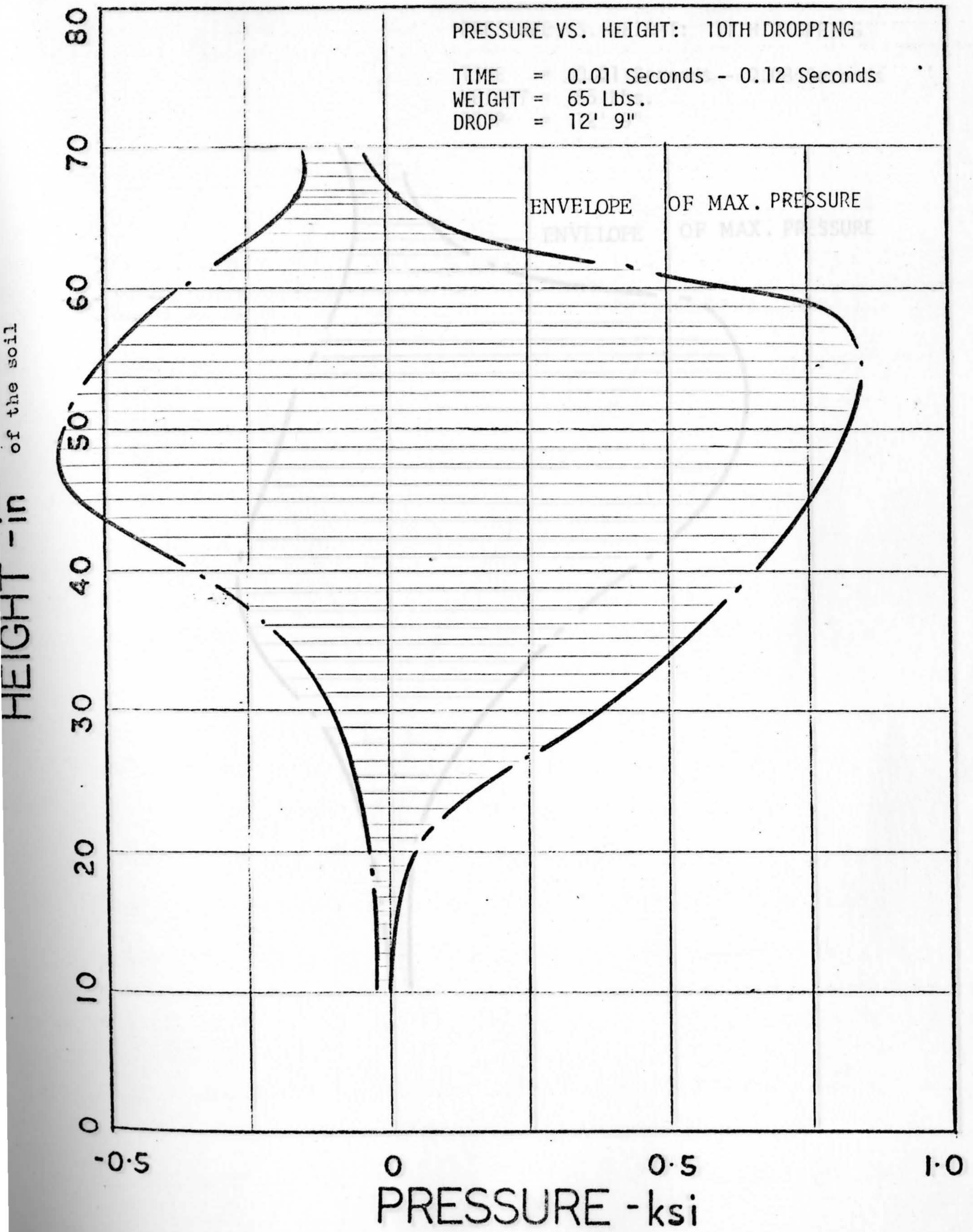
PRESSURE VS. HEIGHT: 10TH DROPPING
TIME = 0.01 Seconds - 0.12 Seconds
WEIGHT = 65 Lbs.
DROP = 12' 9"
ENVELOPE OF MAX. PRESSURE
HEIGHT -in of the soil
0
10
20
30
40
50
60
70
80
-0·5
0
0·5
1·0
PRESSURE -ksi

FIG. 7

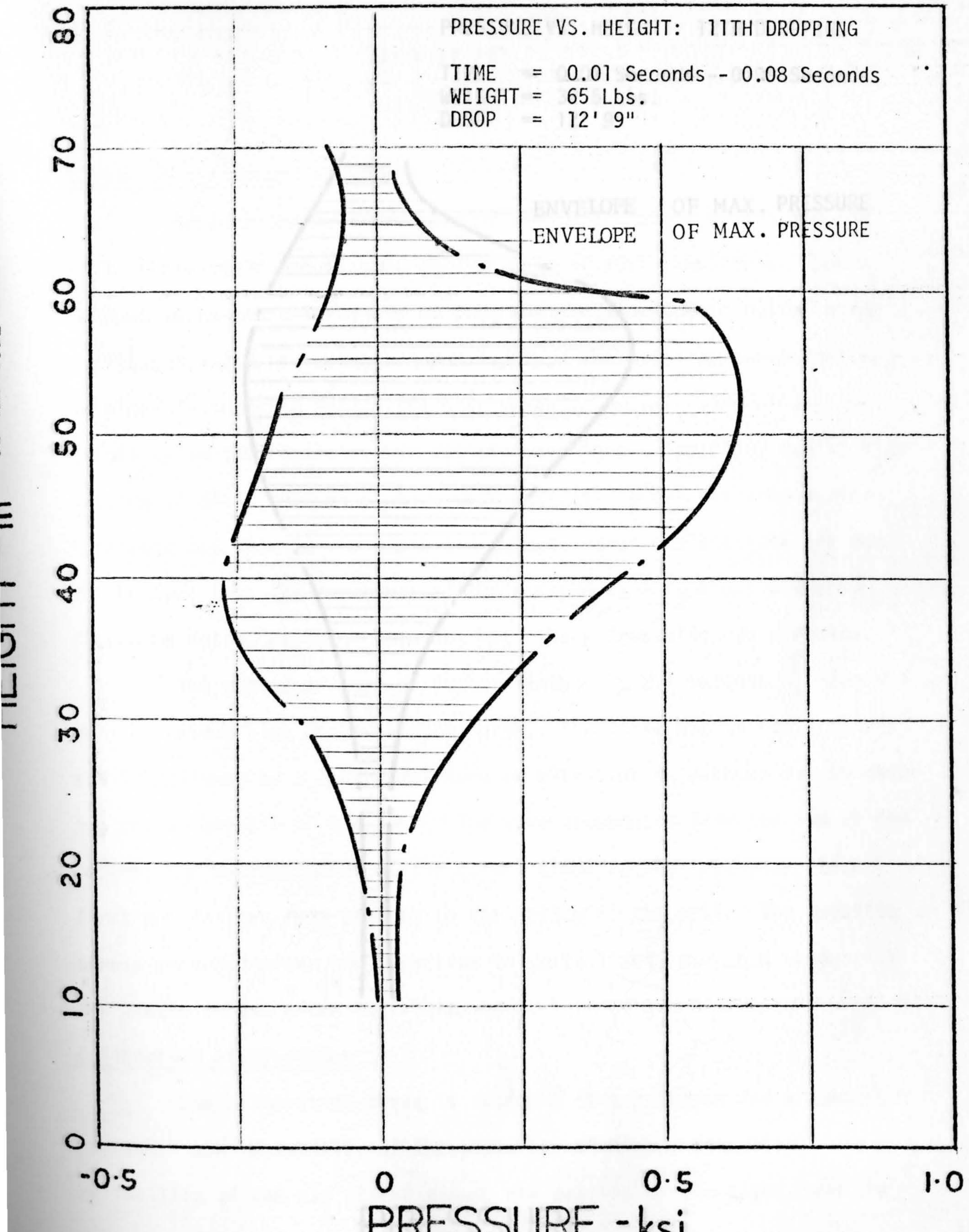
PRESSURE VS. HEIGHT: 11TH DROPPING
TIME = 0.01 Seconds - 0.08 Seconds
WEIGHT = 65 Lbs.
DROP = 12' 9"
ENVELOPE OF MAX. PRESSURE
80
70
60
50
40
30
20
10
0
-0·5
0
0·5
1·0
PRESSURE -ksi
HEIGHT - in

Fig. 8

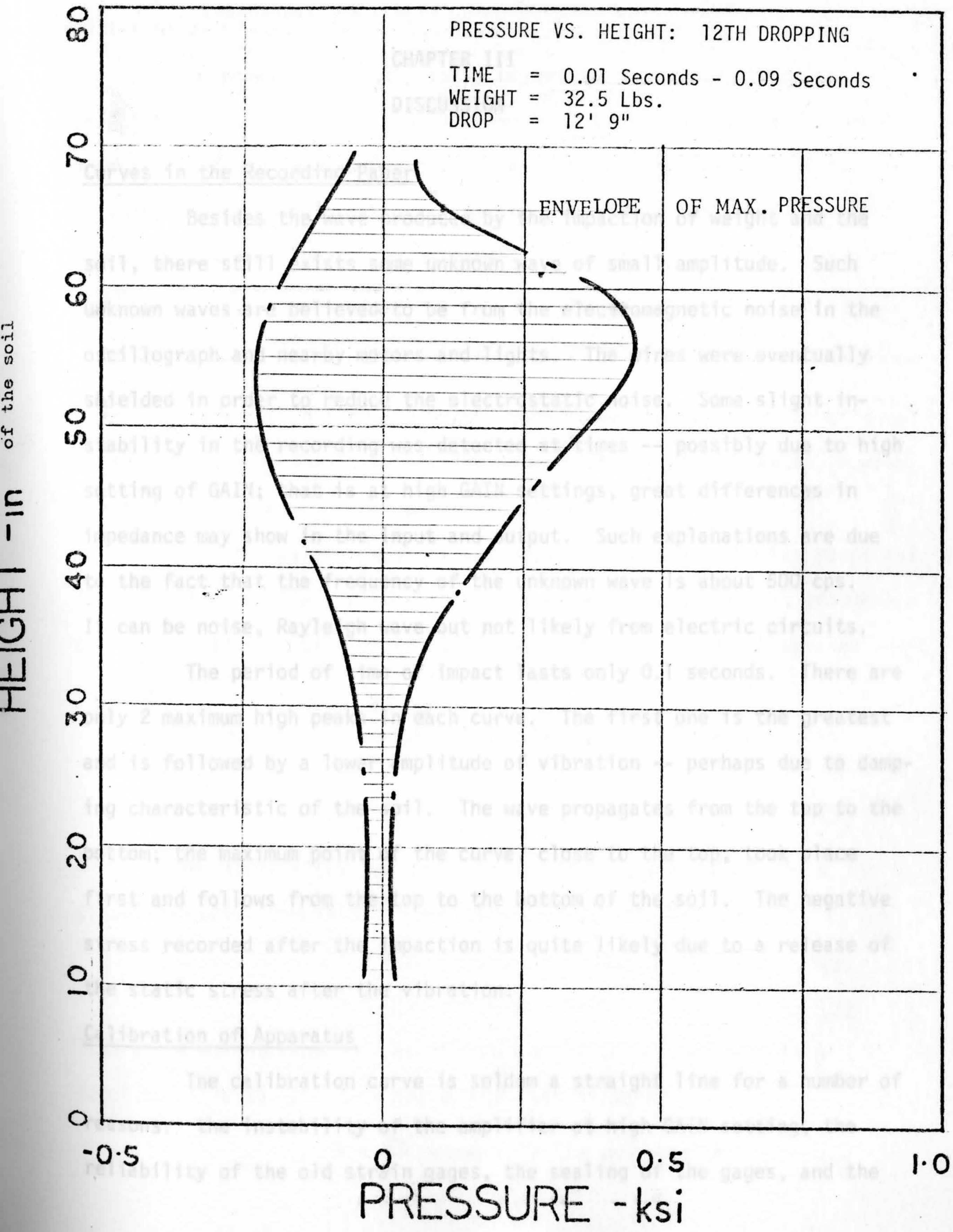
PRESSURE VS. HEIGHT: 12TH DROPPING
TIME = 0.01 Seconds - 0.09 Seconds
WEIGHT = 32.5 Lbs.
DROP = 12' 9"
ENVELOPE OF MAX. PRESSURE
HEIGHT - in of the soil
80
70
60
50
40
30
20
10
0
-0·5
0
0·5
1·0
PRESSURE - ksi

CHAPTER III
DISCUSSION

Curves in the Recording Paper

Besides the wave produced by the impaction of weight and the soil, there still exists some unknown wave of small amplitude. Such unknown waves are believed to be from the electromagnetic noise in the oscillograph and nearby motors and lights. The wires were eventually shielded in order to reduce the electrostatic noise. Some slight instability in the recording was detected at times -- possibly due to high setting of GAIN; that is at high GAIN settings, great differences in impedance may show in the input and output. Such explanations are due to the fact that the frequency of the unknown wave is about 500 cps. It can be noise, Rayleigh wave but not likely from electric circuits.

The period of time of impact lasts only 0.1 seconds. There are only 2 maximum high peaks in each curve. The first one is the greatest and is followed by a lower amplitude of vibration -- perhaps due to damping characteristic of the soil. The wave propagates from the top to the bottom; the maximum point of the curve, close to the top, took place first and follows from the top to the bottom of the soil. The negative stress recorded after the impaction is quite likely due to a release of the static stress after the vibration.

Calibration of Apparatus

The calibration curve is seldom a straight line for a number of reasons: the instability of the amplifier at high GAIN setting, the reliability of the old strain gages, the sealing of the gages, and the stress bars.

The stress decrease, nearly to zero at the one-third of the height from the bottom, is possibly due to the fact that the soil absorbs energy of the wave and is not a good conductor of the wave. Soil is not elastic; energy is being absorbed by its own organic matters in the soil and plastic characteristic of the soil.

Comparison of Experimental Result with Mathematical Result of Richart

Since 1955 Miller and Pursey determined the distribution of total input energy among the three elastic waves to be 67 percent Rayleigh wave, 26 percent shear wave, and 7 percent compression wave.

Because Rayleigh wave is the major wave among the other waves and decays much more slowly with distance than body waves, Richart produced a chart of amplitude ratio vs. dimensionless depth for Rayleigh wave as shown in Figure 11.

The equation of horizontal displacement, after Richart, is:

$$u = \frac{\partial \Phi}{\partial x} + \frac{\partial \Psi}{\partial z} \qquad (1)$$

The expressions for Φ and Ψ, by assuring a solution for a sinusoidal wave travelling in positive x direction, are

$$\Phi = F(z)\ \exp\{i(\omega t - Nx)\} \qquad (2)$$

$$\Psi = G(z)\ \exp\{i(\omega t - Nx)\} \qquad (3)$$

F(z) and G(z) describe the variation in amplitude of the wave as a function of depth, and N is the wave number defined by

$$N = \frac{2\pi}{L} \quad \text{where L is the wave length.} \qquad (4)$$

The three equations of motion in terms of stress can be written:

$$\rho\frac{\partial^2 u}{\partial t^2}=\frac{\partial\sigma_x}{\partial x}+\frac{\partial\tau_{xy}}{\partial y}+\frac{\partial\tau_{xz}}{\partial z}$$

$$\rho\frac{\partial^2 v}{\partial t^2}=\frac{\partial\tau_{yx}}{\partial x}+\frac{\partial\sigma_y}{\partial y}+\frac{\partial\tau_{yz}}{\partial z}\qquad(5)$$

$$\rho\frac{\partial^2 w}{\partial t^2}=\frac{\partial\tau_{zx}}{\partial x}+\frac{\partial\tau_{zy}}{\partial y}+\frac{\partial\sigma_z}{\partial z}$$

Relationships for an elastic medium

$$\sigma_x=\lambda\bar{\varepsilon}+2G\varepsilon_x\qquad\tau_{xy}=\tau_{yx}=G\gamma_{xy}$$

$$\sigma_y=\lambda\bar{\varepsilon}+2G\varepsilon_y\qquad\tau_{yz}=\tau_{zy}=G\gamma_{yz}\qquad(6)$$

$$\sigma_z=\lambda\bar{\varepsilon}+2G\varepsilon_z\qquad\tau_{zx}=\tau_{xz}=G\gamma_{zx}$$

Relationships for strain and rotation in terms of displacement.

$$\varepsilon_x=\frac{\partial u}{\partial x}\qquad\gamma_{xy}=\frac{\partial v}{\partial x}+\frac{\partial u}{\partial y}\qquad 2\bar{\omega}_x=\frac{\partial w}{\partial y}-\frac{\partial v}{\partial z}$$

$$\varepsilon_y=\frac{\partial v}{\partial y}\qquad\gamma_{yz}=\frac{\partial w}{\partial y}+\frac{\partial v}{\partial z}\qquad 2\bar{\omega}_y=\frac{\partial u}{\partial z}-\frac{\partial w}{\partial x}\qquad(7)$$

$$\varepsilon_z=\frac{\partial w}{\partial z}\qquad\gamma_{zx}=\frac{\partial u}{\partial z}+\frac{\partial w}{\partial x}\qquad 2\bar{\omega}_z=\frac{\partial v}{\partial x}-\frac{\partial u}{\partial y}$$

Where $\bar{\omega}$ is the rotation about each axis.

Combining equations (6) and (7) with equation (5) gives

$$\rho\frac{\partial^2 u}{\partial t^2}=(\lambda+G)\frac{\partial\bar{\varepsilon}}{\partial x}+G\nabla^2 u$$

$$\rho \frac{\partial^2 v}{\partial t^2} = (\lambda+G) \frac{\partial \bar{\varepsilon}}{\partial y} + G\nabla^2 v \tag{8}$$

Substituting u and w into equation (8) yields

$$\rho \frac{\partial}{\partial x}\left(\frac{\partial^2 \Phi}{\partial t^2}\right) + \rho \frac{\partial}{\partial z}\left(\frac{\partial^2 \Psi}{\partial t^2}\right) = (\lambda+2G) \frac{\partial}{\partial x}(\nabla^2 \Phi) + G \frac{\partial}{\partial z}(\nabla^2 \Psi) \tag{9}$$

and

$$\rho \frac{\partial}{\partial z}\left(\frac{\partial^2 \Phi}{\partial t^2}\right) - \rho \frac{\partial}{\partial x}\left(\frac{\partial^2 \Psi}{\partial t^2}\right) = (\lambda+2G) \frac{\partial}{\partial z}(\nabla^2 \Phi) - G\frac{\partial}{\partial x}(\nabla^2 \Psi) \tag{10}$$

Equations (9) and (10) are satisfied if

$$\frac{\partial^2 \Phi}{\partial t^2} = \frac{\lambda+2G}{\rho} \nabla^2 \Phi = V_p^2 \nabla^2 \Phi \tag{11}$$

$$\frac{\partial^2 \Psi}{\partial t^2} = \left(\frac{G}{\rho}\right) \nabla^2 \Psi = V_s^2 \nabla^2 \Psi \tag{12}$$

Now, substituting the expression for Φ and Ψ from equations (2) and (3) into equations (11) and (12) yields

$$-\frac{\omega^2}{V_p^2} F(z) = -N^2 F(z) + F''(z) \tag{13}$$

$$-\frac{\omega^2}{V_s^2} G(z) = -N^2 G(z) + G''(z) \tag{14}$$

By rearranging equations (13) and (14), the corresponding results are

$$F''(z) - \left(N^2 - \frac{\omega^2}{V_p^2}\right) F(z) = 0 \tag{15}$$

$$G''(z) - (N^2 - \frac{\omega^2}{V_s^2})\ G(z) = 0 \qquad (16)$$

where F"(z) and G"(z) are derivatives in the respect to z. Now letting

$$q^2 = (N^2 - \frac{\omega^2}{V_p^2}) \qquad (17)$$

and $$s^2 = (N^2 - \frac{\omega^2}{V_s^2}) \qquad (18)$$

Equations (15) and (16) can be rewritten as

$$F''(z) - q^2F(z) = 0 \qquad (19)$$

$$G''(z) = s^2G(z) = 0 \qquad (20)$$

The solutions of equations (19) and (20) can be expressed in the form

$$F(z) = A_1 \exp(-qz) + B_1 \exp(qz) \qquad (21)$$

$$G(z) = A_2 \exp(-sz) + B_2 \exp(sz) \qquad (22)$$

A solution that allows the amplitude A the wave to become infinite with depth cannot be tolerated; therefore,

$$B_1 = B_2 = 0$$

and equations (2) and (3) become

$$\Phi = A_1 \exp\{-qz + i(\omega t - Nx)\} \qquad (23)$$

$$\Psi = A_2 \exp\{-sz + i(\omega t - Nx)\} \qquad (24)$$

The equations of horizontal displacement of Rayleigh wave is

$$u = \frac{\partial\Phi}{\partial x} + \frac{\partial\Psi}{\partial z}$$

Upon substituting the expressions for Φ and Ψ from equations (23) and (24) into the expressions for u, we get

$$u = - A_1 \, i \, N \exp \{-qz + i(\omega t-Nx)\} - A_2 \, s \exp \{-sz + i(\omega t-Nx)\} \tag{25}$$

The relationship of A_2 and A_1 can be solved by equations (23) and (24) using boundary conditions specifying no stress at the surface of a half-space implying that $\sigma_z = 0$ and $\tau_{xy} = 0$ at surface. Therefore, at surface

$$\sigma_z = \lambda \bar{\varepsilon} + 2G\varepsilon_z = \lambda \bar{\varepsilon} + 2G \frac{\partial w}{\partial z} = 0 \tag{26}$$

$$\tau_{zx} = G\gamma_{zx} = G(\frac{\partial w}{\partial x} + \frac{\partial u}{\partial z}) = 0 \tag{27}$$

Using the definitions of u and K and the solutions for Φ and Ψ from equations (23) and (24), the above equations for boundary conditions can be written

$$\sigma_z \Big|_{z=0} = A_1 \{\lambda + 2G)q^2 - \lambda N^2\} - 2i \, A_2 GNs = 0 \tag{28}$$

$$\tau_{zx} \Big|_{z=0} = 2i \, A_1 Nq + A_2 \, (s^2 + N^2) = 0 \tag{29}$$

Upon rearranging equations (28) and (29) become

$$\frac{A_1}{A_2} \, \frac{(\lambda+2G)q^2-\lambda N^2}{2i \, GNs} - 1 = 0 \tag{30}$$

$$\frac{A_1}{A_2} \, \frac{2qiN}{(s^2+N^2)} + 1 = 0 \tag{31}$$

Therefore we get

$$A_2 = - \frac{2qiNA_1}{s^2+N^2} \tag{32}$$

and substitution of A_2 into equation (25) gives

$$u = A_1 \{-iN \exp (-qz) + \frac{2iqsN}{s^2+N^2} \exp (-sz)\} \exp i \, (\omega t-Nx) \tag{33}$$

Rewritten equation (33)

$$u = A_1 \, Ni \, \{ - \exp \; [- \frac{q}{N} (zN)] + \frac{2 \frac{qs}{N^2}}{\frac{s^2}{N^2} + 1} \exp [- \frac{s}{N} (zN)] \}$$

$$x \exp i \; (\omega t \; - Nx) \qquad (34)$$

from equation (34) the variation of u with depth can
be expressed as

$$U(z) = - \exp \{ - \frac{q}{N} (zN) \} + \frac{2 \frac{qs}{N^2}}{\frac{s^2}{N^2} + 1} \exp \{ - \frac{s}{N} (zN) \} \qquad (35)$$

U(z) represent the spatial variations of the displacement u. Equations (17) and (18) can be written as $\frac{q^2}{N^2} = 1 - \alpha^2 K^2$; $\frac{s}{N} = 1 - K^2$

Now U(z) can be evaluated in terms of the wave number N for any given value of Poisson's ratio. If $\nu = 0.25$, $U(z) = - \exp \{-0.8475 \, (zN)\} + 0.5773 \exp \{-0.3933 \, (zN)\}$.

Using this expression a curve due to Richart's mathematical approach relating to lateral pressure at surface was plotted in Fig. 11 and Fig. 12.

The mean curve at 0.05 second interval of all the experiments and the mean curve of the final setting of all the experiments were chosen to represent the experimental result. The two chosen curves were extended to the top surface of the soil for reference. These two curves of pressure transfered to two relating curves relating to the surface lateral pressure were plotted into Fig. 11 and 12 respectively for comparison.

By relating to the amplitude of lateral pressure at surface due to Richart's expression, the deviation of the mean curve of 0.05 second with curve due to Richart's expression is 10 percent approximately. Similarly, the curve of final setting with the curve due to Richart's expression is approximately 30 percent in deviation.

The deviation of the result of Richart's expression with the experimental result is due to the fact that Richart considered only the Rayleigh wave without considering the shear wave and compression waves, but the experiment was influenced by both of them. The most important difference between Richart's result with the experimental result is because Richart's expression is derived from a continuous sinusoidal wave without taking time into the equation while the result of the experiment is only an impulse of shock taking amplitude at different intervals of time into the curve. The wave system has three salient features corresponding to the arrivals of the compression wave, shear wave and Rayleigh wave. A particle at the surface first experiences a displacement in the form of an oscillation at the arrival of the compression wave, followed by a relatively quiet period leading up to another oscillation at the arrival of shear wave. These events are referred to by Lamb as the minor tremor and followed by a much larger magnitude oscillation, the major tremor, at the time of arrival of Rayleigh wave.

The time interval between wave arrivals becomes greater and the amplitude of iscillations becomes smaller with increasing distance from the source. Rayleigh wave is significant at large distance but the experiment is at short distance therefore it was influenced much by both shear and compression wave.

PHYSICAL SET UP

Plate No. 1 Photograph of Physical set up with the steel tank at the back. The 447 oscillograph rest on the BA-4 bridge amplifier at the front.

TRAP DOOR

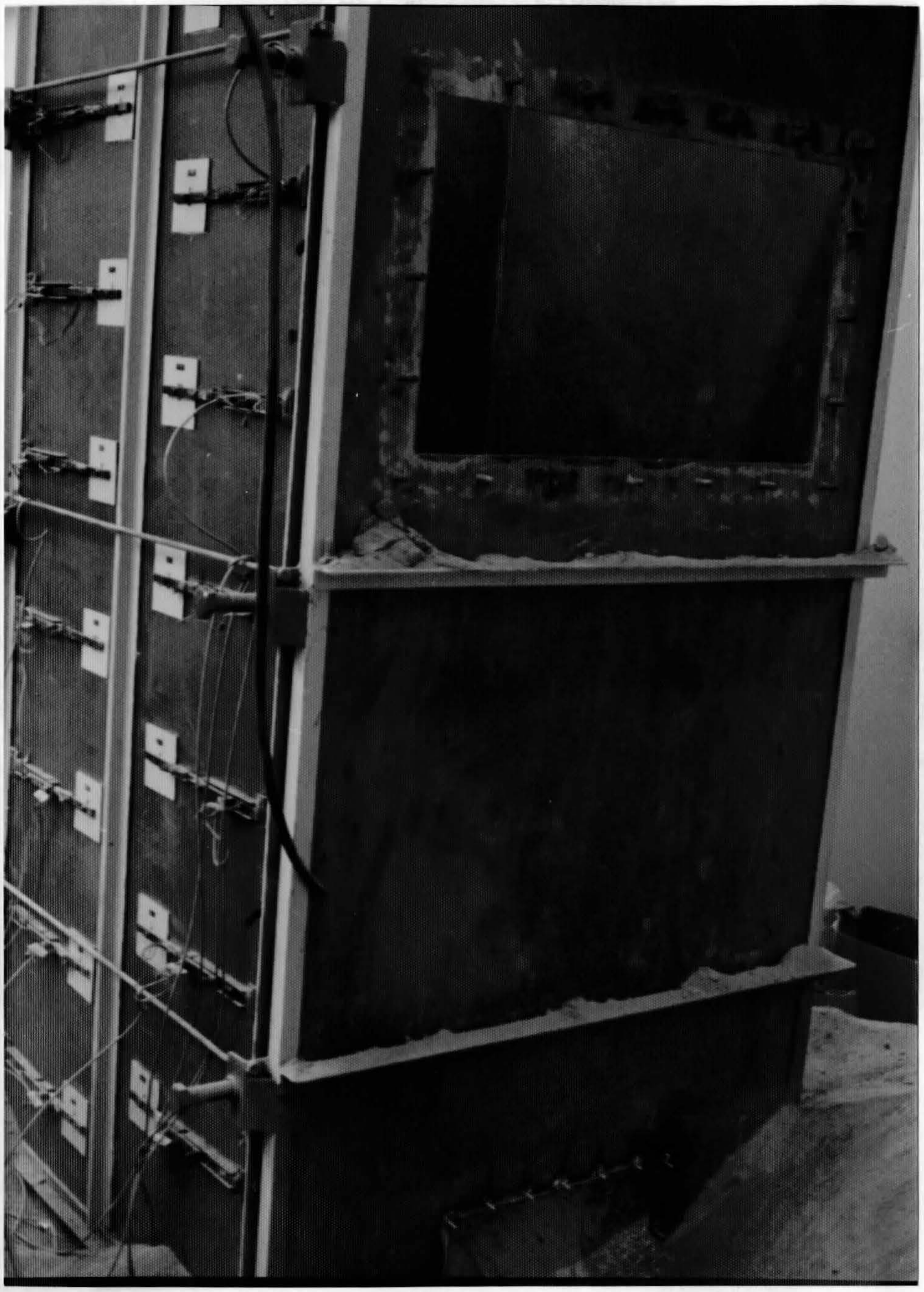

Plate No. 2 Photograph of two trap doors at the side of the steel tank to facilitate loading and unloading.

APPARATUS SET UP FOR CALIBRATION

Plate No. 3 Photograph of apparatus set up for calibration with pulley set up at the front, stress bar and window with corresponding circuit hook-up at the back.

447 OSCILLOGRAPH & BA-4 AMPLIFIER

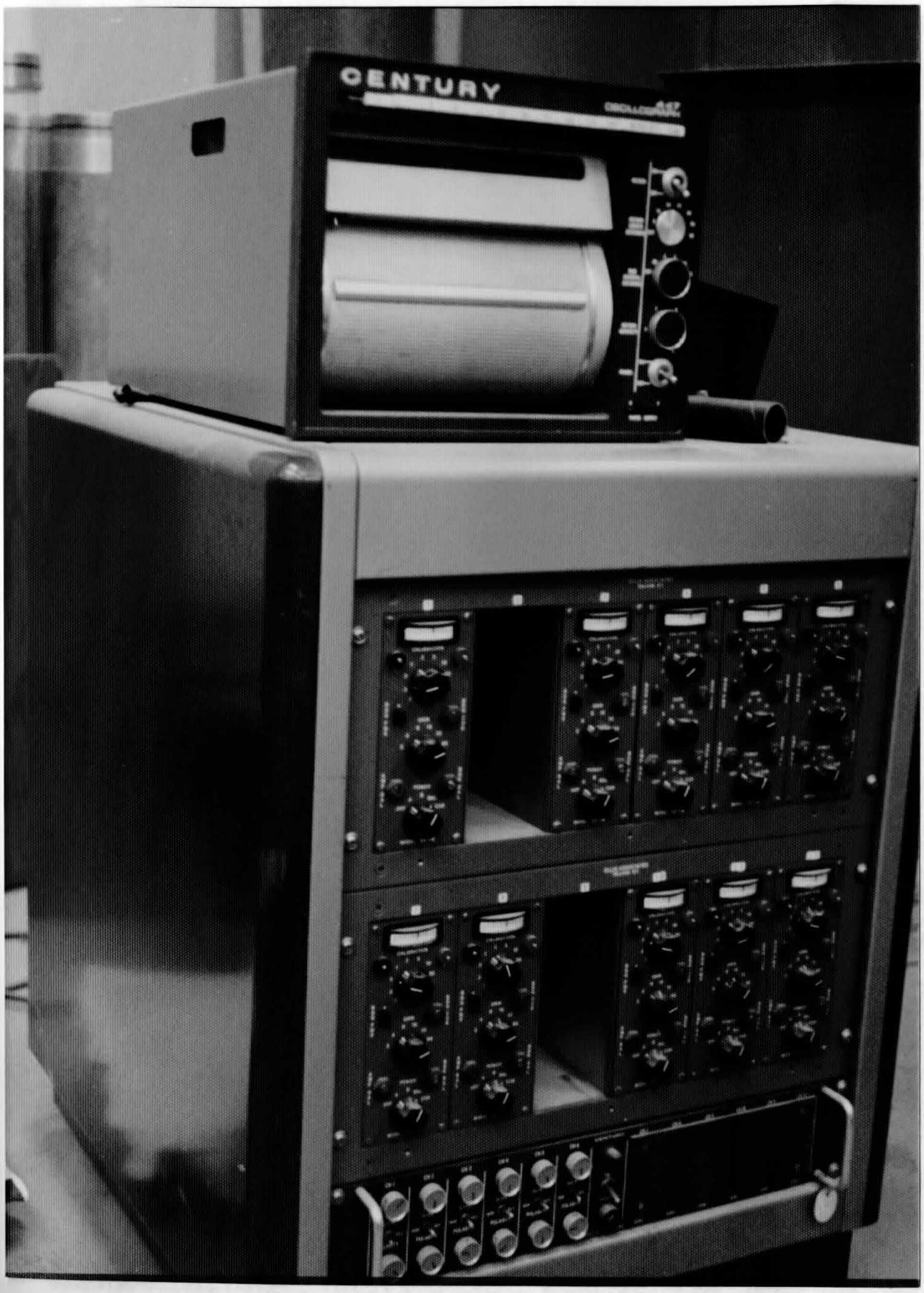
CENTURY
447 OSCILLOGRAPH

Plate No. 4 447 Oscillograph rest on BA-4 Bridge Amplifier with channel no. 2 and 9 out of order and removed.

TWO ARM OPERATION

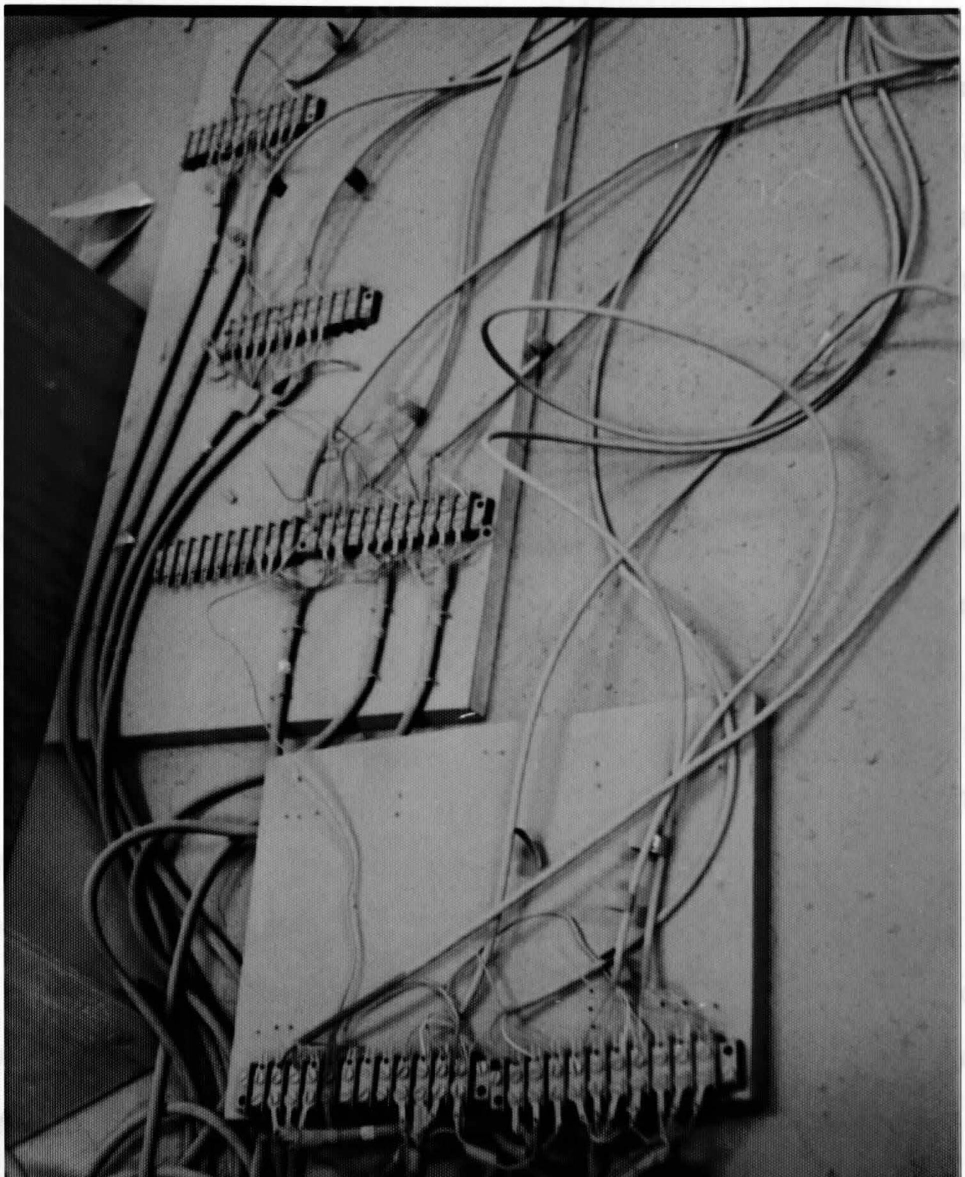

Plate No. 5 Photograph of two arm operation.

CHAPTER IV

CONCLUSION

From the stress distribution curves, a close approximation of the relative lateral force exerted on a vertical wall by a backfill of soil at different time intervals at constant water content but at a variable unknown density can be determined. The results of testing with dry loose sand were reasonably close to the curve results predicted by F.E. Richart, Jr., using a mathematical approach (see Fig. 11).

The experimental findings indicate that maximum stress is locateed at three-fifths (3/5) of the distance from the bottom of the tank, and decreases to nearly zero stress at one third (1/3) of the distance from the bottom.

The curves also show that the resulting pressure is less than the relative zero pressure. This is probably due to the gradual settlement of the loose sand inside the tank and subsequent release during the rebound of the static load on the window plates.

The maximum stress point took place at 0.01 to 0.02 seconds from the moment of contact of the weight with the soil. The vibration response took place in about 0.1 second.

Increasing the dropping weight increased the stress on the window plates, but not in direct proportion.

The water content is believed to have an influence, although not known at this time, on the effects of dynamic loads. This belief was a prime reason for the low water content used in the experiment.

From the view point of wave propagation, sixty-seven percent (67%) of the energy is from the Rayleigh wave, seven percent (7%) of the energy from compression wave, and twenty-six percent (26%) of the energy from shear wave. Rayleigh wave and compression wave are longitudinal waves and were believed to have been picked up by the BA-4 bridge amplifier. The shear wave may have influenced the results but was not picked up by the amplifier. The response due to shear wave is not considered to be picked up by the stress bar.

The maximum pressure picked up on the recording paper was increased by the magnitude of the energy level of the falling weight.

This thesis is admittedly only preliminary, but it is hoped that in the future more experiments will be done to produce more information encompassing of different variables, such as Poisson's ratio void ratio, water content, density, container sizes, arm stiffnesses, etc., and different types of soil.

CHAPTER V

RECOMMENDATIONS

Due to the ever-increasing activity in thesis projects at Youngstown State University, the apparatus of this project is recommended for engineering students interested in soil mechanics and soil dynamics.

The stress rods should be placed about 1/8-inch away from the tank. This would keep the window plates fitting smoothly into the movable wall. When working with soil dynamics, it is hoped that one may improve on the stress bars used to pick up transverse wave responses. It is also hoped that more channel amplifiers could be available, and that a four-arm operation be substituted for the two-arm operation.

A light neoprene plastic seal may be used at the windows on the movable wall and at the corners of the tank in order to give more freedom of both the soil sample and window plates.

A trap door at the bottom of one side of the tank should be built to reduce the amount of labor and time involved in loading and unloading the tank. Also, some strong transparent material of the same deformation characteristics may replace the original trap door. By so doing, observation of the shear plane and other tests could be performed.

Hopefully, in the future students carrying on the research work in soil dynamics will take Poisson's ratio, modulus of linear deformation, modulus of rigidity, shear modulus, wave propagation, continuous medium, homogeneous, isotropic, elastic half-space and more conditions into consideration.

FOOTNOTES

[1] Rausch, E. (1943), "Maschinenfundamente und andere dynamische Bauaufgaben," Vertrieb VDI Verlag G.M.B.H. (Berlin).

[2] Lorenz, H. (1960), "Grunbau-Dynamik," J. Spring (Berlin).

[3] Barkan, D.D. (1962) "Dynamics, of Bases and Foundations" (translated from the Russian by L. Drashevska, and translation edited by G.P. Tschebotarioff), McGraw-Hill Book Co. (New York).

[4] Harris, C.M., and Crede, C.E. (1961), "Shock and Vibration Handbook", McGraw-Hill Book Co. (New York).

[5] Ewing, Jardetzky and Press, 1967, showed that amplitude of the body waves decreases in proportion to the ratio of $1/r$ (r is the distance from the input source) except along the surface of the half-space, where the amplitude decreases as $1/r^2$. The amplitude of the Rayleigh wave decreases as $1/r^{\frac{1}{2}}$.

[6] Richart, F.E., Jr., Hall, J.R., Jr., and Woods, R.D.,(1970) "Vibrations of Soils and Foundations," Prentice-Hall International Series, Englewood Cliffs, N.J.

[7] Jones, R. (1958), "In-Situ Measurement of the Dynamic Properties of Soil by Vibration Methods" Geotechnique, Vol. 8, No. 1, Mar., pp. 1-21.

[8] "Proceedings of the Symposium on Soil Structure Interaction" University of Arizona, Sept. 1964.

[9] Robert L. Wiegel (1970) "Earthquake Engineering" Prentice-Hall International Series, Englewood Cliffs, N.J.

APPENDIX A

SIEVE ANALYSIS AND TESTS OF SOIL PARAMETERS

TABLE 1

TEST OF WATER CONTENT   DATE Sep 26 '77

SCALE NO. 28375

	Sample 1	Sample 2	Sample 3
1. Weight of the container	38.16gm.	38.65gm.	37.76gm.
2. Weight of sand + water + container	215.13gm.	217.42gm.	240.48gm.
3. Weight of sand + container.	208.17gm.	212.11gm.	234.40gm.
4. Weight of sand	170.56gm.	173.46gm.	196.74gm.
5. Weight of water	6.41gm.	5.31gm.	6.08gm.
6. Water content	0.038	0.031	0.031
7. Volume of the container	100 c.c.	100 c.c.	100 c.c.
8. Density	1.77 gm./cc	1.79 gm./cc	2.03 gm./cc
VOID RATIO ESTIMATION			
9. Volume of sand	63.64 c.c.	64.72 c.c.	73.41 c.c.
10. Volume of void	36.36 c.c.	35.28 c.c.	26.59 c.c.
11. Void Ratio	0.57	0.55	0.36

DEVIATION

	Mean	Deviation
12. Water content	0.033	0.15
13. Density	1.86	0.09
14. Void Ratio	0.49	0.27

TABLE 2

SIEVE ANALYSIS MARCH 5 1978

Weight of the pan	396.5 gm.
Weight of the pan + sample soil	2332 gm.
Weight of the sample soil	195.5 gm.

SIEVE SIZE	WEIGHT OF THE SOIL RETAINED	PERCENT PASSING (ACCUMULATING)
1/4"	1.6 gm.	100
0.187"	0.7 gm.	99.92
40	1723.5 gm.	99.88
60	101.2 gm.	10.83
100	76.4 gm.	5.65
200	23.3 gm.	1.65
pan	8.8 gm.	0.45
	1935.5 gm.	

Figure 9

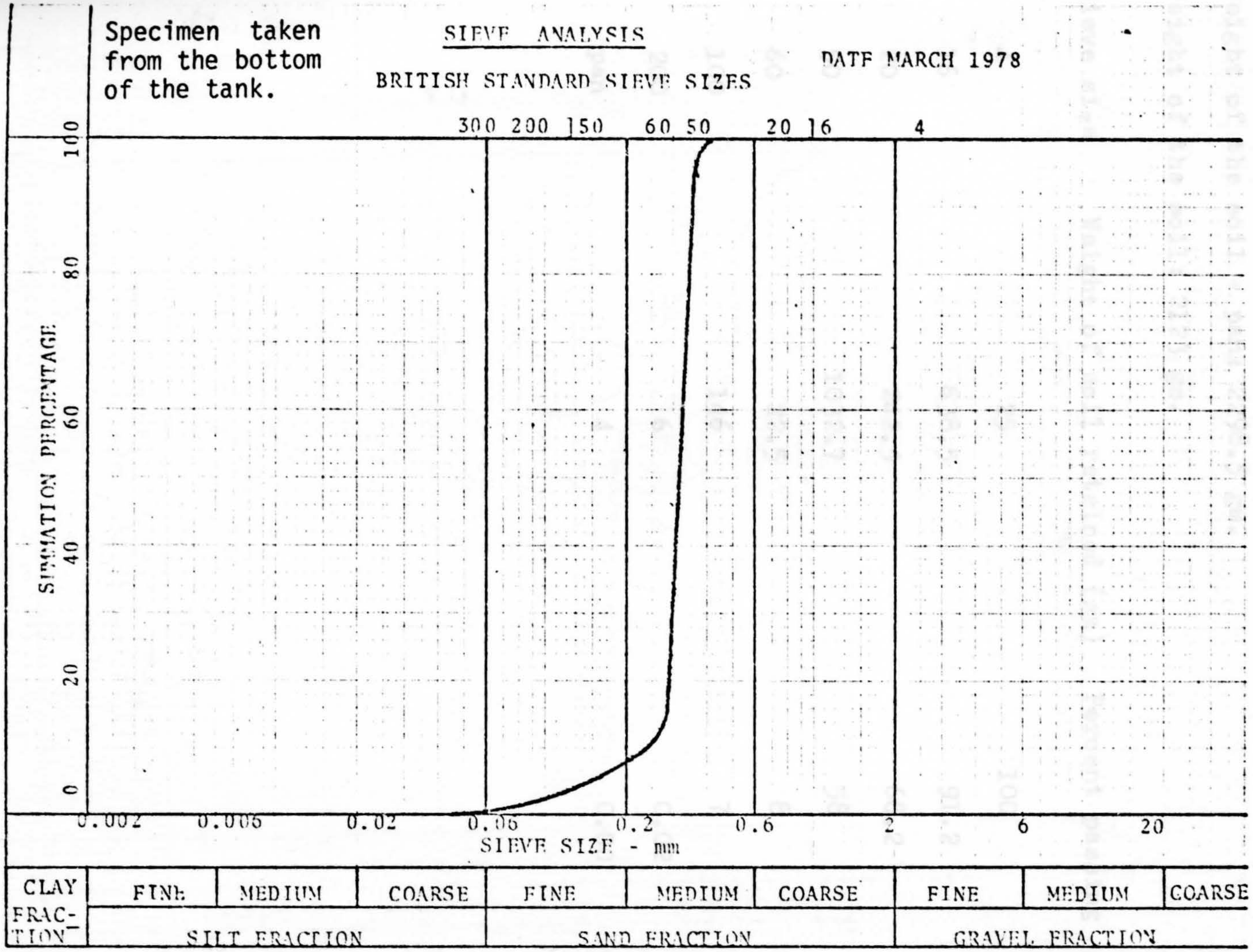

Specimen taken from the bottom of the tank.

TABLE 3 SIEVE ANALYSIS

No. 3257

Oct. 1977

Weight of the pan: 175.8 gm.

Weight of the soil + pan: 2298.5 gm.

Weight of the soil: 2123 gm.

Sieve size	Weight of soil retained (gm)	Percent passing
4	25	100
16	638.5	91.2
20	242.9	68.2
50	1032.7	58
60	22.5	8
100	146	7
200	6	0.02
pan	4	0.00

Figure 10

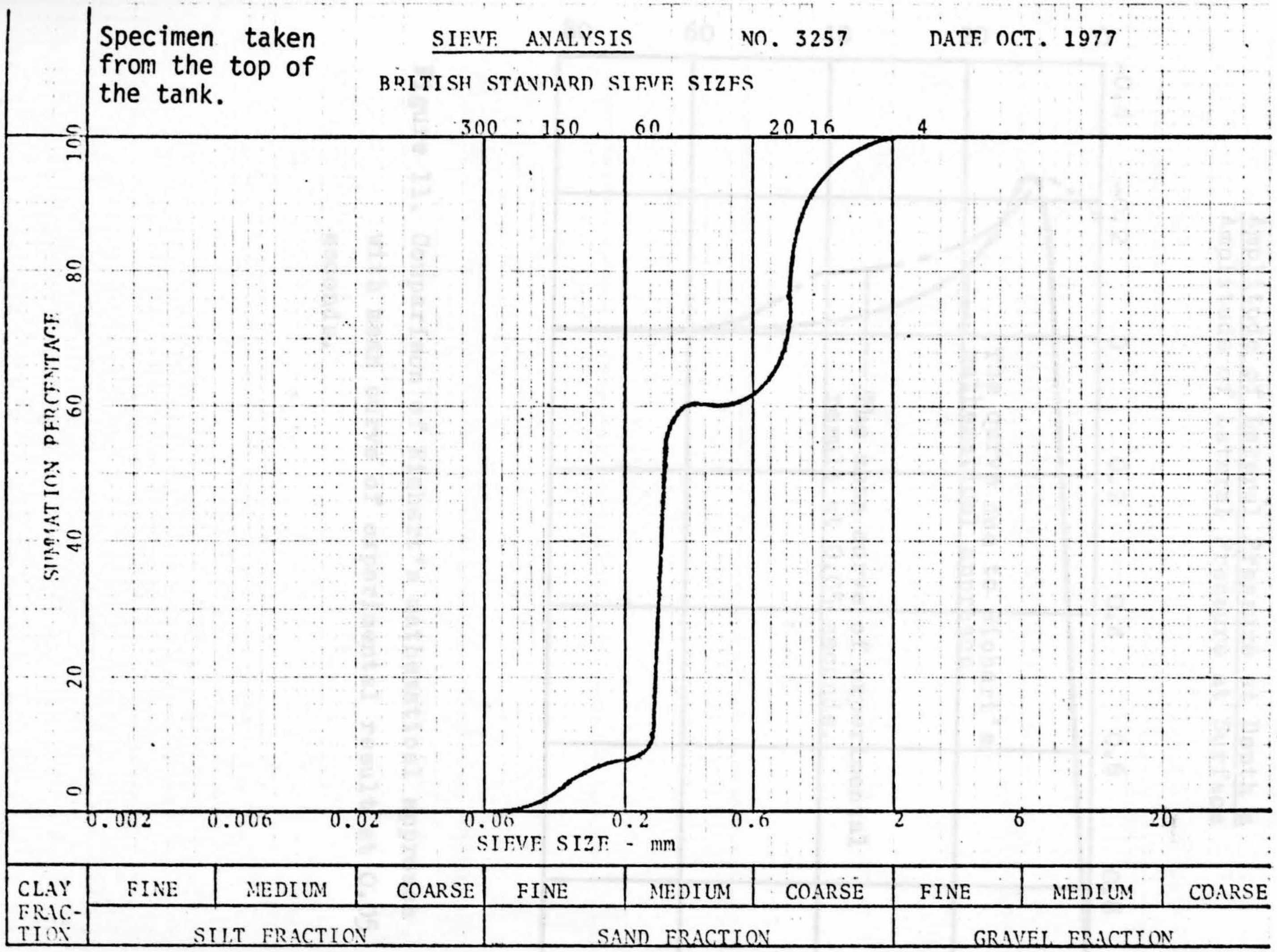
Specimen taken from the top of the tank.
SIEVE ANALYSIS
NO. 3257
DATE OCT. 1977
BRITISH STANDARD SIEVE SIZES
300
150
60
20
16
4
100
80
60
40
20
0
SUMMATION PERCENTAGE
0.002
0.006
0.02
0.06
0.2
0.6
2
6
20
SIEVE SIZE - mm
CLAY FRACTION
FINE
MEDIUM
COARSE
FINE
MEDIUM
COARSE
FINE
MEDIUM
COARSE
SILT FRACTION
SAND FRACTION
GRAVEL FRACTION

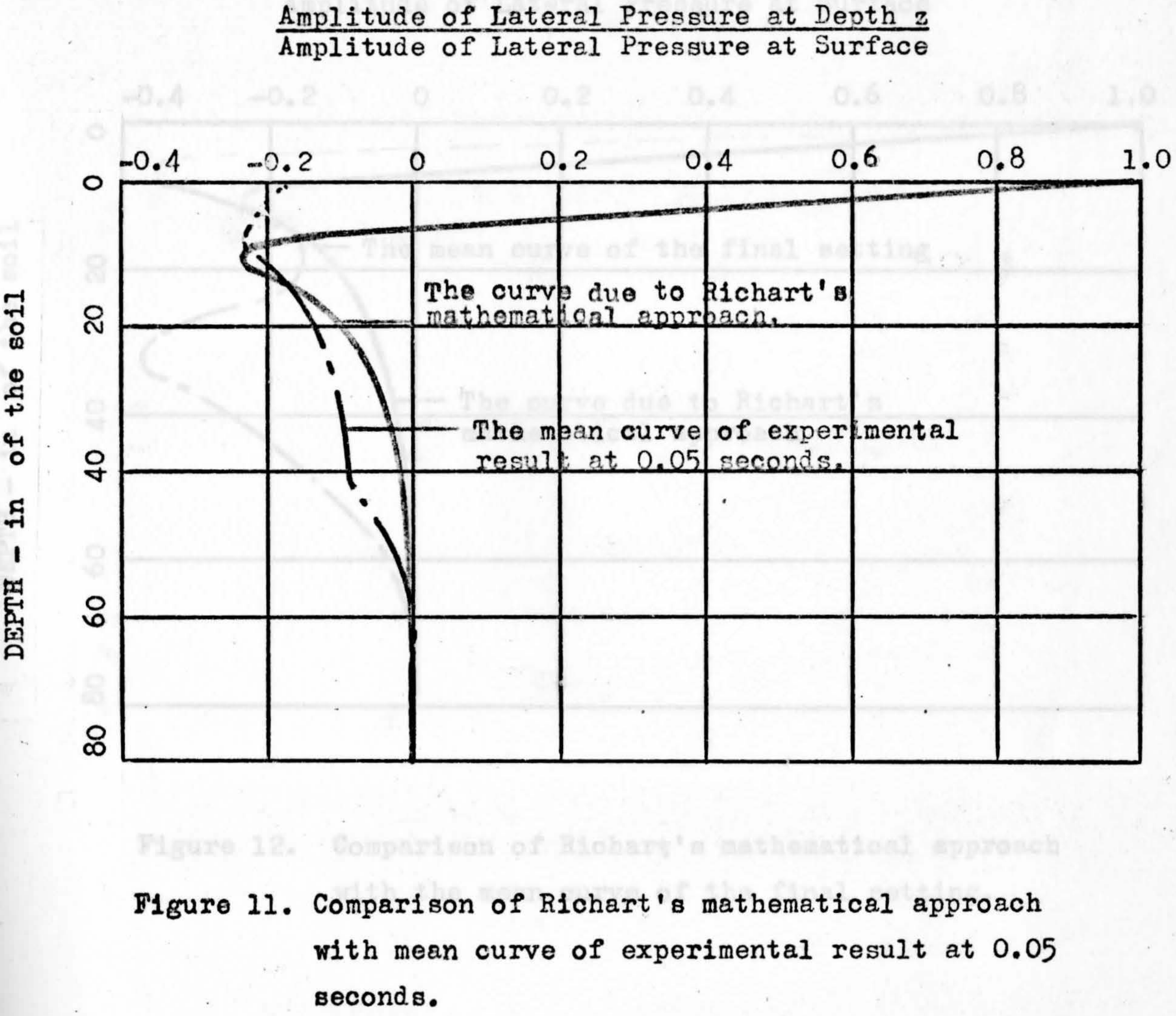

Figure 11. Comparison of Richart's mathematical approach with mean curve of experimental result at 0.05 seconds.

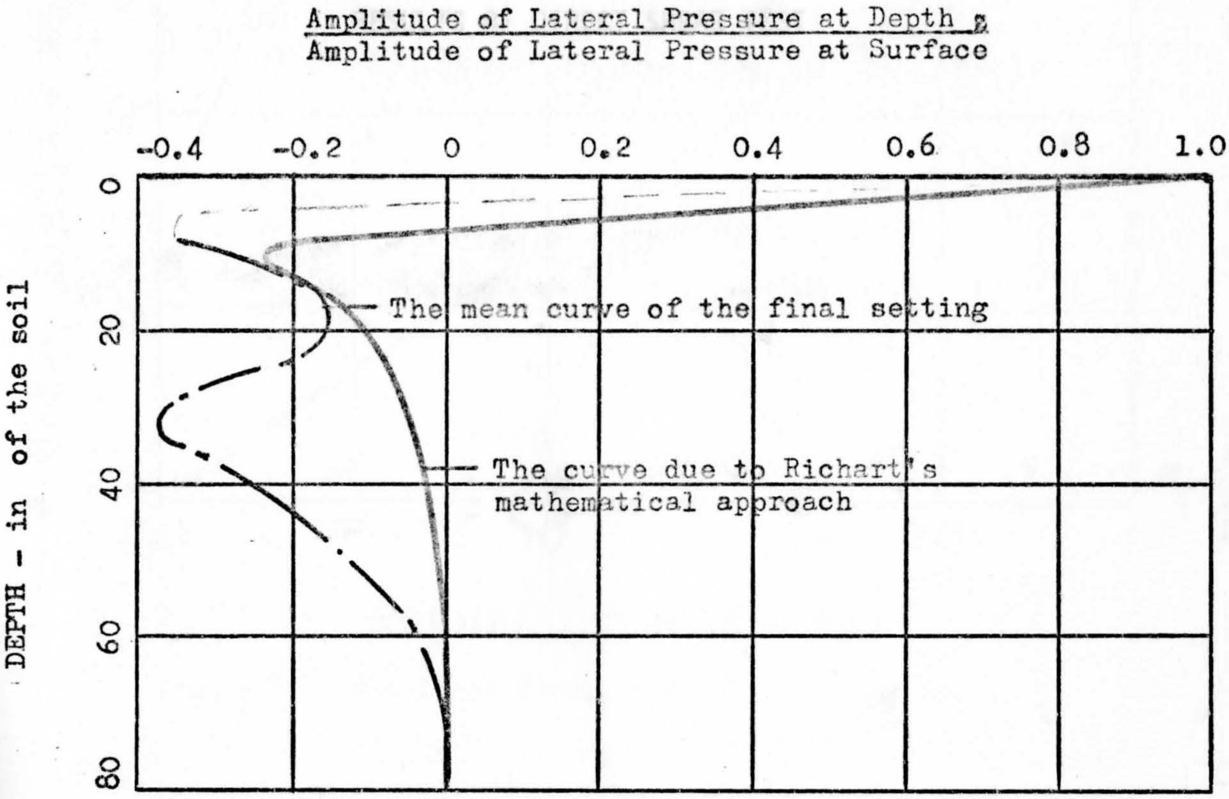

Figure 12. Comparison of Richart's mathematical approach with the mean curve of the final setting.

RESULTS OF DIRECT SHEAR TEST

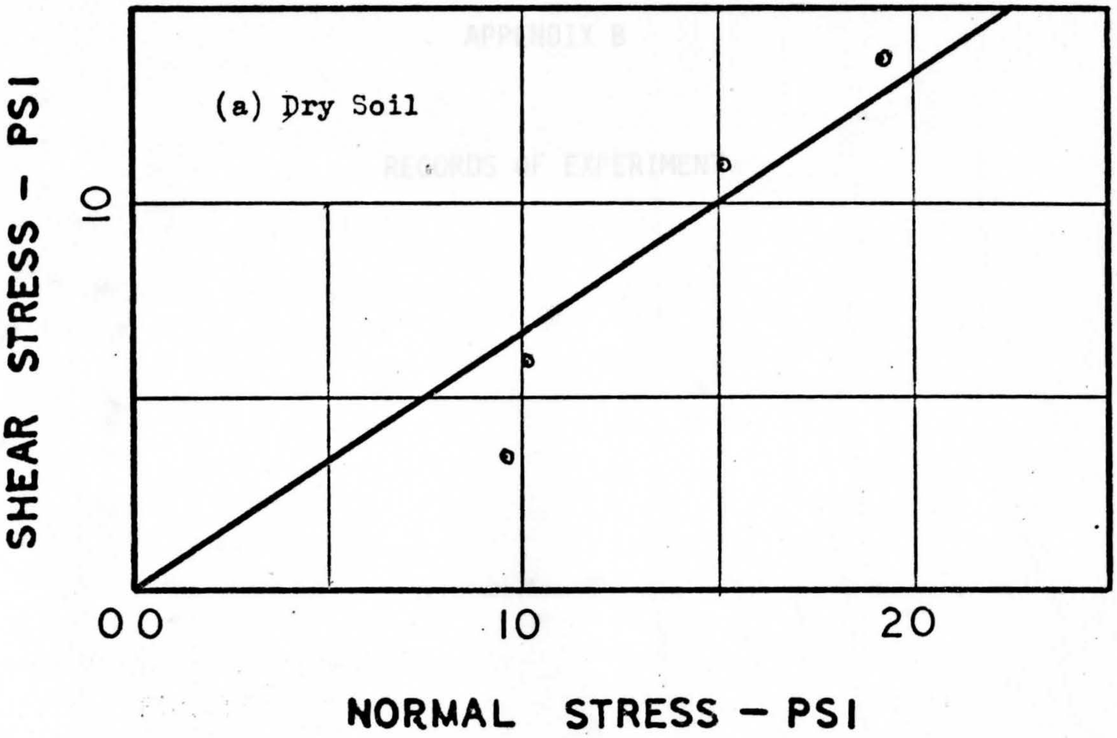

Figure 13. Result of Direct Shear Test on Dry Soil.

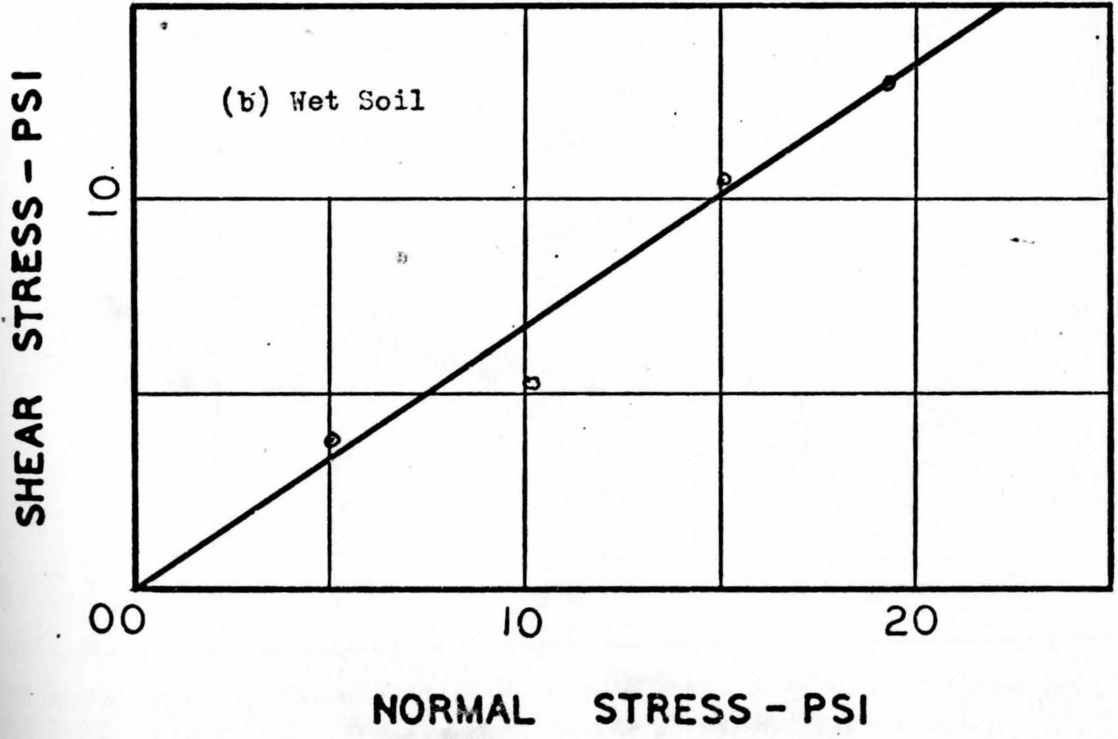

Figure 14. Result of Direct Shear Test on Wet Soil.

APPENDIX B

RECORDS OF EXPERIMENT

FIGURE 15

RECORD OF EXPERIMENTAL RESULTS

WEIGHT = 65LB.

HEIGHT = 12' 9"

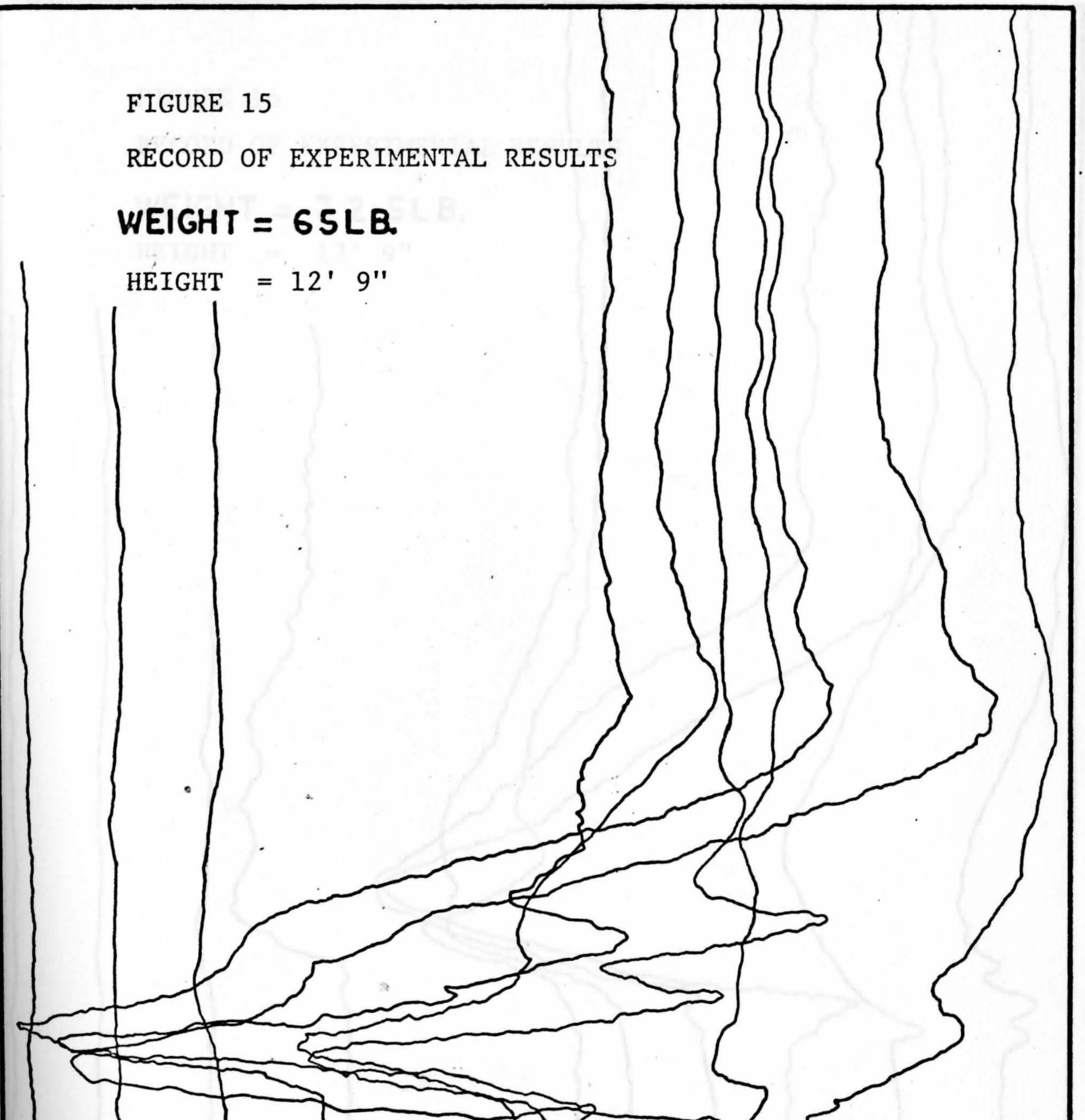

* The amplitude and the magnification varies for each drop. Therefore, the reading was interpreted with respect to calibration charts.

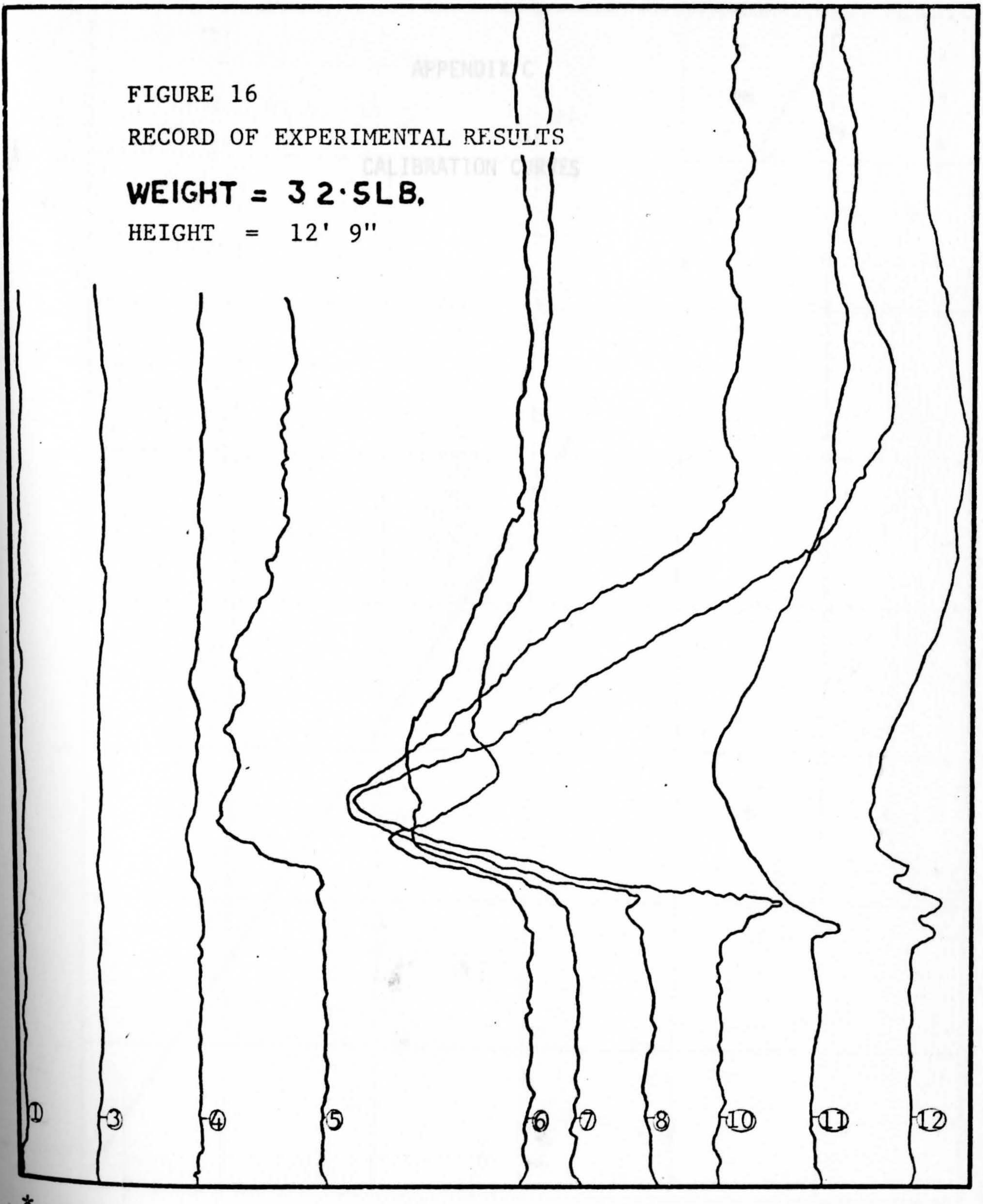

FIGURE 16

RECORD OF EXPERIMENTAL RESULTS

WEIGHT = 32·5LB.

HEIGHT = 12' 9"

* The amplitude and the magnification varies for each drop. Therefore, the reading was interpreted with respect to calibration charts.

APPENDIX C

CALIBRATION CURVES

Fig. 17

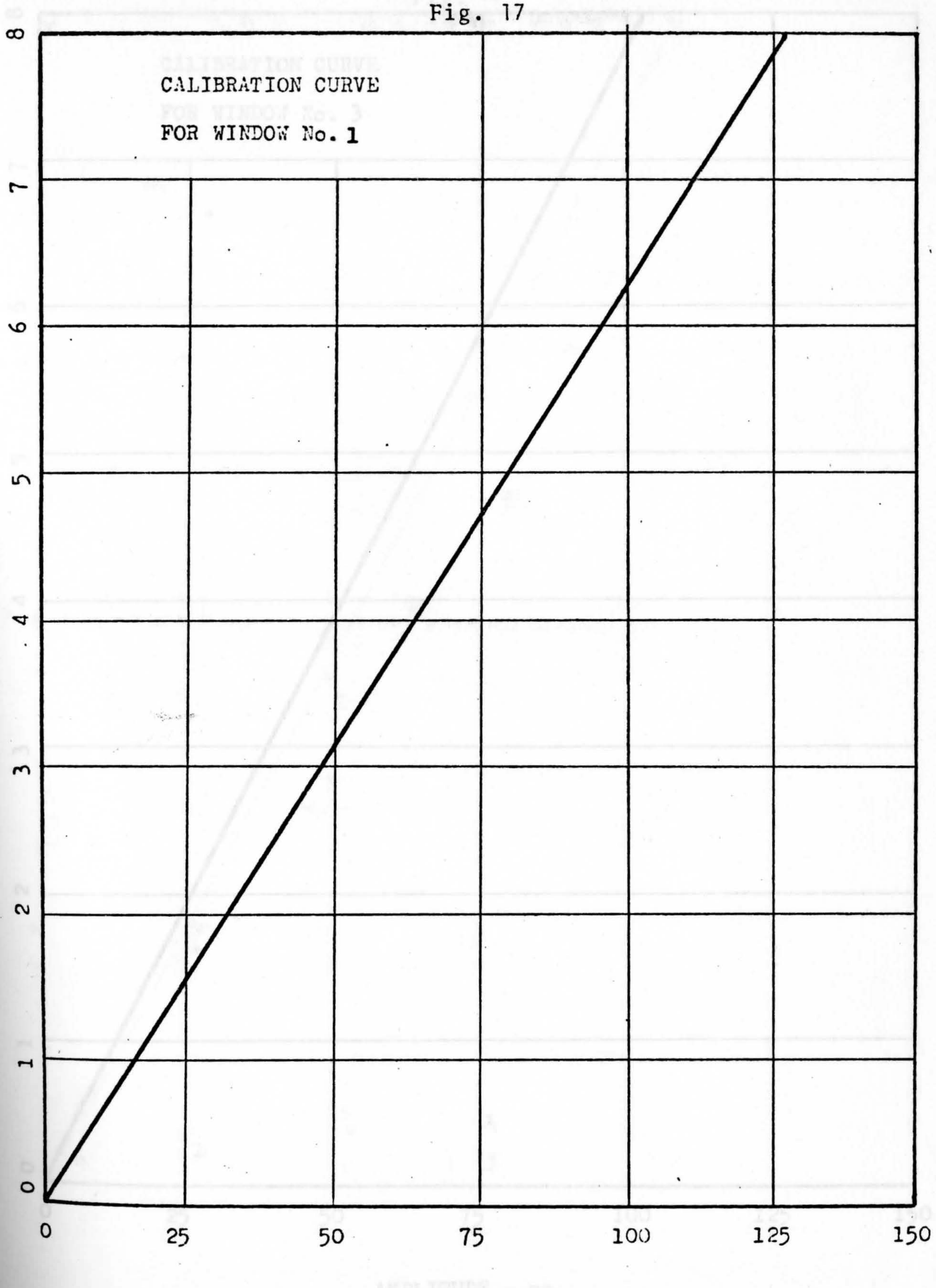
CALIBRATION CURVE
FOR WINDOW No. 1
LOAD - kip
0
1
2
3
4
5
6
7
8
0
25
50
75
100
125
150
AMPLITUDE - mm

Fig. 18

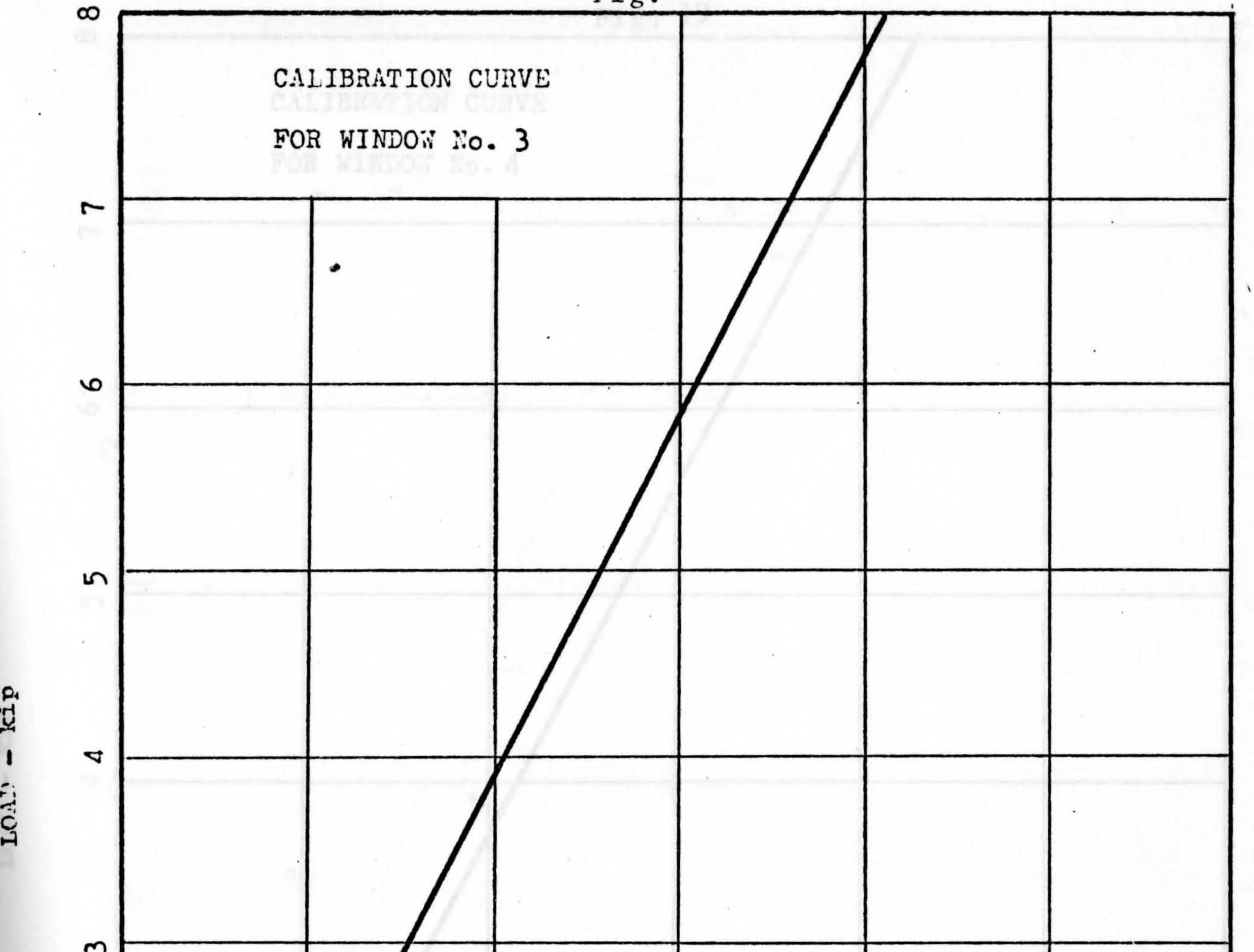
CALIBRATION CURVE
FOR WINDOW No. 3
LOAD - kip
0
1
2
3
4
5
6
7
8
0
25
50
75
100
125
150
AMPLITUDE - mm

Fig. 19

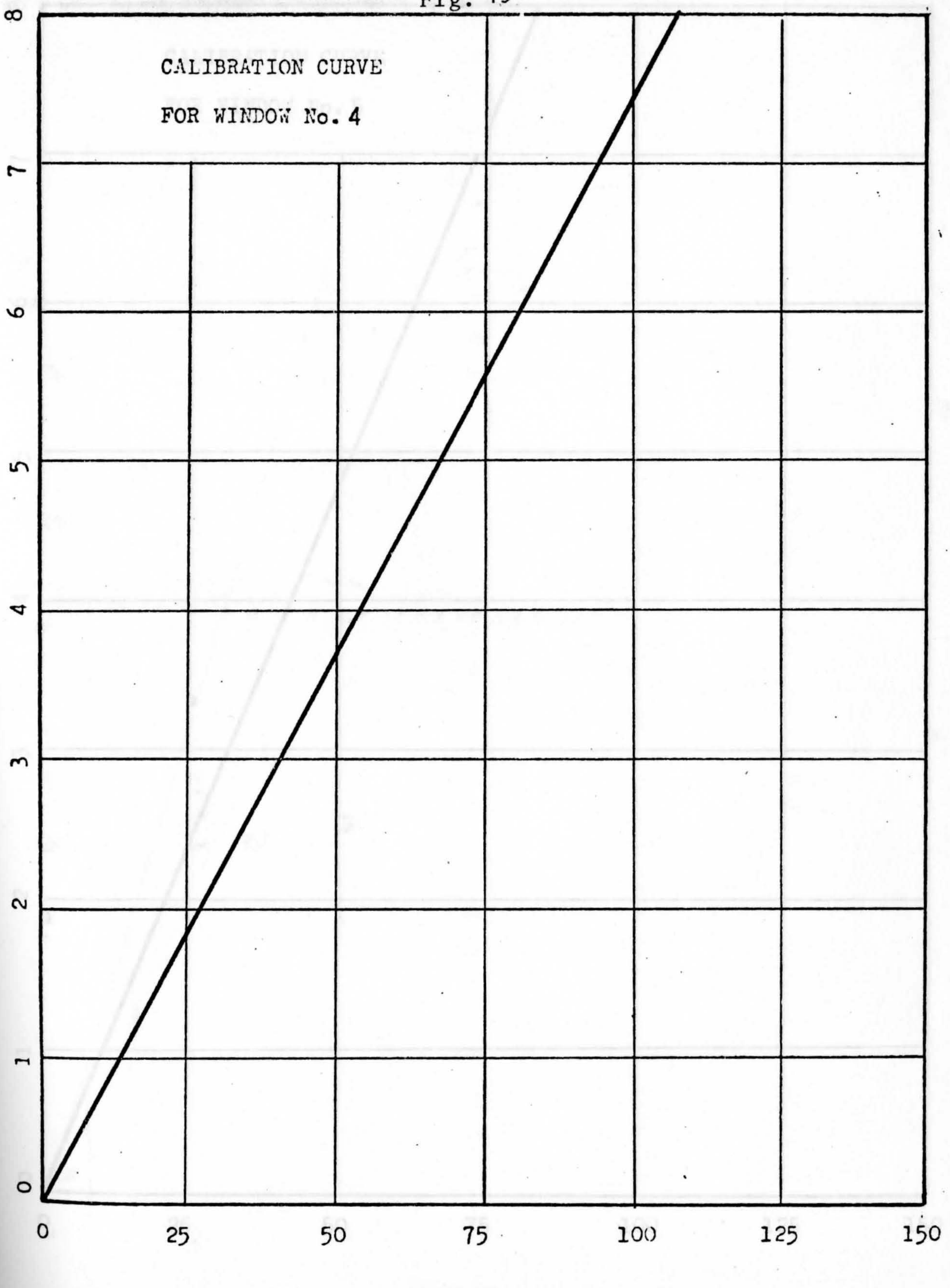
CALIBRATION CURVE
FOR WINDOW No. 4
LOAD - kip
AMPLITUDE - mm
0
1
2
3
4
5
6
7
8
0
25
50
75
100
125
150

Fig. 20

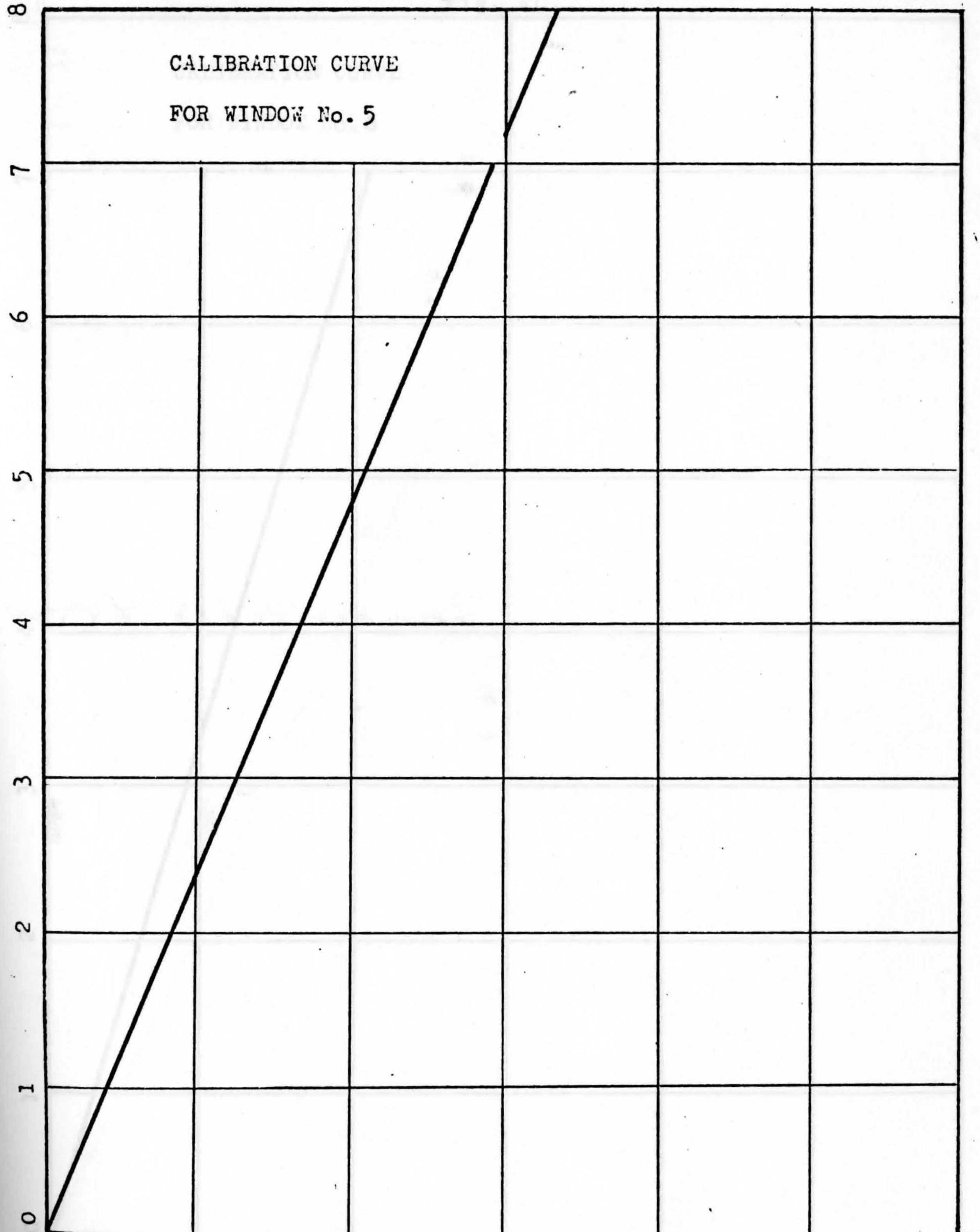
CALIBRATION CURVE
FOR WINDOW No. 5
LOAD - kip
0
1
2
3
4
5
6
7
8
0
25
50
75
100
125
150
AMPLITUDE - mm

Fig. 21

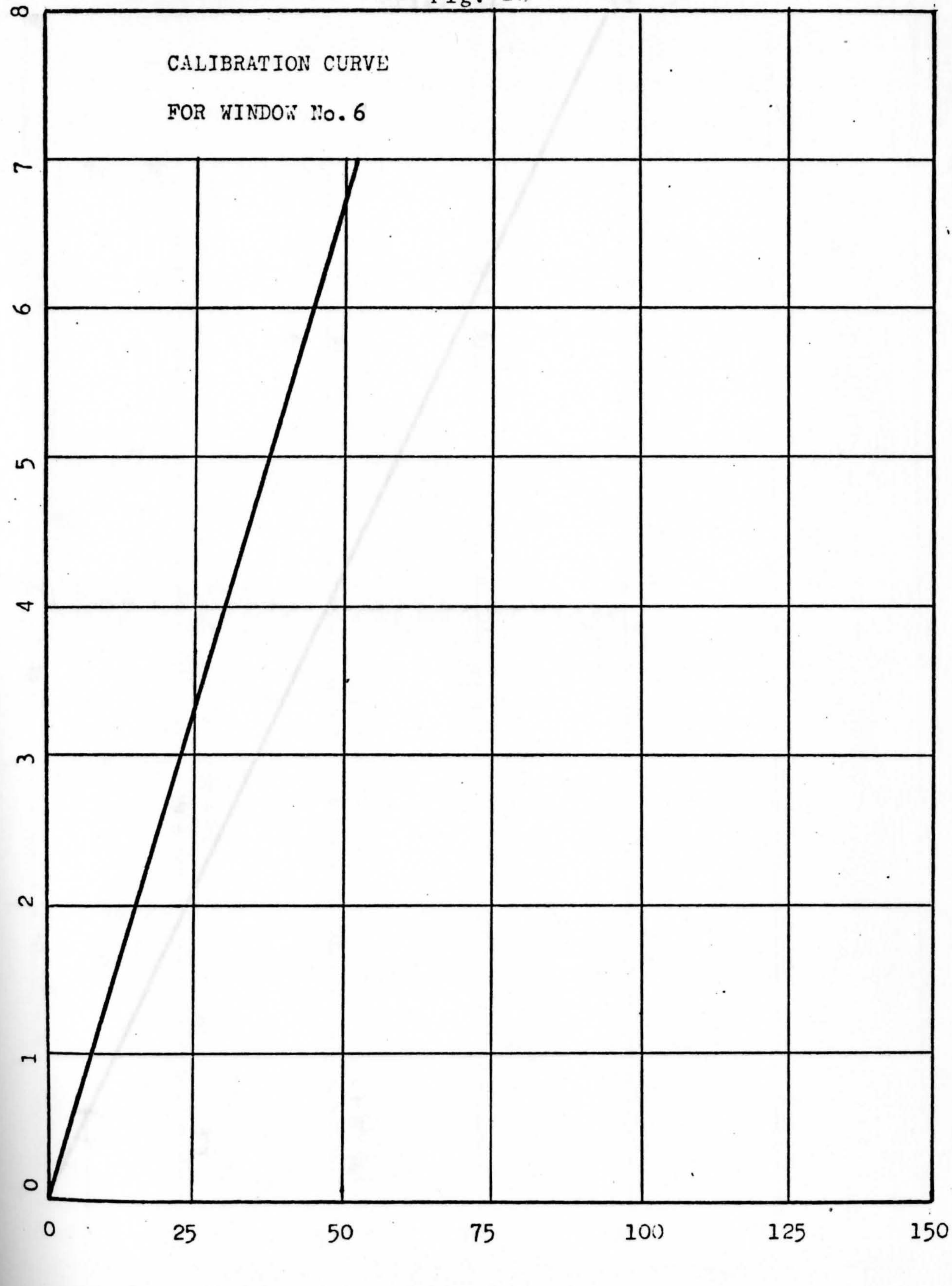
CALIBRATION CURVE
FOR WINDOW No. 6
LOAD - kip
0
1
2
3
4
5
6
7
8
0
25
50
75
100
125
150
AMPLITUDE - mm

Fig. 22

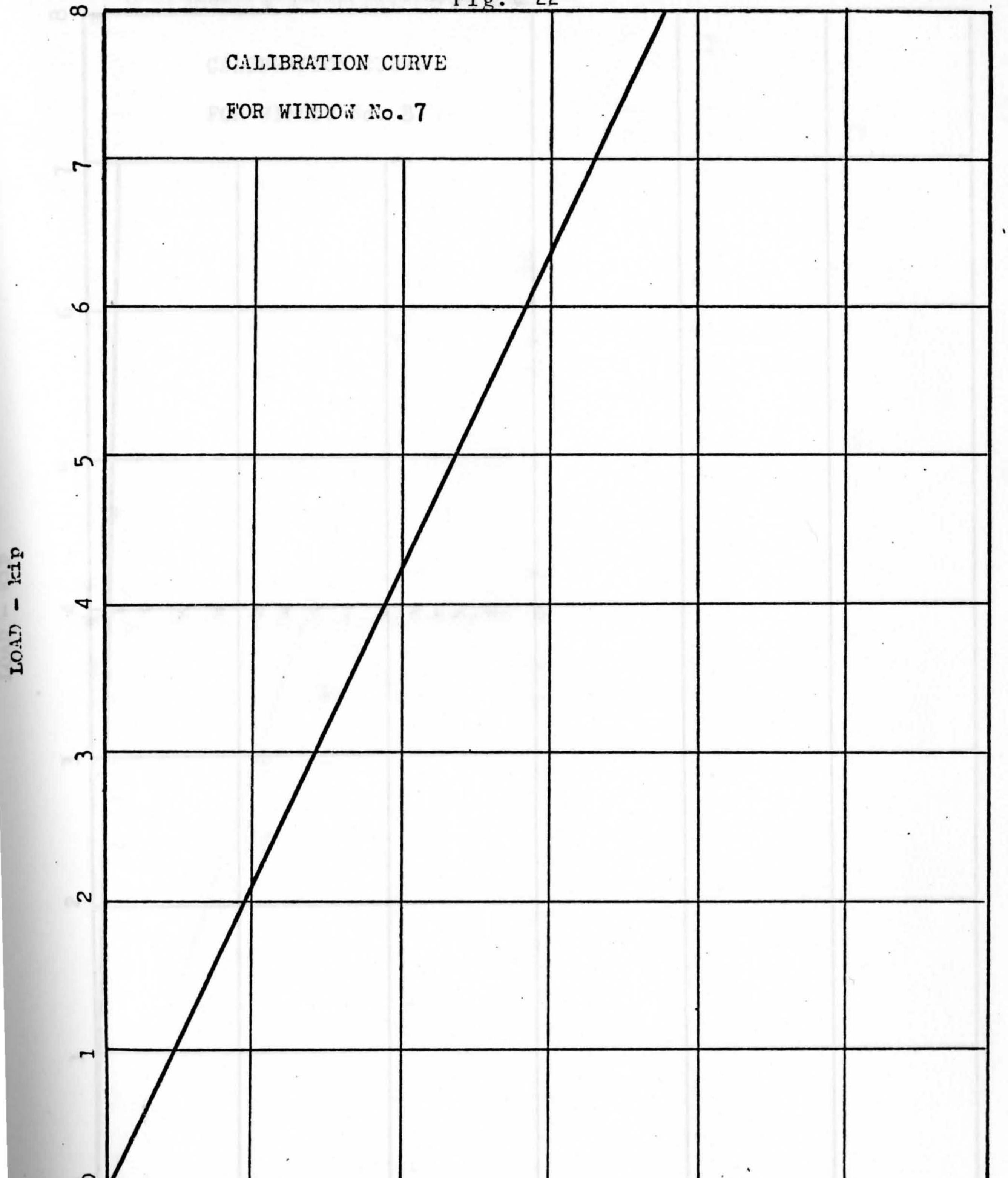
CALIBRATION CURVE
FOR WINDOW No. 7
LOAD - kip
0
1
2
3
4
5
6
7
8
0
25
50
75
100
125
150
AMPLITUDE - mm

Fig. 23

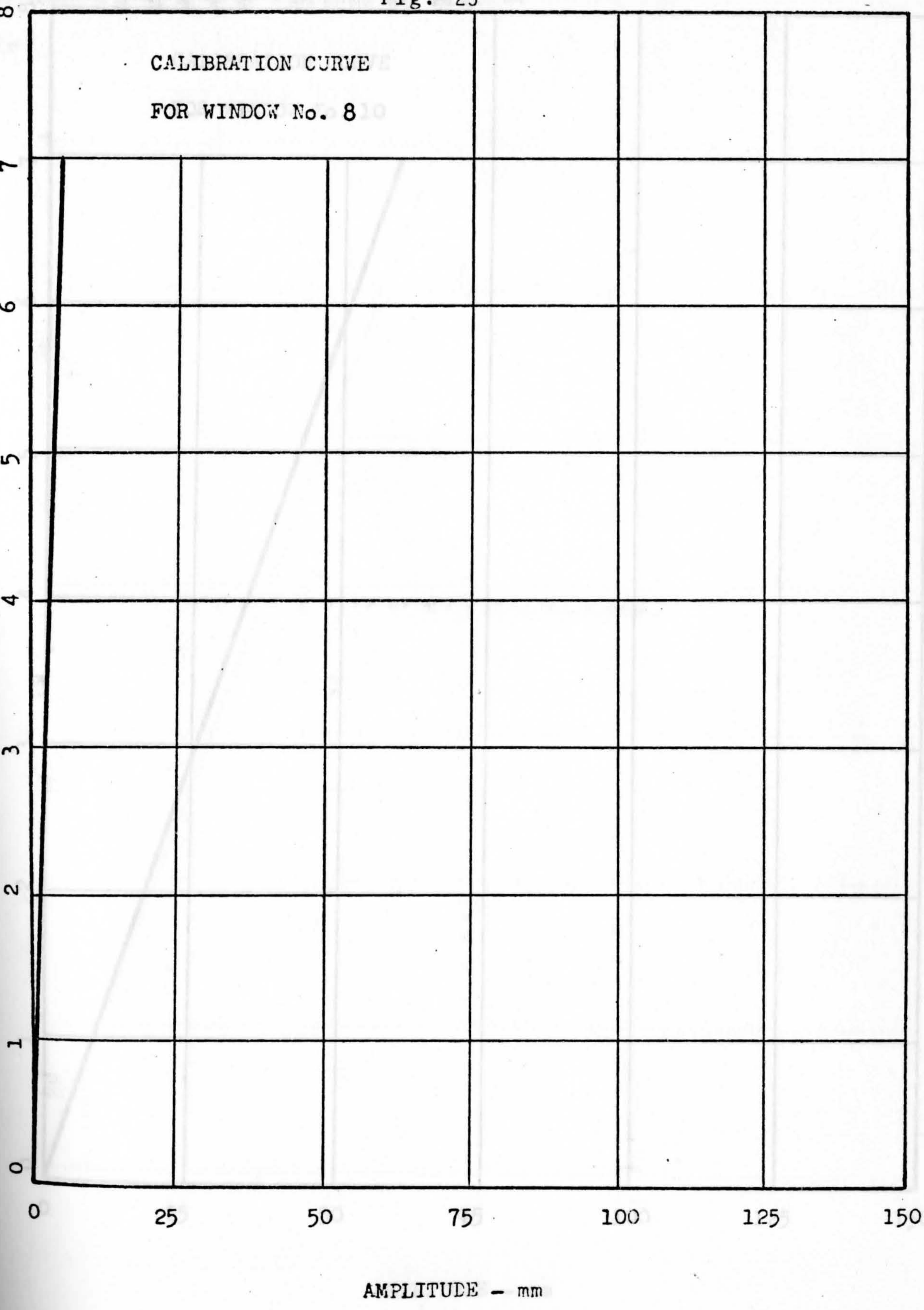
CALIBRATION CURVE
FOR WINDOW No. 8
LOAD - Kip
0
1
2
3
4
5
6
7
8
0
25
50
75
100
125
150
AMPLITUDE - mm

Fig. 24

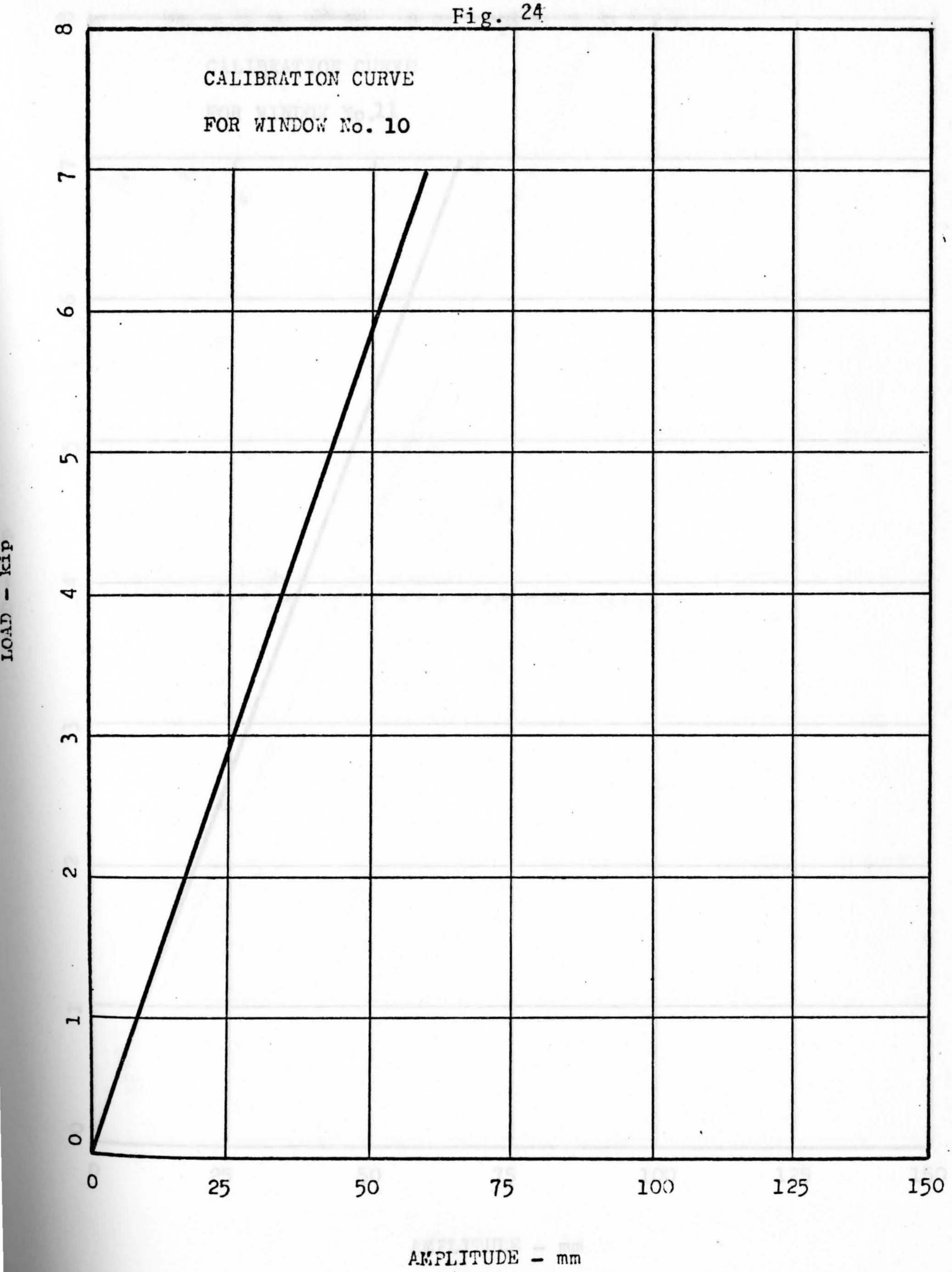
CALIBRATION CURVE
FOR WINDOW No. 10
LOAD - kip
0
1
2
3
4
5
6
7
8
AMPLITUDE - mm
0
25
50
75
100
125
150

Fig. 25

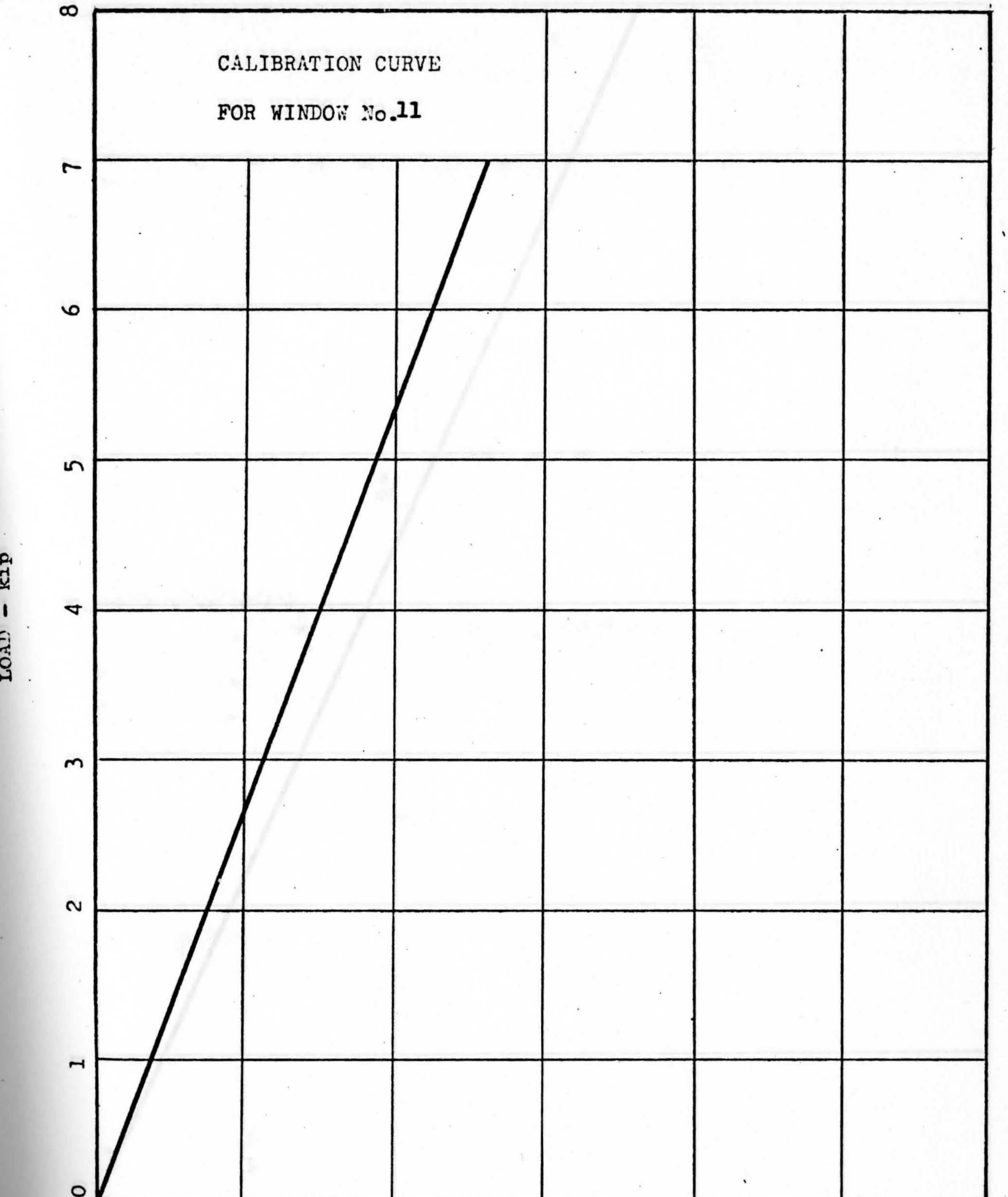
CALIBRATION CURVE
FOR WINDOW No.11
LOAD - kip
0
1
2
3
4
5
6
7
8
0
25
50
75
100
125
150
AMPLITUDE - mm

Fig. 26

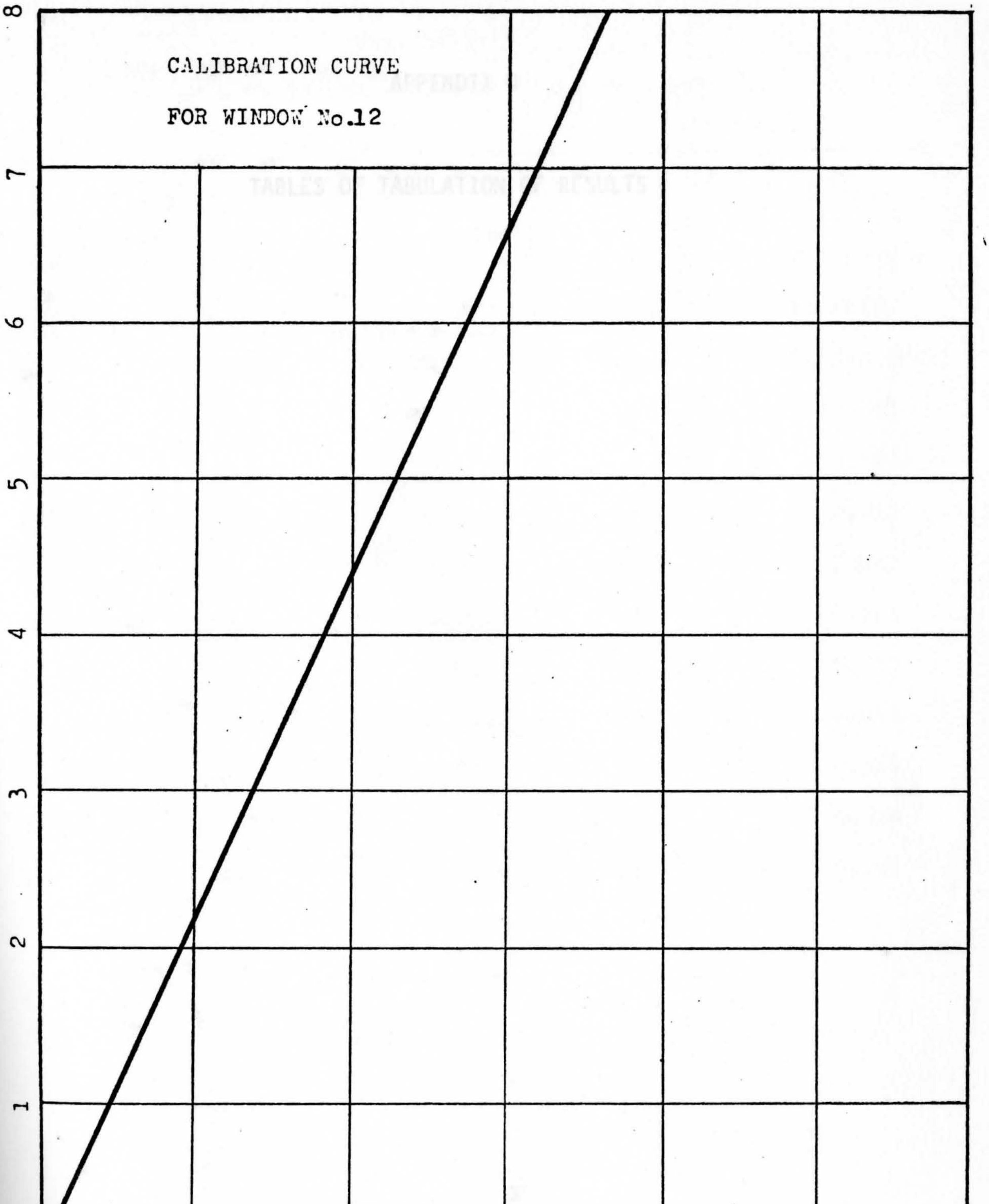
CALIBRATION CURVE
FOR WINDOW No.12
LOAD - kip
0
1
2
3
4
5
6
7
8
0
25
50
75
100
125
150
AMPLITUDE - mm

APPENDIX D

TABLES OF TABULATION OF RESULTS

TABLE 4

9th DROPPING

WT = 65 lb. DROP = 12'-9" ENERGY = 827 ft-#

	at 0.01 sec.		at 0.02 sec.	
WINDOW NO.	DISPLACEMENT (mm.)	RELATING STRESS (ksi)	DISPLACEMENT (mm.)	RELATING STRESS (ksi)
1	0	0	-0.1	-0.038
3	0	0	0.5	0.0234
4	0	0	2.7	0.013
5	4	0.0225	11.5	0.065
6	19	0.1543	-9	-0.073
7	9	0.05	22	0.119
8	7	0.0054	80	0.063
10	89	0.64	76	0.546
11	0	0	3	0.019
12	-1	-0.005	-16	-0.087

TABLE 5

9th DROPING

WT = 65 lb. DROP = 12'-9" ENERGY = 827 ft-#

	at 0.03 sec.		at 0.04 sec.	
WINDOW NO.	DISPLACEMENT (mm.)	RELATING STRESS (ksi)	DISPLACEMENT (mm.)	RELATING STRESS (ksi)
1	0	0	0	0
3	1	0.047	1	0.047
4	3	0.014	2	0.01
5	-35	-0.197	-29	-0.163
6	-13	-0.106	-29	-0.236
7	2	0.012	- 3	-0.018
8	52	0.041	37.5	0.029
10	60	0.431	33.5	0.241
11	0	0	1.5	0.009
12	-14	-0.076	22	-0.1196

TABLE 6

9th DROPPING

WT = 65 lb. DROP = 12'-9" ENERGY = 827 ft-#

	at 0.05 sec.		at 0.06 sec.	
WINDOW NO.	DISPLACEMENT (mm.)	RELATING STRESS (ksi)	DISPLACEMENT (mm.)	RELATING STRESS (ksi)
1	0	0	0	0
3	1	0.047	0	0
4	1.2	0.006	1	0.005
5	-40	-0.225	-40	-0.225
6	-28	-0.228	-27	-0.219
7	-11	-0.06	-21	-0.11
8	-0.2	-0.0015	-31	-0.024
10	-0.1	-0.007	-30.5	-0.219
11	1	0.006	-4	-0.025
12	25	-0.136	-28	-0.152

TABLE 7

9th DROPPING

WT = 65 lb. DROP = 12'-9" ENERGY = 827 ft-#

	at 0.07 sec.		at 0.08 sec.	
WINDOW NO.	DISPLACEMENT (mm.)	RELATING STRESS (ksi)	DISPLACEMENT (mm.)	RELATING STRESS (ksi)
1	0	0	0	0
3	0	0	0	0
4	0	0	0	0
5	-45	-0.253	-45	-0.253
6	-28	-0.228	-27	-0.219
7	-31	-0.1685	-29	0.157
8	-40	-0.031	-37	-0.029
10	-43	-0.309	-36	-0.259
11	-5	-0.031	-4	-0.002
12	-29	-0.158	-28	-0.152

TABLE 8

9th DROPPING

WT = 65 lb. DROP = 12'-9" ENERGY = 827 ft-#

WINDOW NO.	at 0.09 sec. DISPLACEMENT (mm)	at 0.09 sec. RELATING STRESS (ksi)	at 0.1 sec. DISPLACEMENT (mm)	at 0.1 sec. RELATING STRESS (ksi)
1	0	0	0	0
3	0	0	0.5	0.023
4	0	0	0.5	0.002
5	-43	-0.242	-42	-0.236
6	-27	-0.219	-27	-0.219
7	-26	-0.14	-23	-0.12
8	-37	-0.029	-35	-0.027
10	-34	-0.244	-32	-0.23
11	-8.5	-0.053	-6	-0.037
12	-25	-0.136	-24	-0.131

TABLE 9

9th DROPPING

WT = 65 lb. DROP = 12'-9" ENERGY = 827 ft-#

	at 0.11 sec.		at 0.12 sec.	
WINDOW NO.	DISPLACEMENT (mm)	RELATING STRESS (ksi)	DISPLACEMENT (mm)	RELATING STRESS (ksi)
1	0	0	0	0
3	0.5	0.023	0.5	0.023
4	0.5	0.002	0.5	0.002
5	-42	-0.236	-42	-0.236
6	-26	-0.211	-26	-0.211
7	-22.5	-0.14	-22	-0.141
8	-33	-0.026	-30	-0.023
10	-26	-0.187	-25	-0.180
11	-2	-0.012	-1	-0.006
12	-23	-0.125	-23	-0.125

TABLE 10

9th and 10th DROPPING

WT = 65 lb. DROP = 12'-9" ENERGY = 827 ft-#

	9th DROPPING at 0.016 sec.		10th DROPPING at 0.017 sec.	
WINDOW NO.	DISPLACEMENT (mm)	RELATING STRESS (ksi)	DISPLACEMENT (mm)	RELATING STRESS (ksi)
1	0	0	0	0
3	0.5	0.023	0	0
4	2	0.01	3.2	0.016
5	42	0.236	49	0.276
6	28	0.22	79	0.642
7	33	0.172	56.5	0.301
8	77	0.058	101	0.789
10	95	0.712	118	0.848
11	6	0.044	- 2.5	-0.016
12	-16	-0.088	-2.5	-0.014

TABLE 11

10th DROPPING

WT = 65 lb. DROP = 12'-9" ENERGY = 827 ft-#

	at 0.01 sec.		at 0.02 sec.	
WINDOW NO.	DISPLACEMENT (mm)	RELATING STRESS (ksi)	DISPLACEMENT (mm)	RELATING STRESS (ksi)
1	0	0	0	0
3	0	0	0	0
4	0.5	0.002	2	0.009
5	3	0.017	53	0.298
6	4	0.033	41	0.333
7	6.5	0.057	45.5	0.241
8	16	0.125	72	0.563
10	120	0.863	120	0.863
11	-5.5	-0.034	-3	-0.019
12	16	0.087	-6	-0.033

TABLE 12

10th DROPPING

WT = 65 lb. DROP = 12'-9" ENERGY = 827 ft-#

	at 0.03 sec.		at 0.04 sec.	
WINDOW NO.	DISPLACEMENT (mm)	RELATING STRESS (ksi)	DISPLACEMENT (mm)	RELATING STRESS (ksi)
1	0	0	0	0
3	0	0	0	0
4	4.5	0.021	1	0.004
5	-6	-0.034	4	0.023
6	-6.5	-0.053	-24	-0.195
7	3.5	0.002	2.5	0.014
8	59	0.461	1	0.008
10	86	0.618	53	0.381
11	-3	-0.019	-1	-0.006
12	-3.5	-0.019	-14	-0.076

TABLE 13

10th DROPPING

WT = 65 lb. DROP = 12'-9" ENERGY = 827ft-#

	at 0.05 sec.		at 0.06 sec.	
WINDOW NO.	DISPLACEMENT (mm)	RELATING STRESS (ksi)	DISPLACEMENT (mm)	RELATING STRESS (ksi)
1	0	0	0	0
3	1	0.04	1	0.04
4	-1	-0.004	-2	-0.009
5	-14	-0.079	-21	-0.118
6	-26.5	-0.215	-35	-0.284
7	-1.5	-0.009	-9.5	-0.053
8	-39	-0.305	-62.5	-0.488
10	-6	-0.043	-37	-0.266
11	0.5	0.003	-0.5	-0.003
12	-17.5	-0.095	-21	-0.114

TABLE 14

10th DROPPING

WT = 65 lb. DROP= 12'-9" ENERGY = 827 ft-#

	at 0.07 sec.		at 0.08 sec.	
WINDOW NO.	DISPLACEMENT (mm)	RELATING STRESS (ksi)	DISPLACEMENT (mm)	RELATING STRESS (ksi)
1	0	0	0	0
3	0	0	0	0
4	-3.5	-0.016	-3	-0.014
5	-32	-0.18	-29.5	-0.166
6	-39	-0.317	-35.5	-0.288
7	-28	-0.15	-27	-0.144
8	-75.5	-0.590	-71.5	-0.559
10	-53.5	-0.385	-52	-0.374
11	-4.5	-0.028	-3	-0.019
12	-13.5	-0.073	-11	-0.06

TABLE 15

11th DROPPING

WT = 65 lb. DROP = 12'-9" ENERGY = 827 ft-#

WINDOW NO.	at 0.01 sec. DISPLACEMENT (mm)	at 0.01 sec. RELATING STRESS (ksi)	at 0.02 sec. DISPLACEMENT (mm)	at 0.02 sec. RELATING STRESS (ksi)
1	0	0	0	0
3	0	0	0	0
4	2.5	0.012	0.5	0.002
5	21	0.118	34	0.191
6	21	0.171	12.5	0.102
7	34	0.184	40	0.214
8	51	0.04	61	0.048
10	38	0.273	40	0.288
11	5.5	0.0344	-0.5	-0.003
12	5	0.027	-3	-0.016

TABLE 16

11th DROPPING

WT = 65 lb. DROP = 12'-9" ENERGY = 827 ft-#

WINDOW NO.	at 0.03 sec. DISPLACEMENT (mm)	at 0.03 sec. RELATING STRESS (ksi)	at 0.04 sec. DISPLACEMENT (mm)	at 0.04 sec. RELATING STRESS (ksi)
1	0	0	0	0
3	0	0	0	0
4	2.5	0.012	2	0.009
5	24	0.135	14	0.079
6	14	0.114	2.5	0.02
7	27	0.144	17	0.094
8	55	0.043	8.5	0.007
10	14	0.101	-17	-0.122
11	1	0.006	-4	-0.025
12	-6	-0.033	-7	-0.038

TABLE 17

11th DROPPING

WT = 65 lb. DROP = 12'-9" ENERGY = 827 ft-#

	at 0.05 sec.		at 0.06 sec.	
WINDOW NO.	DISPLACEMENT (mm)	RELATING STRESS (ksi)	DISPLACEMENT (mm)	RELATING STRESS (ksi)
1	0	0	0	0
3	0	0	0	0
4	0	0	0.5	0.002
5	-1	-0.006	-7	-0.039
6	-23	-0.187	-33	-0.268
7	6.5	-0.034	3.5	0.002
8	-7	-0.006	-13	-0.01
10	-17	-0.122	-22	-0.158
11	-6	-0.038	-5	-0.031
12	-4	-0.022	-1	-0.005

TABLE 18

11th DROPPING

WT = 65 lb. DROP = 12'-9" ENERGY = 827 ft-#

	at 0.07 sec.		at 0.08 sec.	
WINDOW NO.	DISPLACEMENT (mm)	RELATING STRESS (ksi)	DISPLACEMENT (mm)	RELATING STRESS (ksi)
1	0	0	0	0
3	0	0	0	0
4	0	0	0	0
5	-4	-0.023	-1.5	-0.008
6	-29	-0.236	-24	-0.195
7	6.5	0.034	7.5	0.041
8	-12.5	-0.01	-8	-0.006
10	-22	-0.158	-15.5	-0.111
11	-3	-0.019	-1	-0.006
12	0	0	1	0.005

TABLE 19

11th DROPPING

WT = 65 lb. DROP = 12'-9" ENERGY = 827 ft-#

at 0.016 sec.

WINDOW NO.	DISPLACEMENT (mm)	RELATING STRESS (ksi)
1	0	0
3	0	0
4	3.2	0.016
5	31.5	0.185
6	24	0.2
7	59.5	0.31
8	89	0.522
10	86.5	0.623
11	2.5	0.016
12	1	0.005

TABLE 20

12th DROPPING

WT = 32.5 lb. DROP = 12'-9" ENERGY = 414 ft-#

	at 0.01 sec.		at 0.02 sec.	
WINDOW NO.	DISPLACEMENT (mm)	RELATING STRESS (ksi)	DISPLACEMENT (mm)	RELATING STRESS (ksi)
1	0	0	0	0
3	0	0	0	0
4	0.5	0.002	0.5	0.002
5	1.5	0.008	14	0.079
6	8.5	0.069	4.5	0.037
7	15	0.094	29.5	0.16
8	20.5	0.016	48	0.038
10	26	0.187	57	0.41
11	8.5	0.053	18	0.113
12	2	0.011	6.5	0.035

TABLE 21

12th DROPPING

WT = 32.5 lb. DROP = 128-9" ENERGY = 414 ft-#

	at 0.03 sec.		at 0.04 sec.	
WINDOW NO.	DISPLACEMENT (mm)	RELATING STRESS (ksi)	DISPLACEMENT (mm)	RELATING STRESS (ksi)
1	0	0	0	0
3	0	0	0	0
4	1.5	0.007	0	0
5	15	0.084	9.5	0.053
6	8	0.065	0	0
7	24	0.131	16	0.087
8	5.5	0.004	7.5	0.006
10	25	0.18	-3	-0.022
11	11.5	0.072	4	0.025
12	0.5	0.003	-6	-0.033

TABLE 22

12th DROPPING

WT = 32.5 lb. DROP = 12'-9" ENERGY = 414 ft-#

WINDOW NO.	at 0.05 sec.		at 0.06 sec.	
	DISPLACEMENT (mm)	RELATING STRESS (ksi)	DISPLACEMENT (mm)	RELATING STRESS (ksi)
1	0	0	0	0
3	0	0	0	0
4	0	0	0	0
5	6.5	0.037	6.5	0.037
6	-2	-0.016	-2.5	-0.02
7	-9.5	-0.053	10	0.056
8	-13.5	-0.011	-12	-0.009
10	-22	-0.158	-29.5	-0.212
11	-3	-0.019	-4	-0.025
12	-8	-0.044	-8	-0.044

TABLE 23

12th DROPPING

WT = 32.5 lb. DROP = 12'-9" ENERGY = 414 ft-#

	at 0.07 sec.		at 0.08 sec.	
WINDOW NO.	DISPLACEMENT (mm)	RELATING STRESS (ksi)	DISPLACEMENT (mm)	RELATING STRESS (ksi)
1	0	0	0	0
3	0	0	0	0
4	0	0	0	0
5	5.5	0.031	5.5	0.031
6	-3.5	-0.028	-4	-0.033
7	9	0.05	9.5	0.053
8	-13	-0.01	-15	-0.013
10	-23.5	-0.1689	-22	-0.158
11	-4	-0.025	-2.5	-0.016
12	-5	-0.027	-2.5	-0.014

TABLE 24

12th DROPPING

WT = 32.5 lb. DROP = 12'-9" ENERGY = 414 ft-#

	at 0.09 sec.		at 0.018 sec.	
WINDOW NO.	DISPLACEMENT (mm)	RELATING STRESS (ksi)	DISPLACEMENT (mm)	RELATING STRESS (ksi)
1	0	0	0	0
3	0	0	0	0
4	0	0	1	0.005
5	7.5	0.042	17	0.096
6	-3.5	-0.028	12.5	0.102
7	11.5	0.063	28	0.15
8	-13	-0.01	51	0.04
10	-21	-0.151	63	0.453
11	0	0	15	0.094
12	-2	-0.011	7	0.038

APPENDIX E

CHARTS OF EXPERIMENTAL RESULTS

Fig. 27

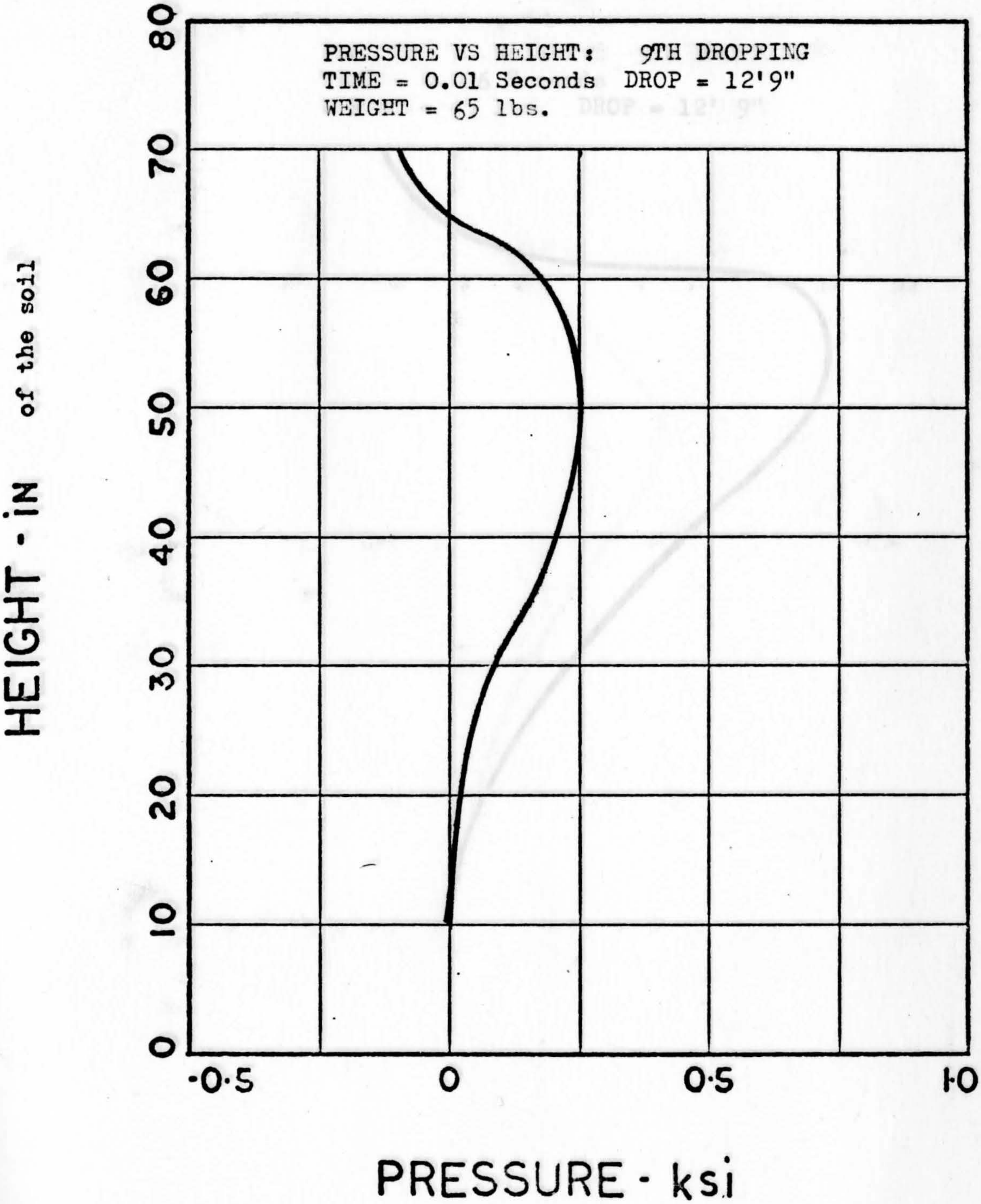
PRESSURE VS HEIGHT: 9TH DROPPING
TIME = 0.01 Seconds DROP = 12'9"
WEIGHT = 65 lbs.
HEIGHT - iN of the soil
80
70
60
50
40
30
20
10
0
-0·5
0
0·5
1·0
PRESSURE - ksi

Fig. 28

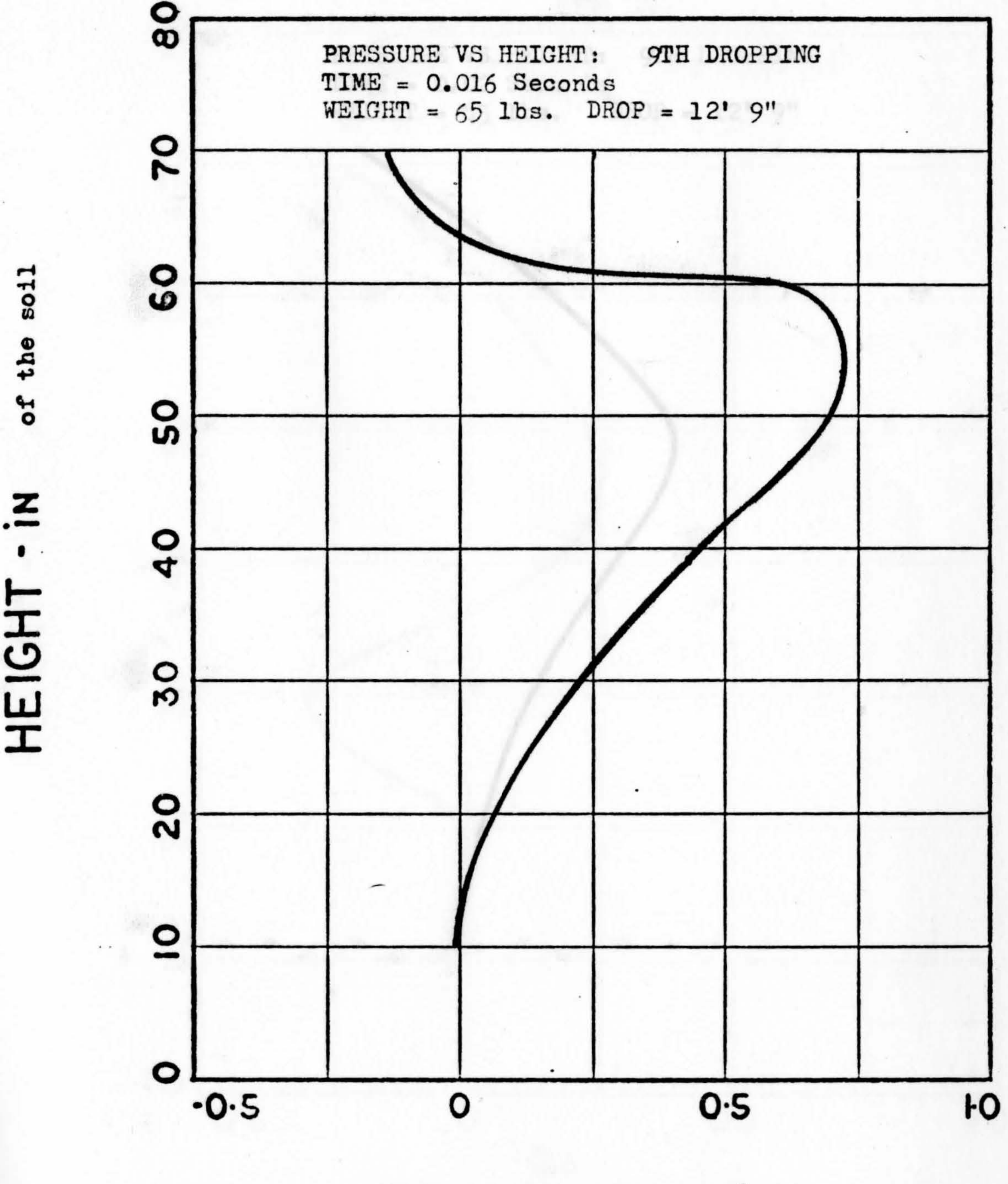
PRESSURE VS HEIGHT: 9TH DROPPING
TIME = 0.016 Seconds
WEIGHT = 65 lbs. DROP = 12' 9"
HEIGHT - iN of the soil
80
70
60
50
40
30
20
10
0
-0·5
0
0·5
1·0
PRESSURE - ksi

Fig. 29

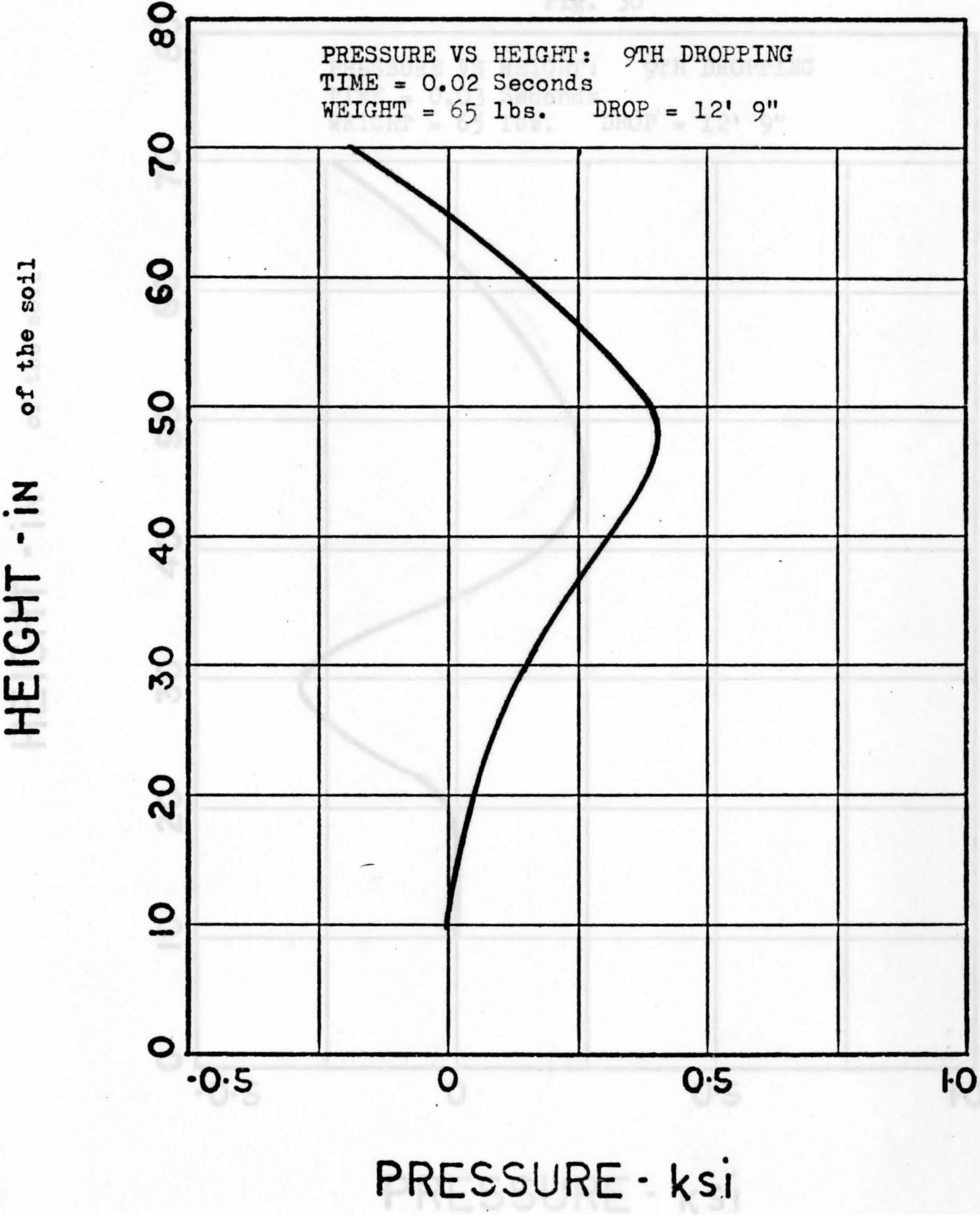
PRESSURE VS HEIGHT: 9TH DROPPING
TIME = 0.02 Seconds
WEIGHT = 65 lbs. DROP = 12' 9"
HEIGHT - iN of the soil
80
70
60
50
40
30
20
10
0
-0·5
0
0·5
1·0
PRESSURE - ksi

Fig. 30

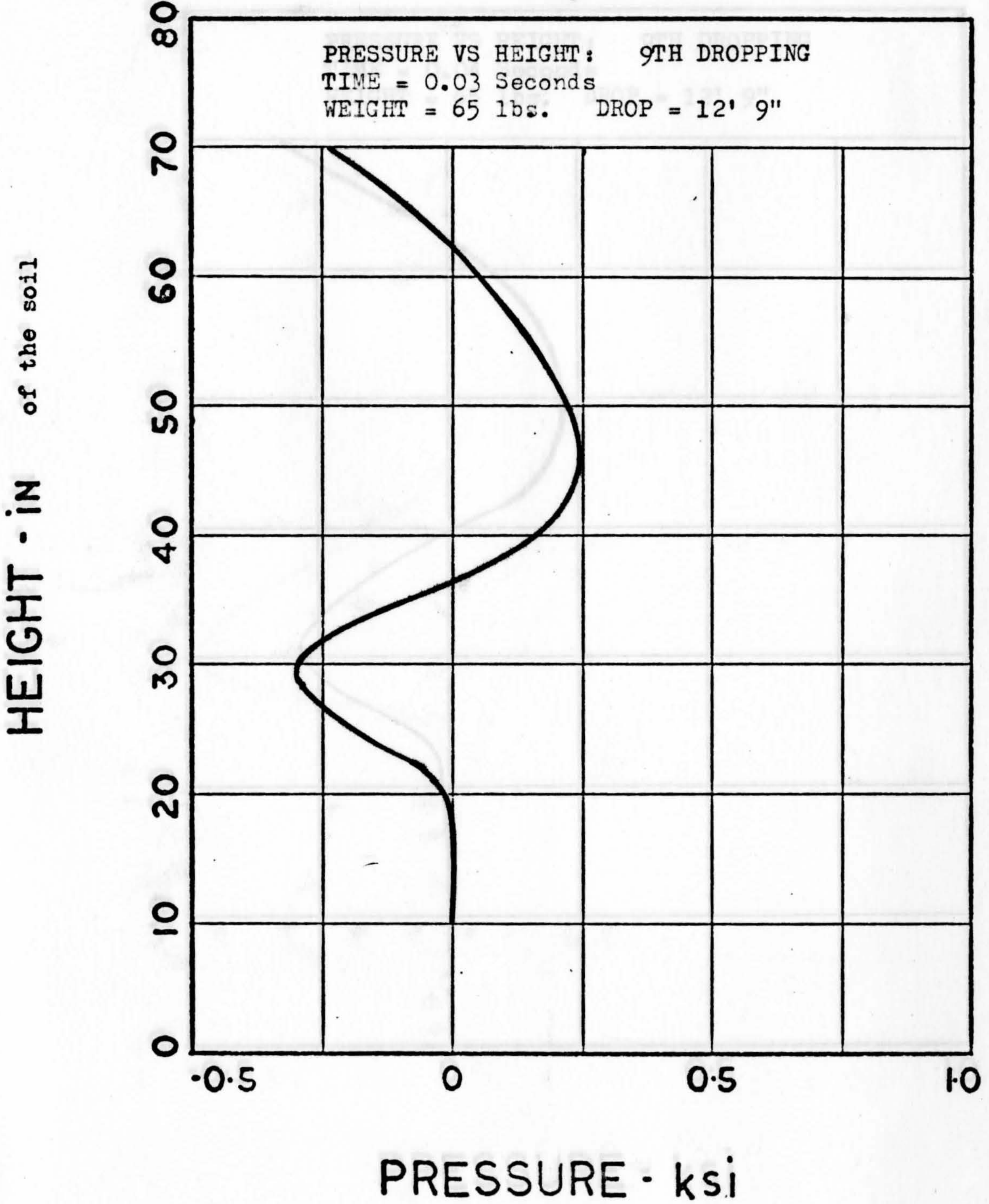
PRESSURE VS HEIGHT: 9TH DROPPING
TIME = 0.03 Seconds
WEIGHT = 65 lbs. DROP = 12' 9"
HEIGHT - iN of the soil
PRESSURE - ksi
0
10
20
30
40
50
60
70
80
-0·5
0
0·5
1·0

Fig. 31

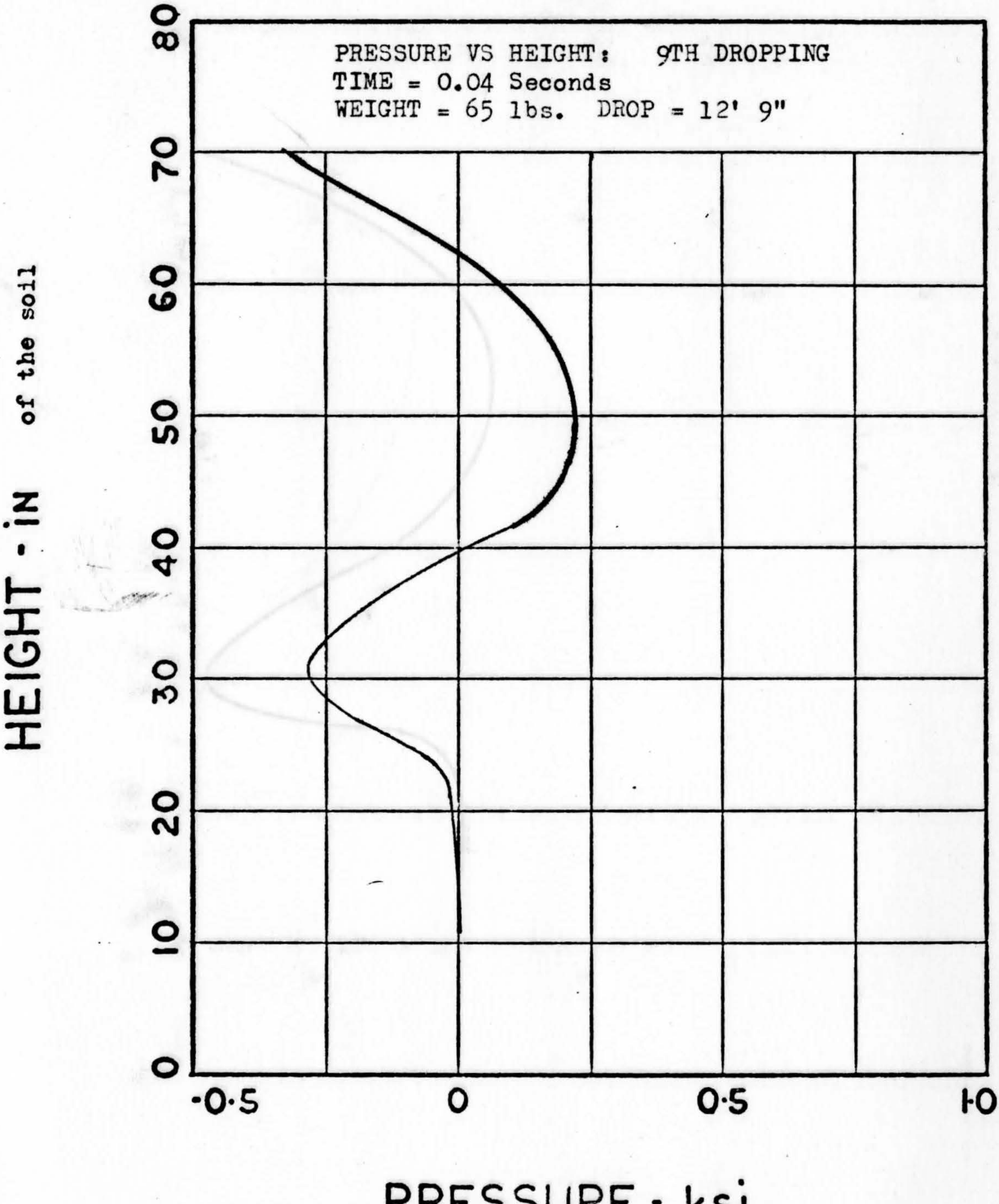
PRESSURE VS HEIGHT: 9TH DROPPING
TIME = 0.04 Seconds
WEIGHT = 65 lbs. DROP = 12' 9"
HEIGHT - iN of the soil
PRESSURE - ksi
80
70
60
50
40
30
20
10
0
-0·5
0
0·5
1·0

Fig. 32

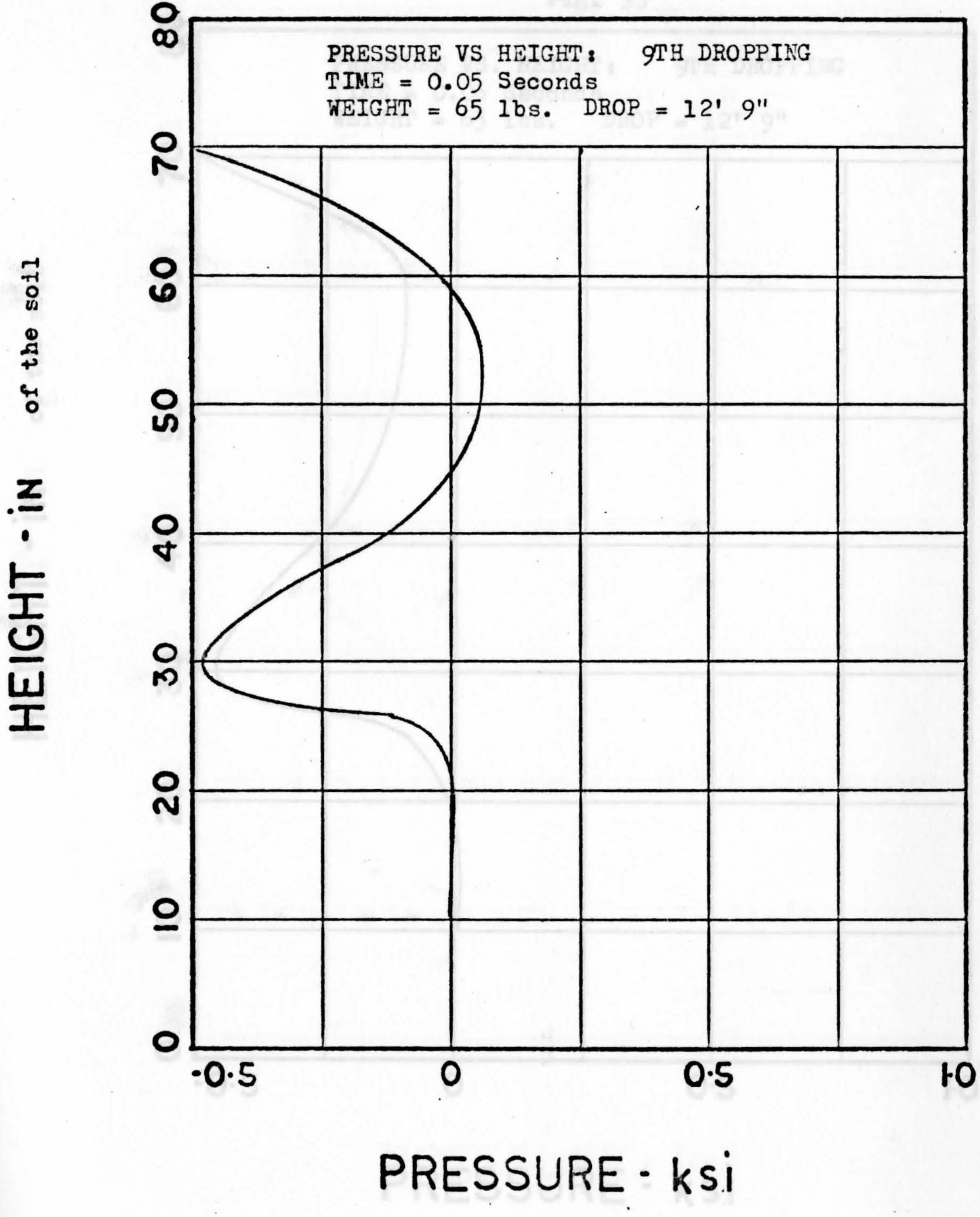
PRESSURE VS HEIGHT: 9TH DROPPING
TIME = 0.05 Seconds
WEIGHT = 65 lbs. DROP = 12' 9"
HEIGHT - iN of the soil
80
70
60
50
40
30
20
10
0
-0·5
0
0·5
1·0
PRESSURE - ksi

Fig. 33

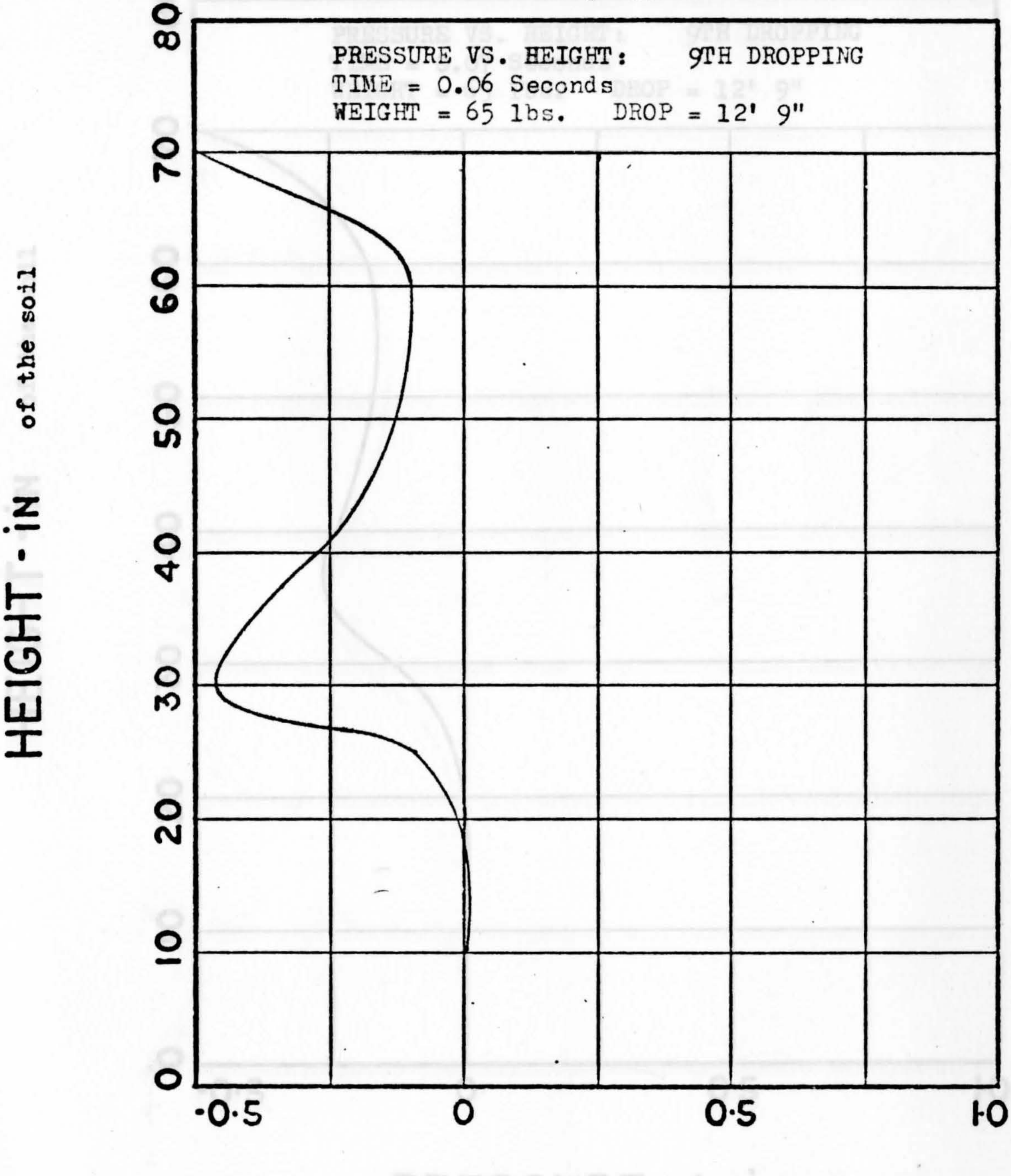

PRESSURE VS. HEIGHT: 9TH DROPPING
TIME = 0.06 Seconds
WEIGHT = 65 lbs. DROP = 12' 9"

Fig. 34

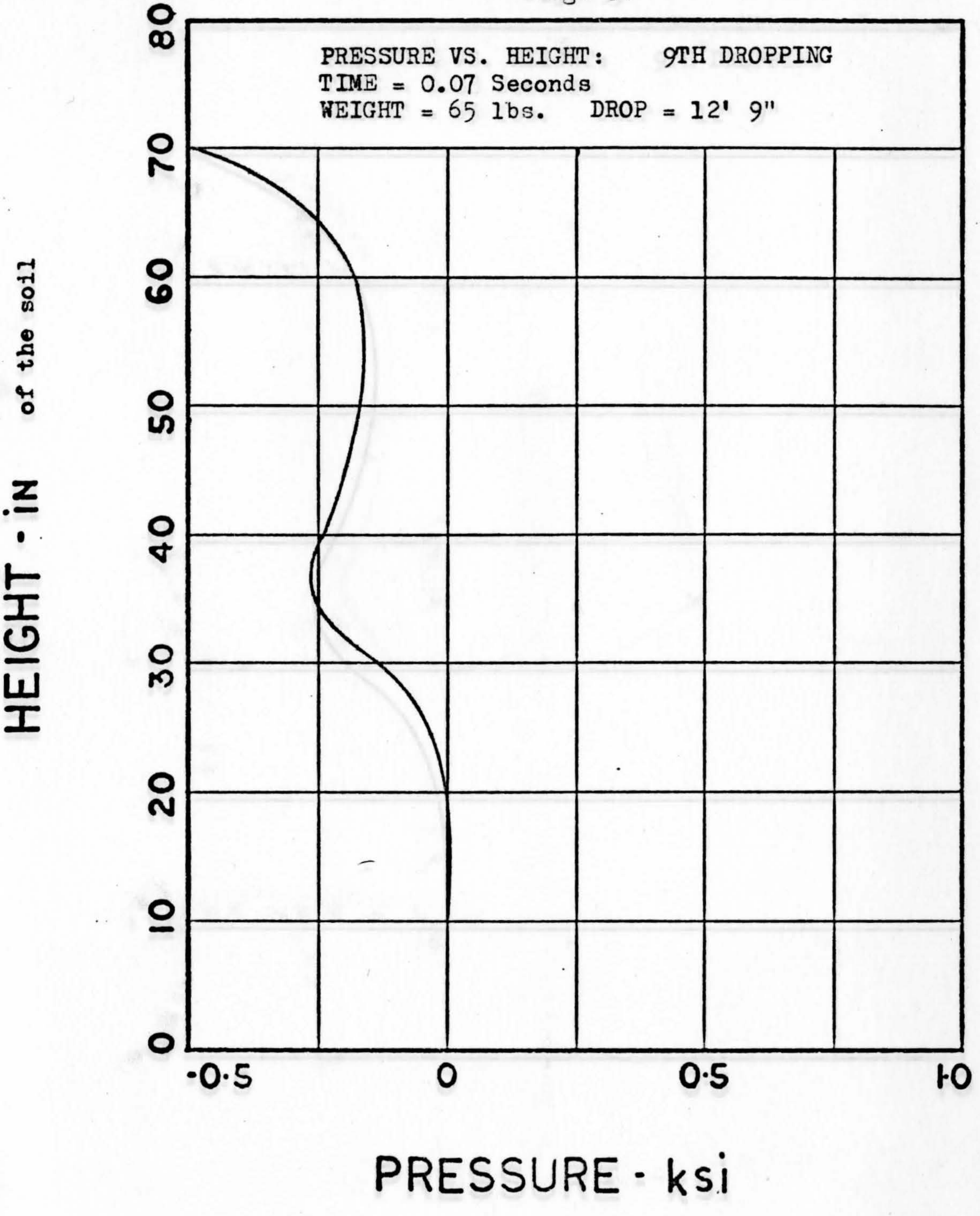
PRESSURE VS. HEIGHT: 9TH DROPPING
TIME = 0.07 Seconds
WEIGHT = 65 lbs. DROP = 12' 9"
HEIGHT - IN of the soil
0
10
20
30
40
50
60
70
80
-0·5
0
0·5
1·0
PRESSURE - ksi

Fig. 35

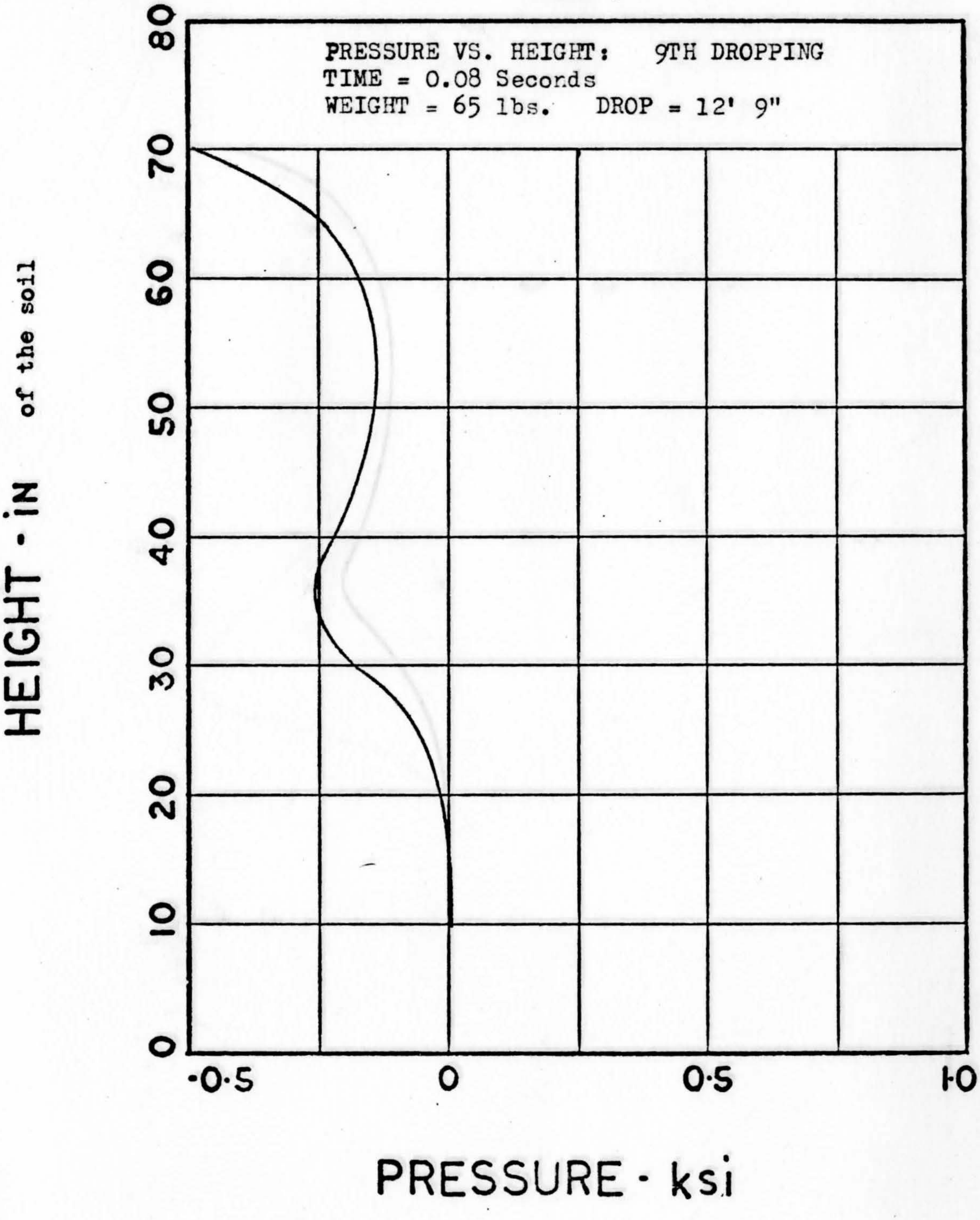
PRESSURE VS. HEIGHT: 9TH DROPPING
TIME = 0.08 Seconds
WEIGHT = 65 lbs. DROP = 12' 9"
HEIGHT - IN of the soil
0
10
20
30
40
50
60
70
80
-0·5
0
0·5
1·0
PRESSURE - ksi

Fig. 36

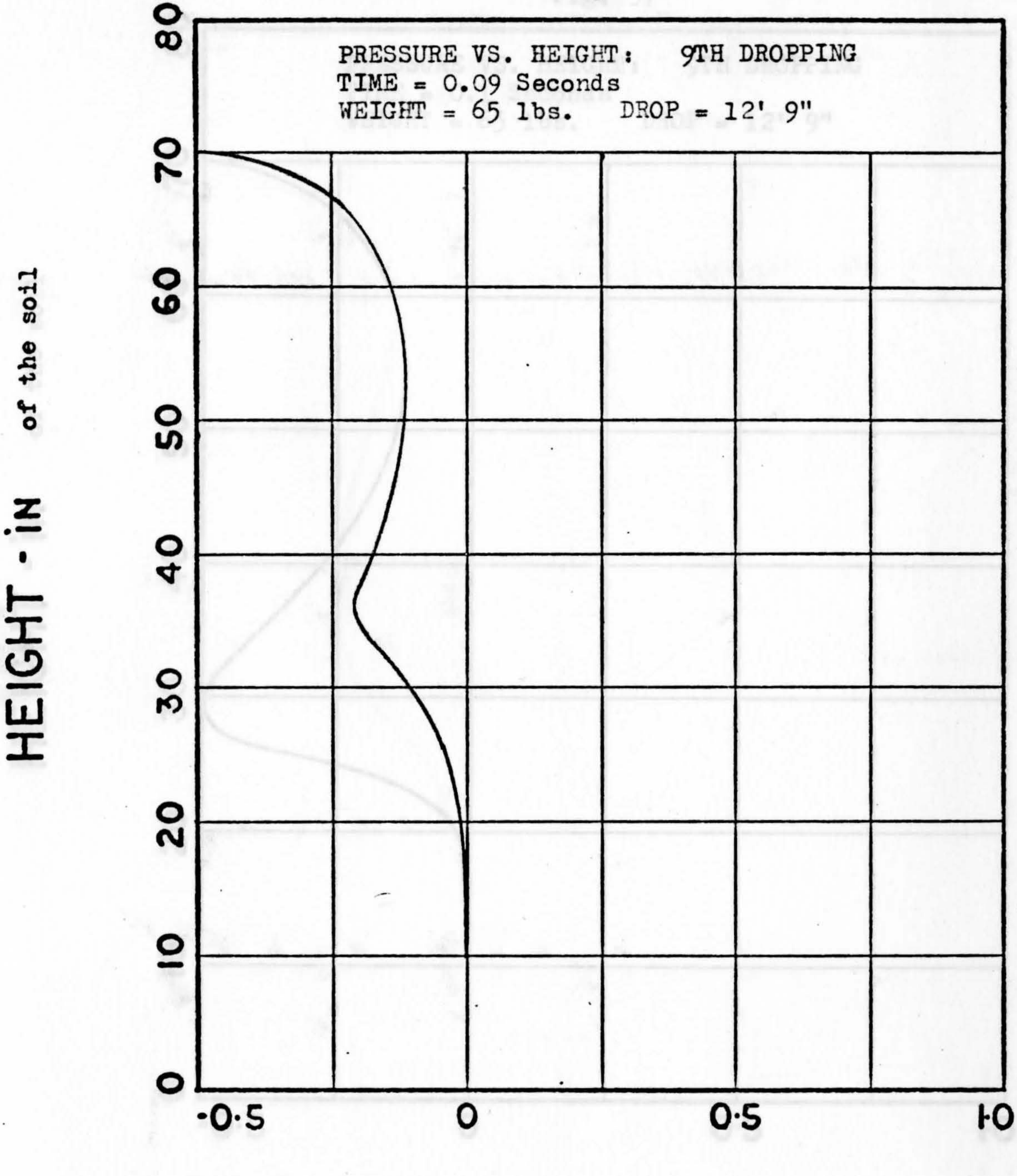
PRESSURE VS. HEIGHT: 9TH DROPPING
TIME = 0.09 Seconds
WEIGHT = 65 lbs. DROP = 12' 9"
HEIGHT - IN of the soil
PRESSURE - ksi
0
10
20
30
40
50
60
70
80
-0·5
0
0·5
1·0

Fig. 37

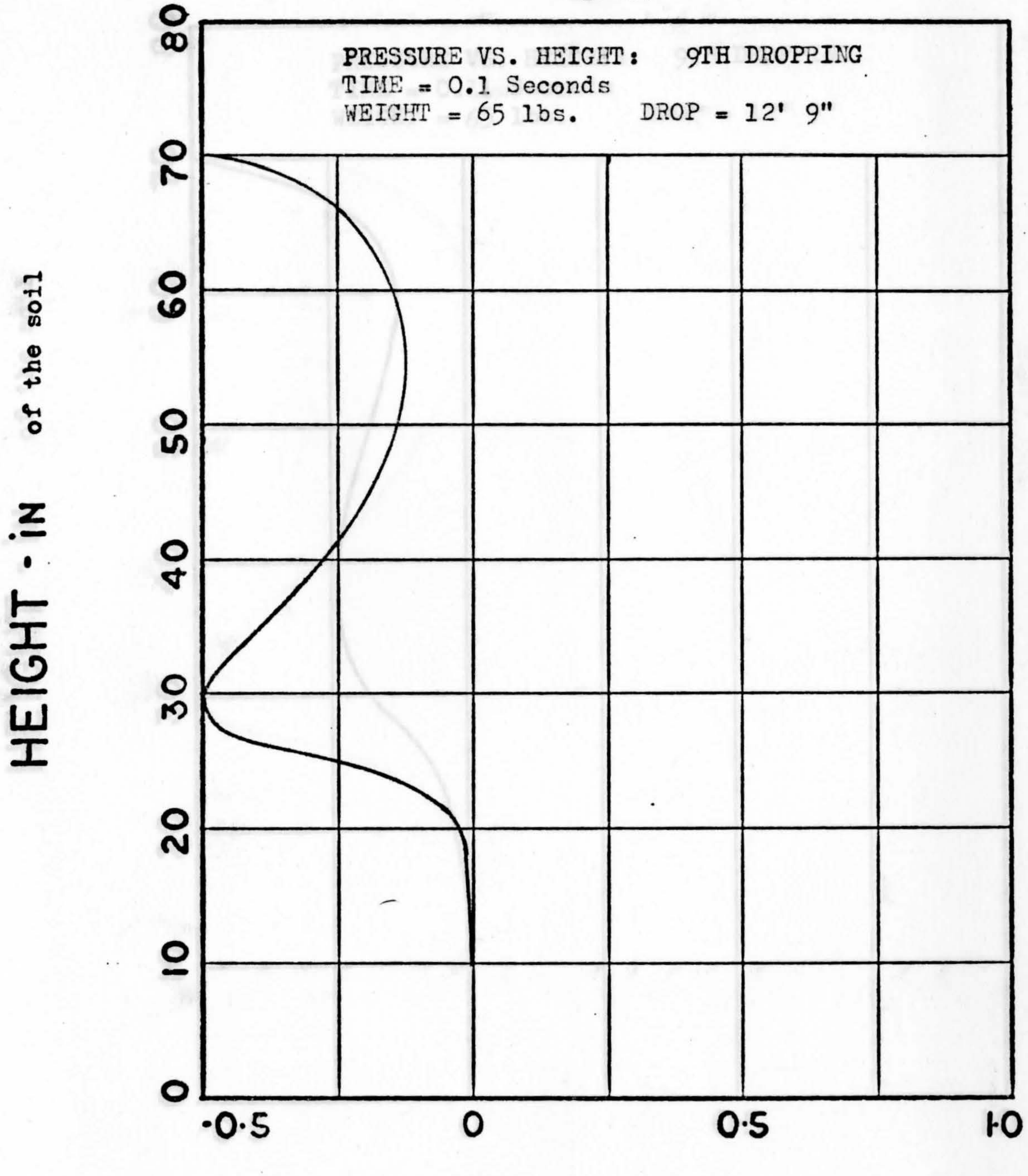
PRESSURE VS. HEIGHT: 9TH DROPPING
TIME = 0.1 Seconds
WEIGHT = 65 lbs. DROP = 12' 9"
HEIGHT - IN of the soil
0
10
20
30
40
50
60
70
80
-0·5
0
0·5
1·0
PRESSURE - ksi

Fig. 38

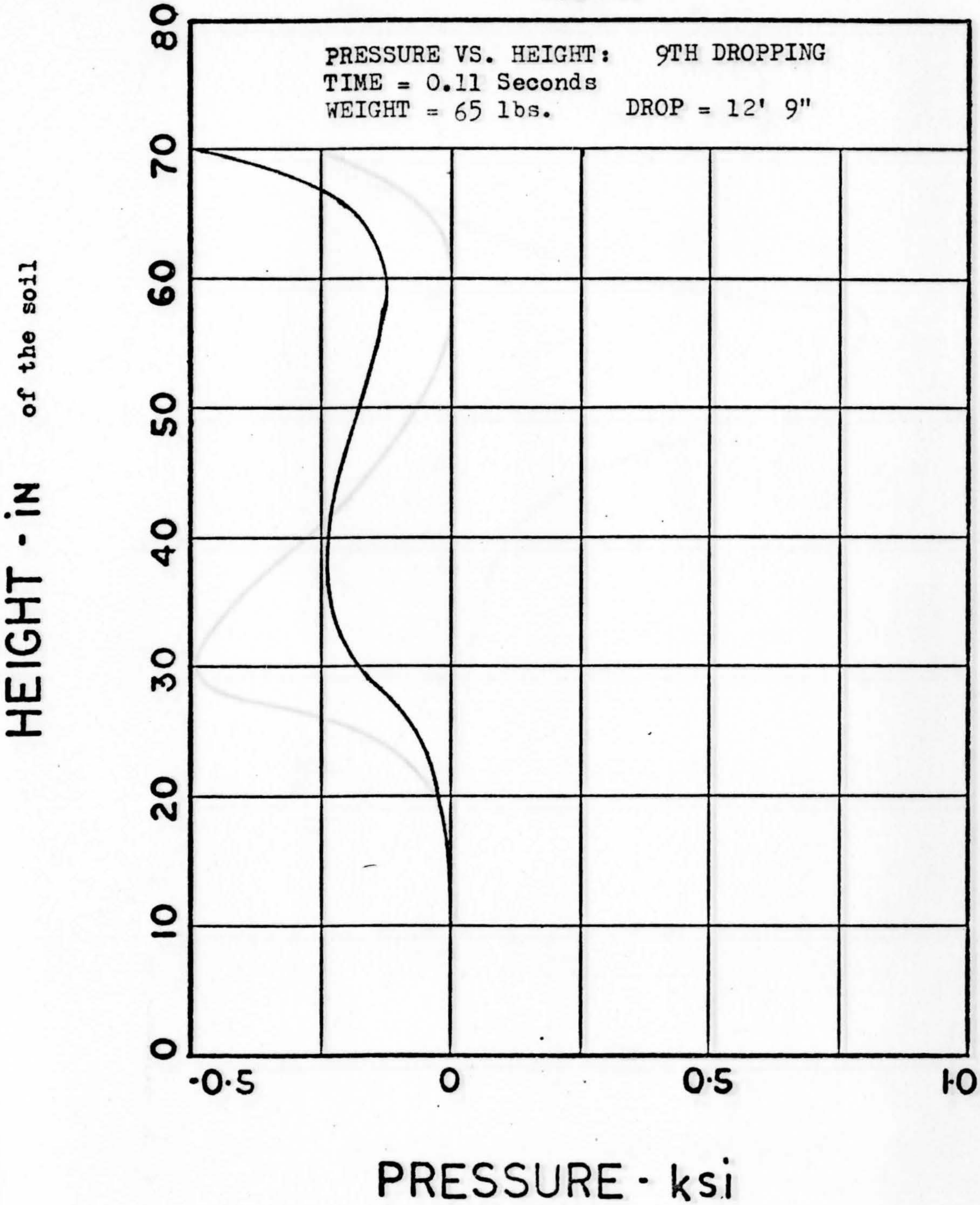
PRESSURE VS. HEIGHT: 9TH DROPPING
TIME = 0.11 Seconds
WEIGHT = 65 lbs. DROP = 12' 9"
HEIGHT - in of the soil
0
10
20
30
40
50
60
70
80
-0·5
0
0·5
1·0
PRESSURE - ksi

Fig. 39

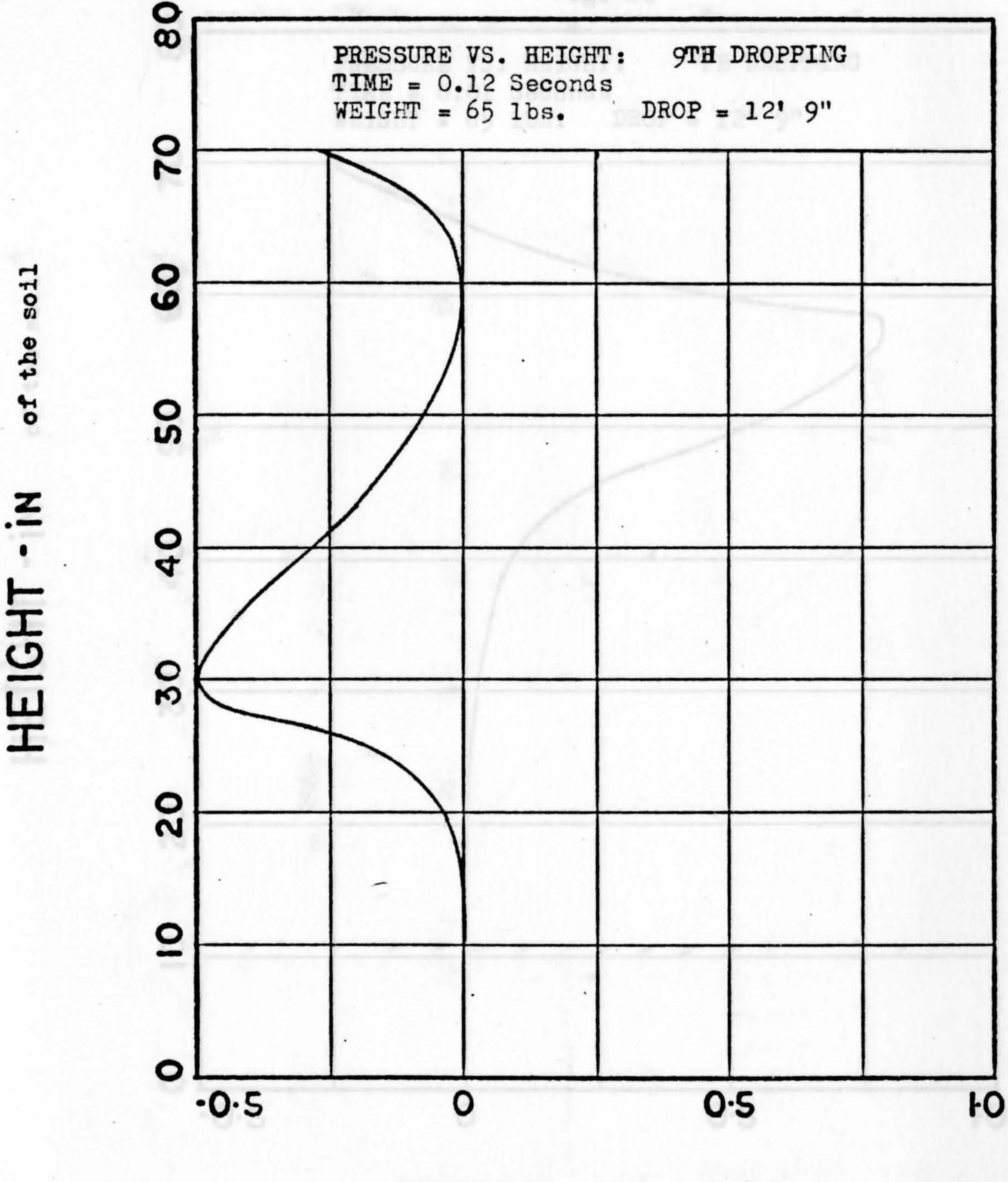
PRESSURE VS. HEIGHT: 9TH DROPPING
TIME = 0.12 Seconds
WEIGHT = 65 lbs. DROP = 12' 9"
HEIGHT - IN of the soil
80
70
60
50
40
30
20
10
0
-0.5
0
0.5
1.0
PRESSURE - ksi

Fig. 40

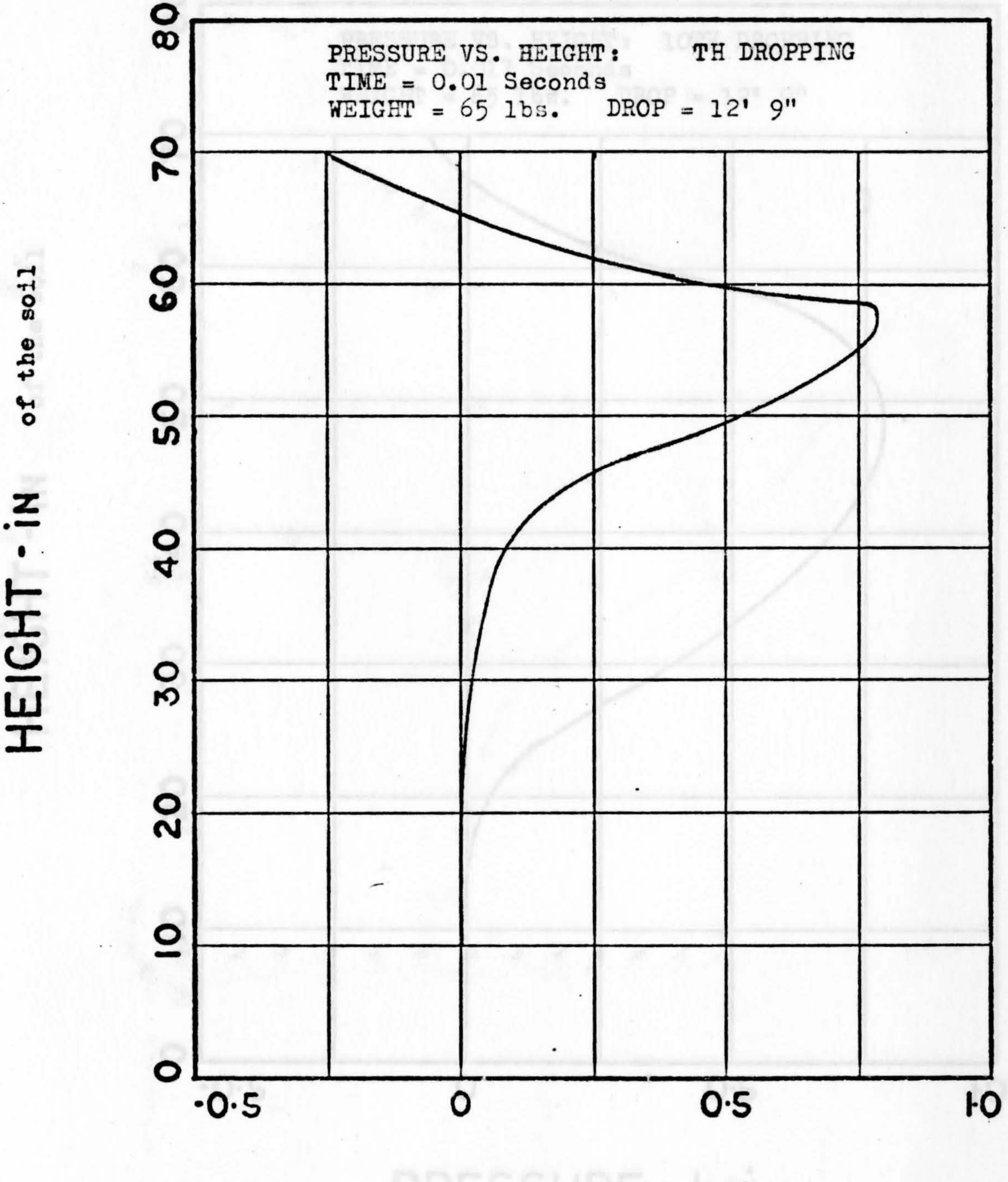
PRESSURE VS. HEIGHT: TH DROPPING
TIME = 0.01 Seconds
WEIGHT = 65 lbs. DROP = 12' 9"
HEIGHT - IN of the soil
0
10
20
30
40
50
60
70
80
PRESSURE - ksi
-0.5
0
0.5
1.0

Fig. 41

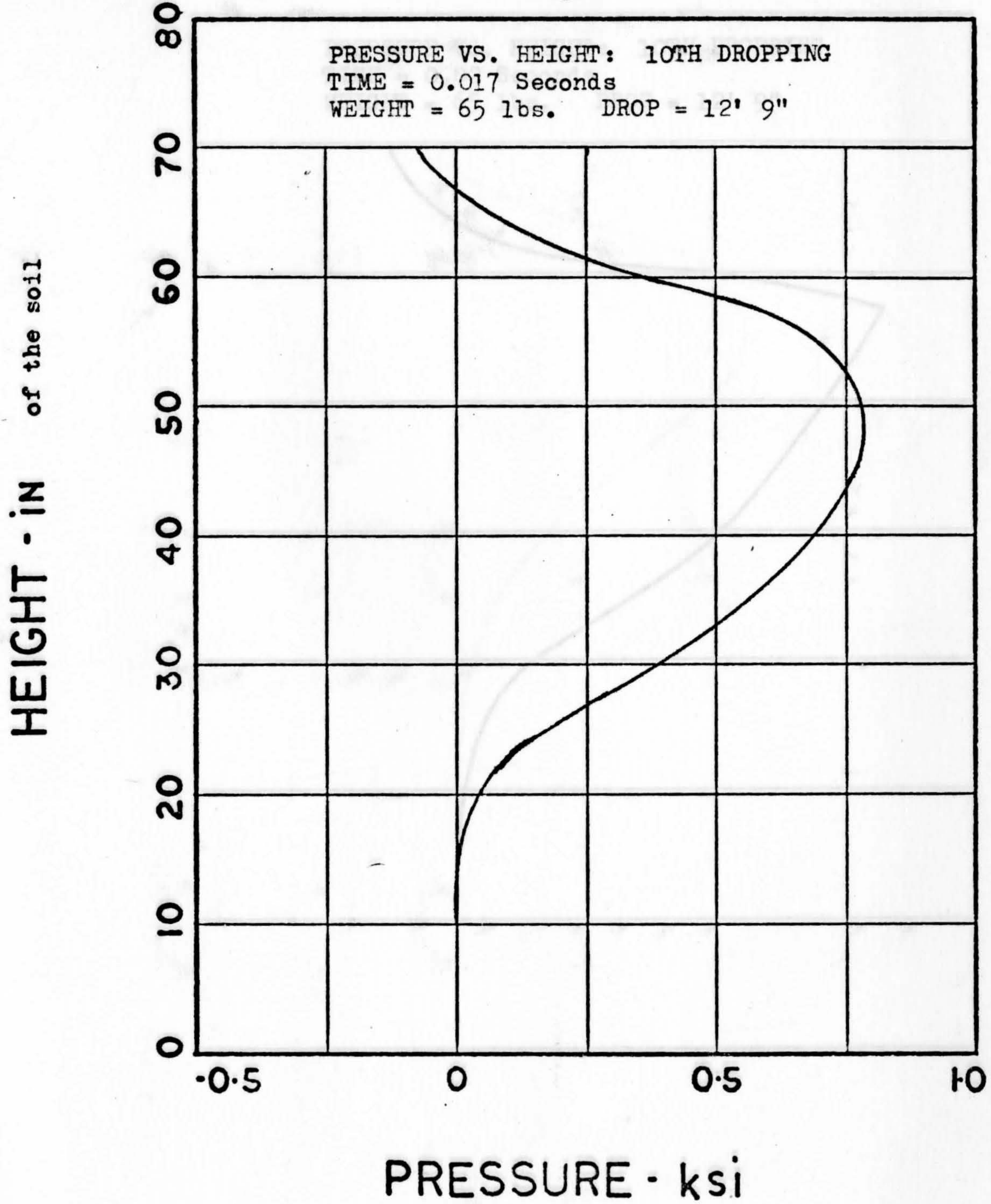
PRESSURE VS. HEIGHT: 10TH DROPPING
TIME = 0.017 Seconds
WEIGHT = 65 lbs. DROP = 12' 9"
HEIGHT - in of the soil
0
10
20
30
40
50
60
70
80
-0·5
0
0·5
1·0
PRESSURE - ksi

Fig. 42

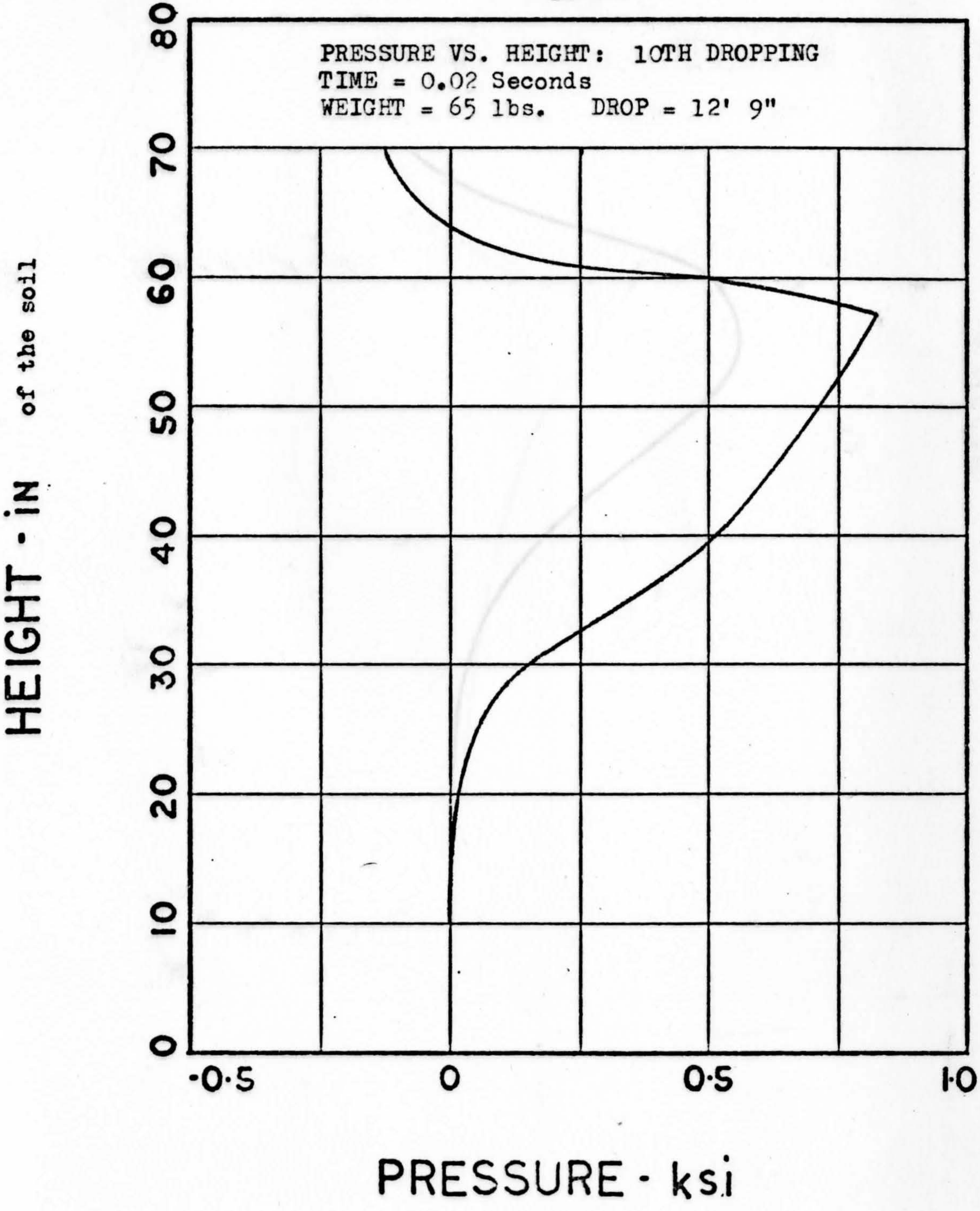
PRESSURE VS. HEIGHT: 10TH DROPPING
TIME = 0.02 Seconds
WEIGHT = 65 lbs. DROP = 12' 9"
HEIGHT - IN of the soil
0
10
20
30
40
50
60
70
80
-0.5
0
0.5
1.0
PRESSURE - ksi

Fig. 43

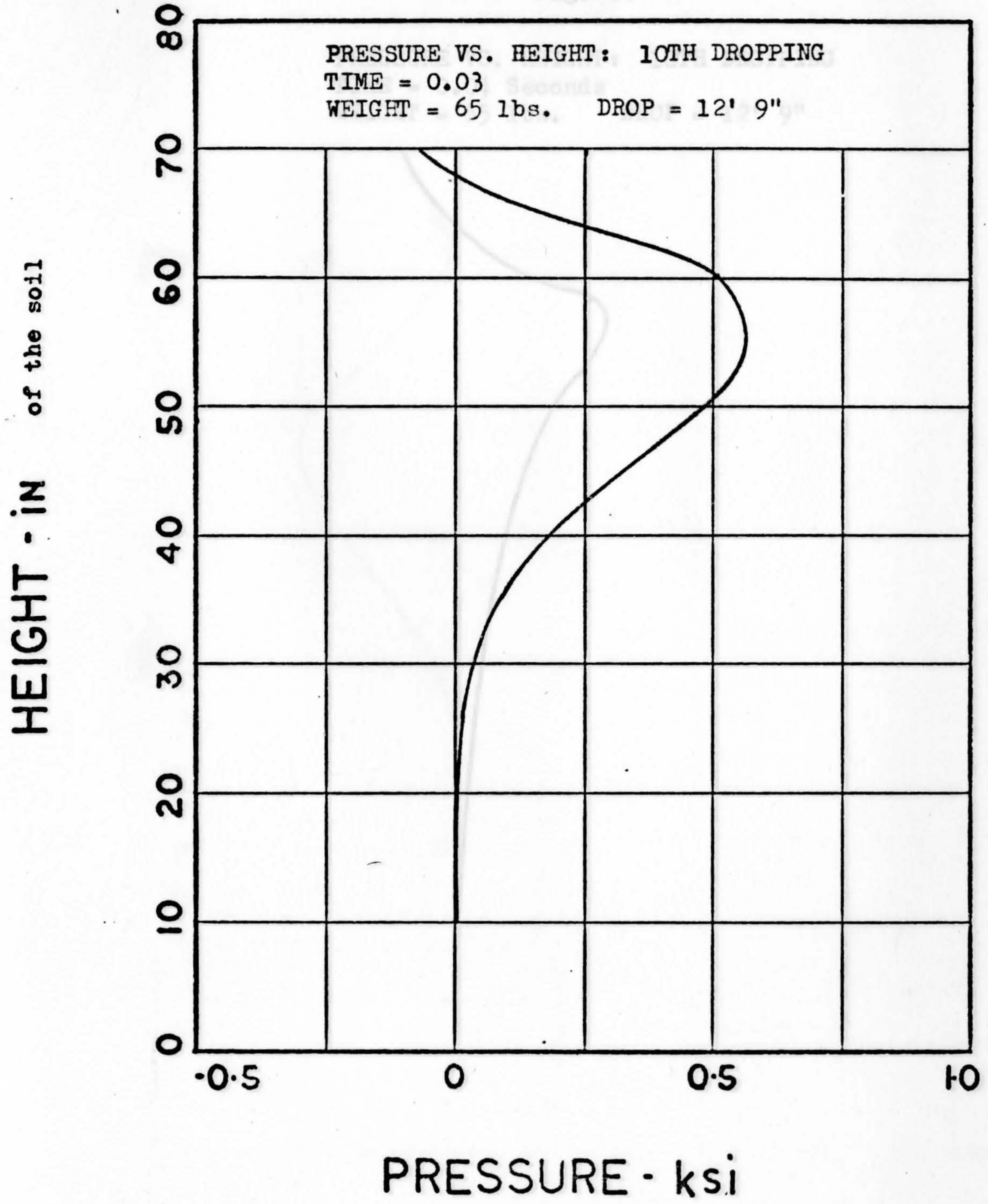
PRESSURE VS. HEIGHT: 10TH DROPPING
TIME = 0.03
WEIGHT = 65 lbs. DROP = 12' 9"
HEIGHT - IN of the soil
80
70
60
50
40
30
20
10
0
-0·5
0
0·5
1·0
PRESSURE - ksi

Fig. 44

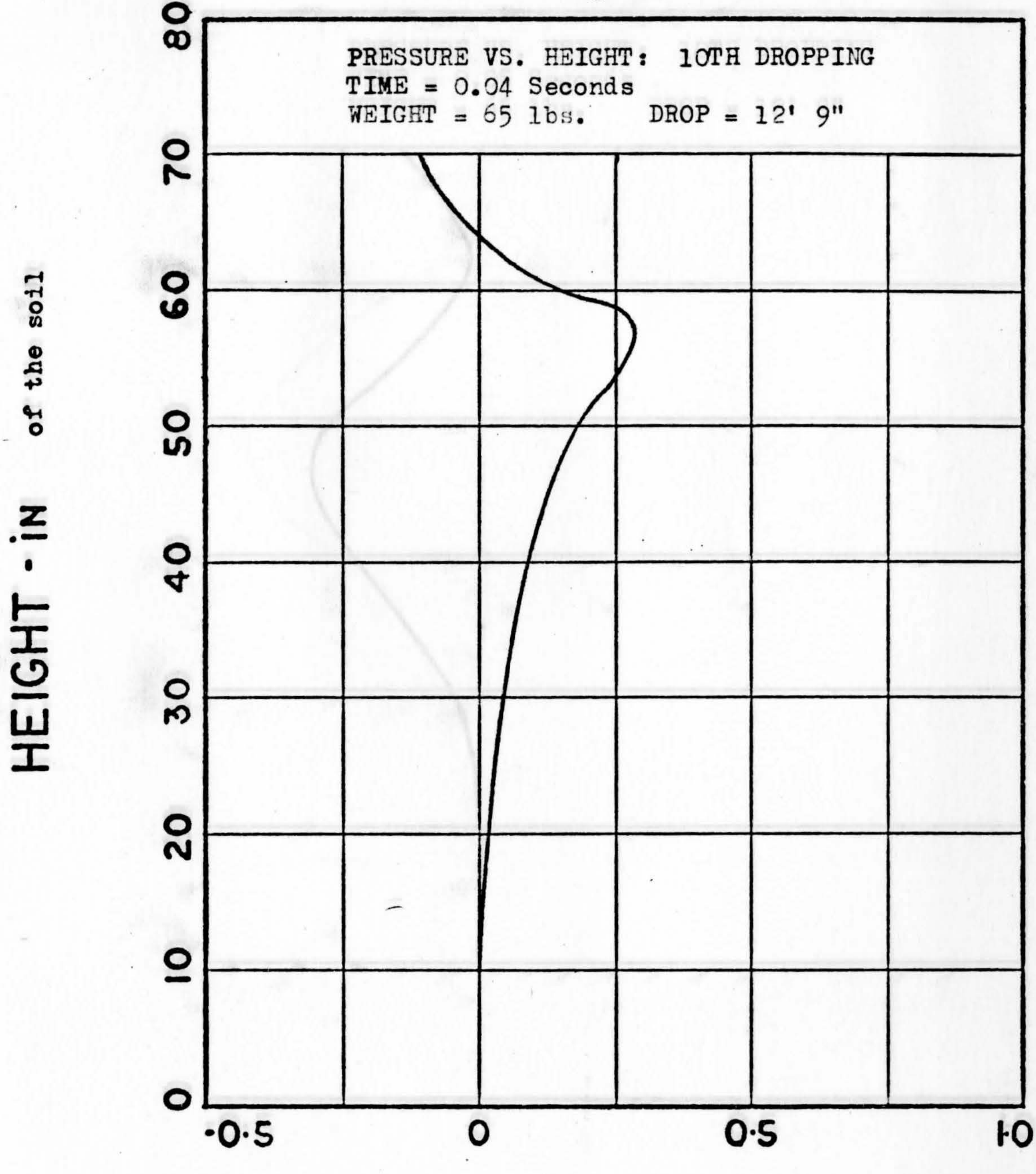
PRESSURE VS. HEIGHT: 10TH DROPPING
TIME = 0.04 Seconds
WEIGHT = 65 lbs. DROP = 12' 9"
HEIGHT - in of the soil
80
70
60
50
40
30
20
10
0
-0.5
0
0.5
1.0
PRESSURE - ksi

Fig. 45

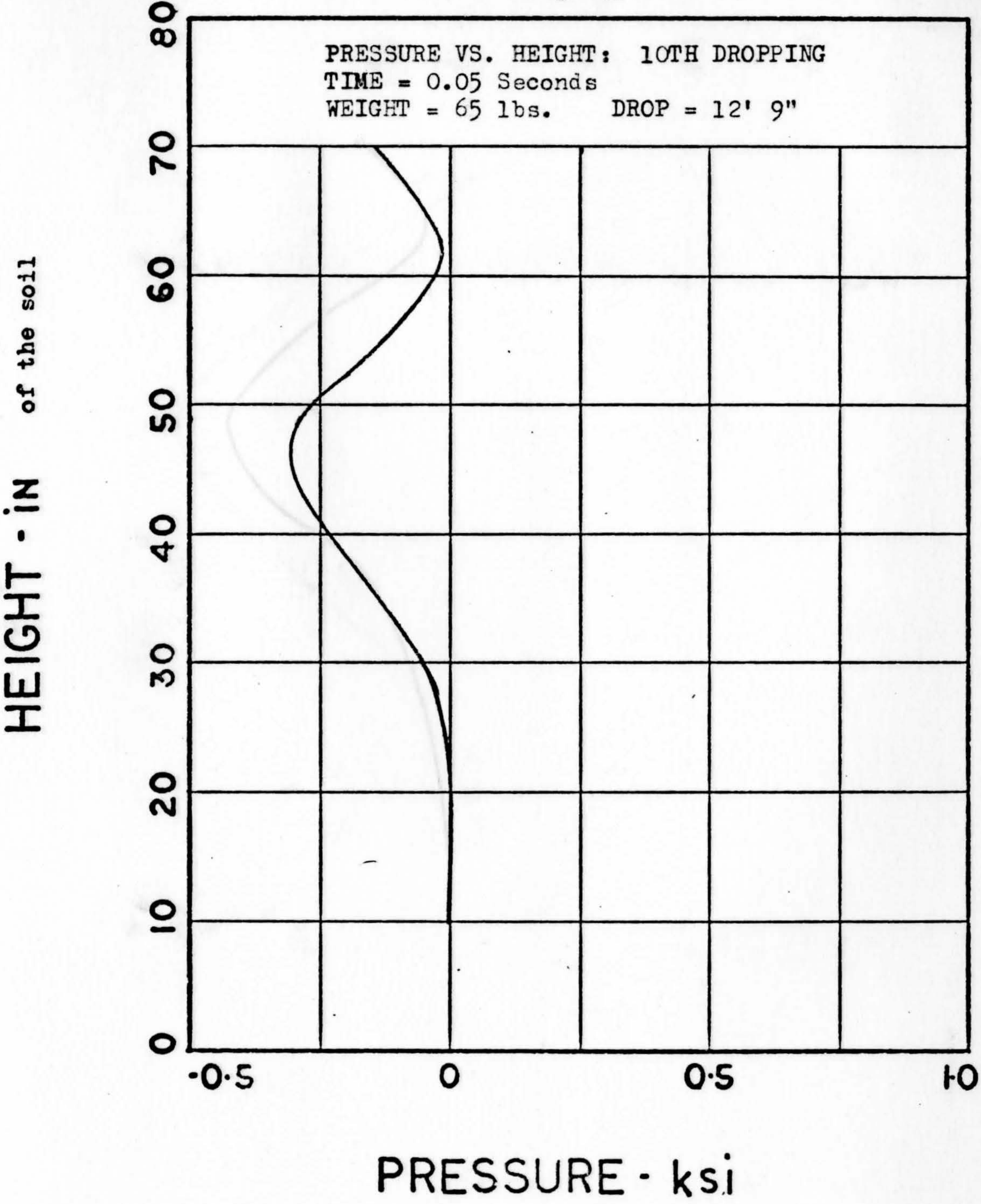
PRESSURE VS. HEIGHT: 10TH DROPPING
TIME = 0.05 Seconds
WEIGHT = 65 lbs. DROP = 12' 9"
HEIGHT - IN of the soil
80
70
60
50
40
30
20
10
0
-0.5
0
0.5
1.0
PRESSURE - ksi

Fig. 46

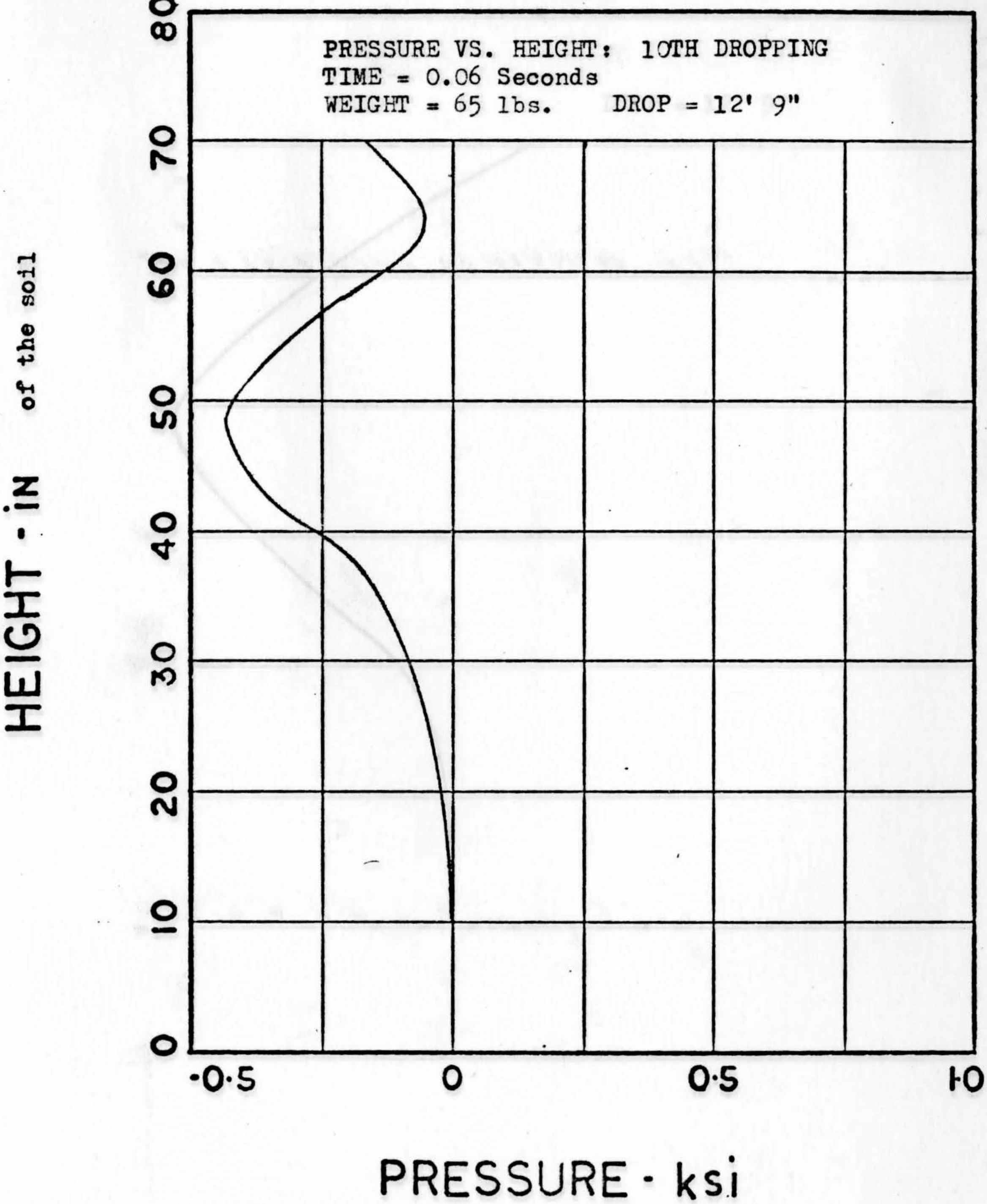
PRESSURE VS. HEIGHT: 10TH DROPPING
TIME = 0.06 Seconds
WEIGHT = 65 lbs. DROP = 12' 9"
HEIGHT - IN of the soil
PRESSURE - ksi
80
70
60
50
40
30
20
10
0
-0.5
0
0.5
1.0

Fig. 47

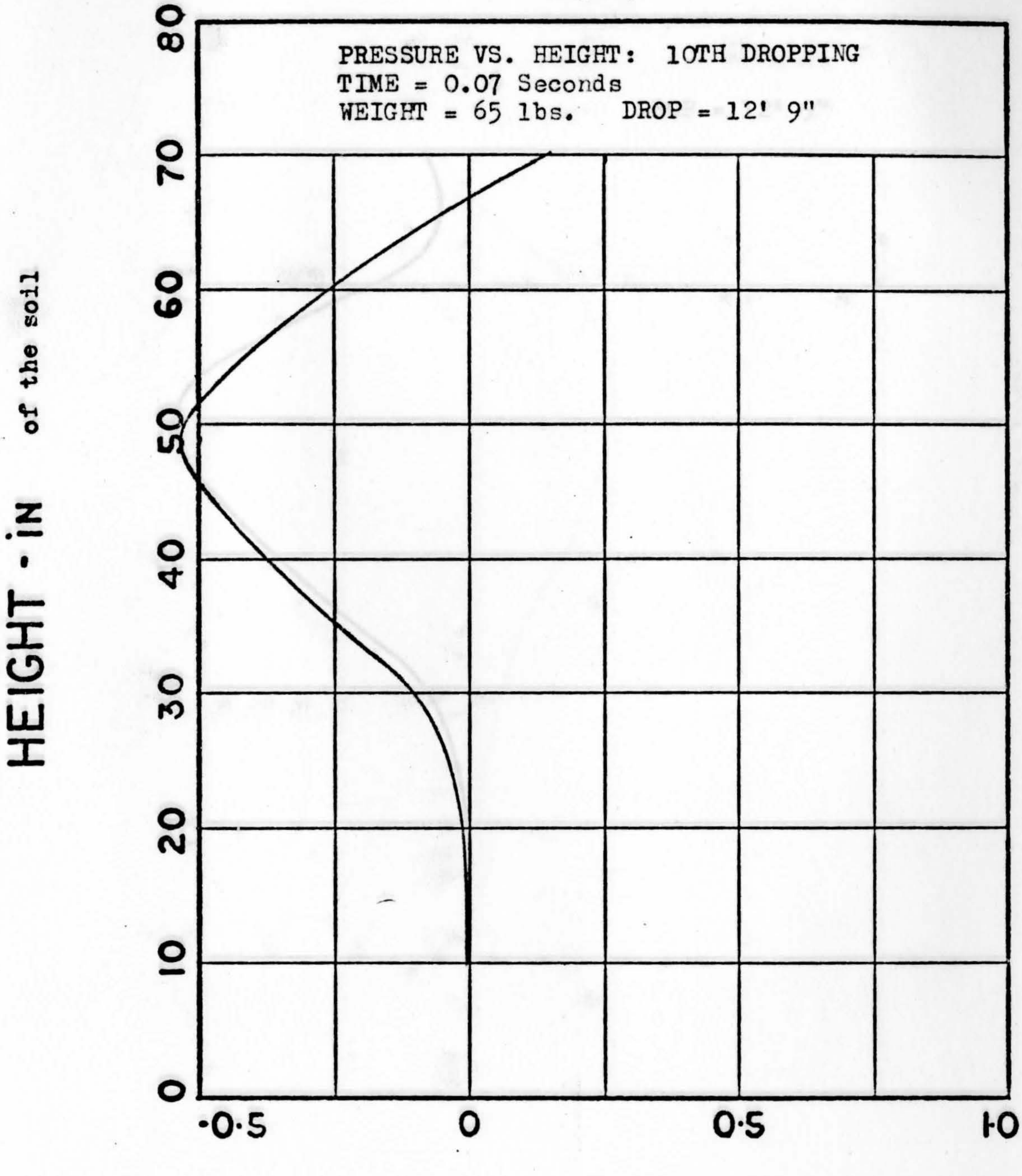
PRESSURE VS. HEIGHT: 10TH DROPPING
TIME = 0.07 Seconds
WEIGHT = 65 lbs. DROP = 12' 9"
HEIGHT - IN of the soil
80
70
60
50
40
30
20
10
0
-0.5
0
0.5
1.0
PRESSURE - ksi

Fig. 48

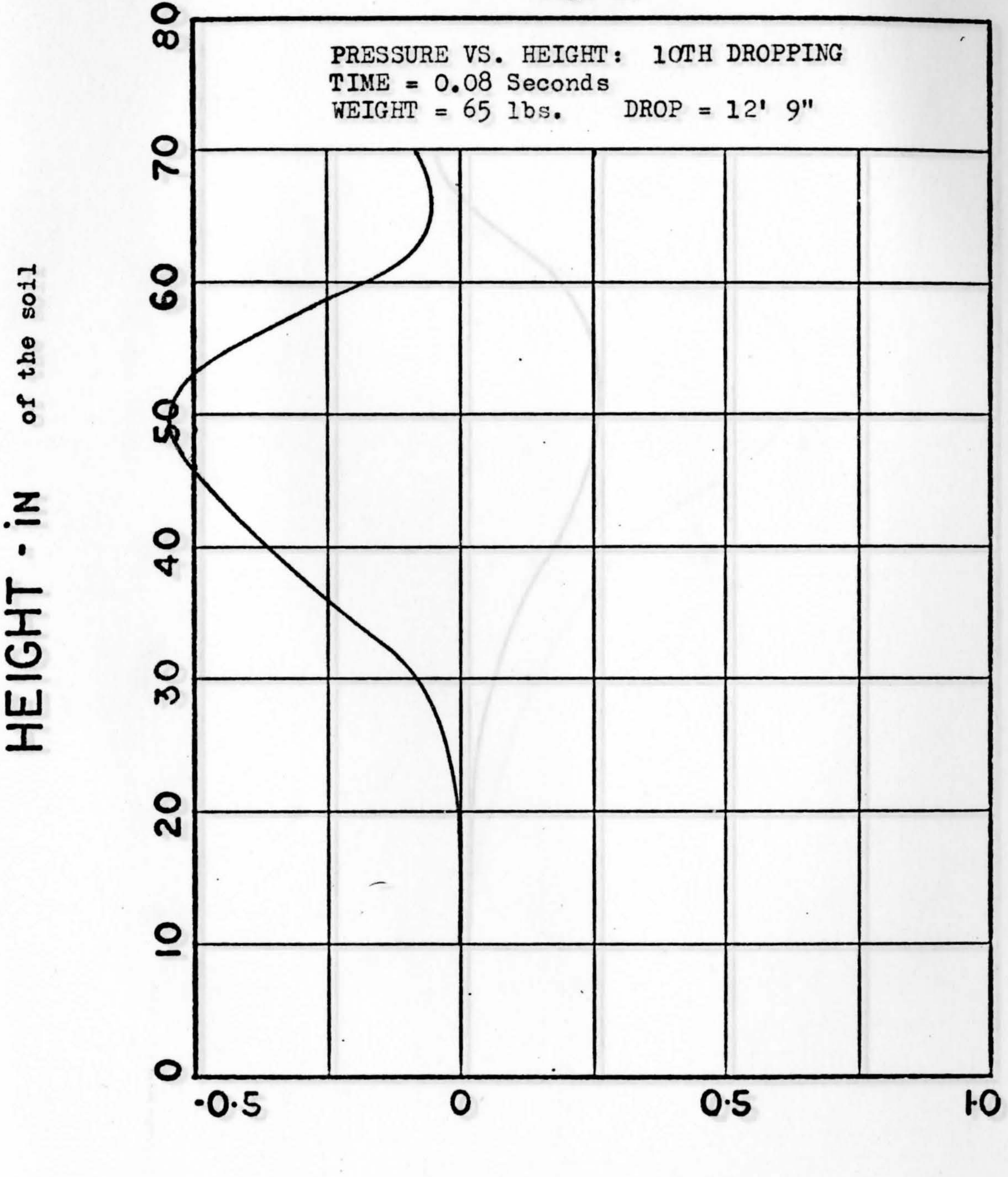
PRESSURE VS. HEIGHT: 10TH DROPPING
TIME = 0.08 Seconds
WEIGHT = 65 lbs. DROP = 12' 9"
HEIGHT - iN of the soil
0
10
20
30
40
50
60
70
80
-0.5
0
0.5
1.0
PRESSURE - ksi

Fig. 49

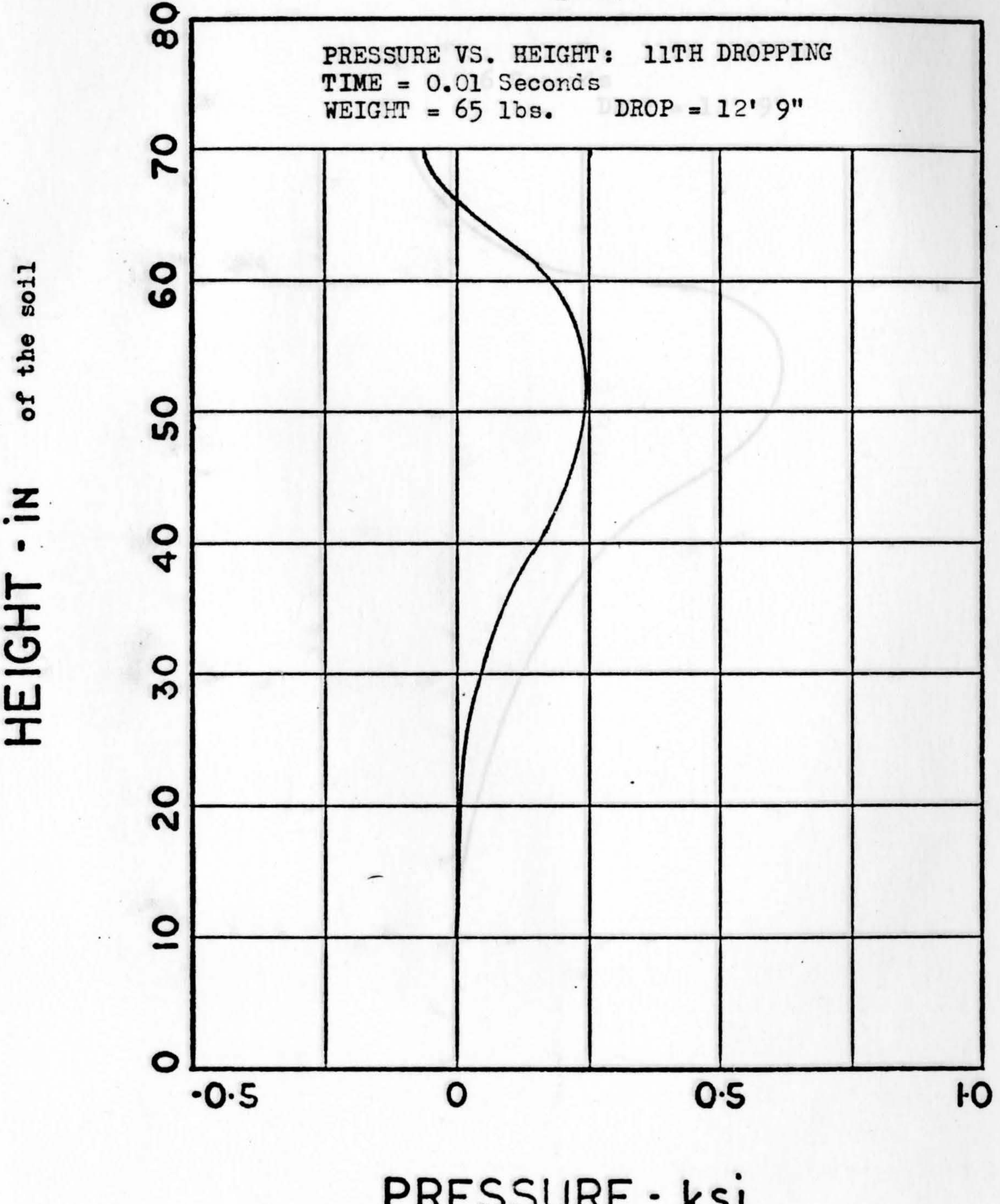
PRESSURE VS. HEIGHT: 11TH DROPPING
TIME = 0.01 Seconds
WEIGHT = 65 lbs. DROP = 12' 9"
HEIGHT - IN of the soil
80
70
60
50
40
30
20
10
0
-0·5
0
0·5
1·0
PRESSURE - ksi

Fig. 50

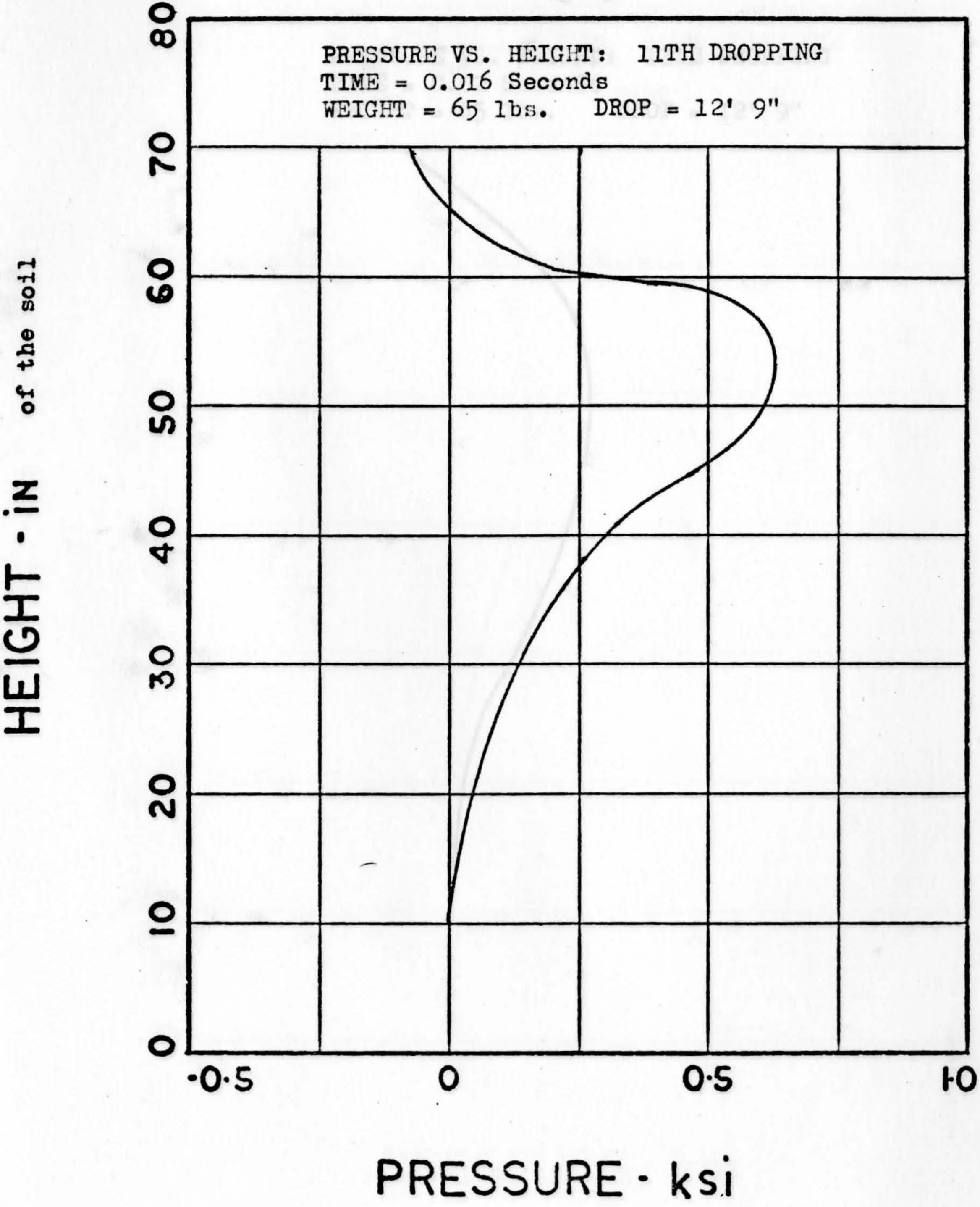
PRESSURE VS. HEIGHT: 11TH DROPPING
TIME = 0.016 Seconds
WEIGHT = 65 lbs. DROP = 12' 9"
HEIGHT - iN of the soil
0
10
20
30
40
50
60
70
80
-0.5
0
0.5
1.0
PRESSURE - ksi

Fig. 51

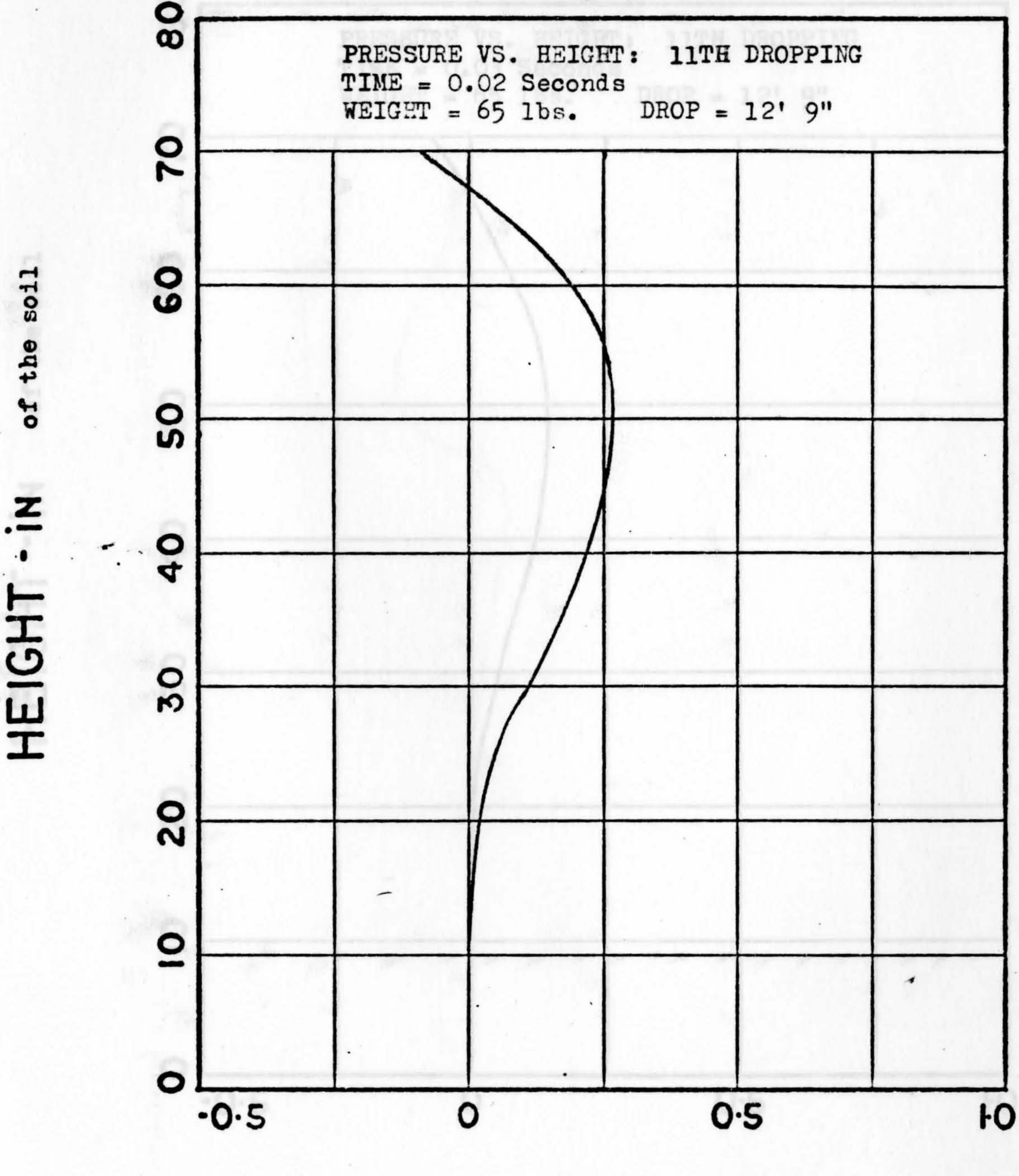
PRESSURE VS. HEIGHT: 11TH DROPPING
TIME = 0.02 Seconds
WEIGHT = 65 lbs. DROP = 12' 9"
HEIGHT - IN of the soil
0
10
20
30
40
50
60
70
80
-0·5
0
0·5
1·0
PRESSURE - ksi

Fig. 52

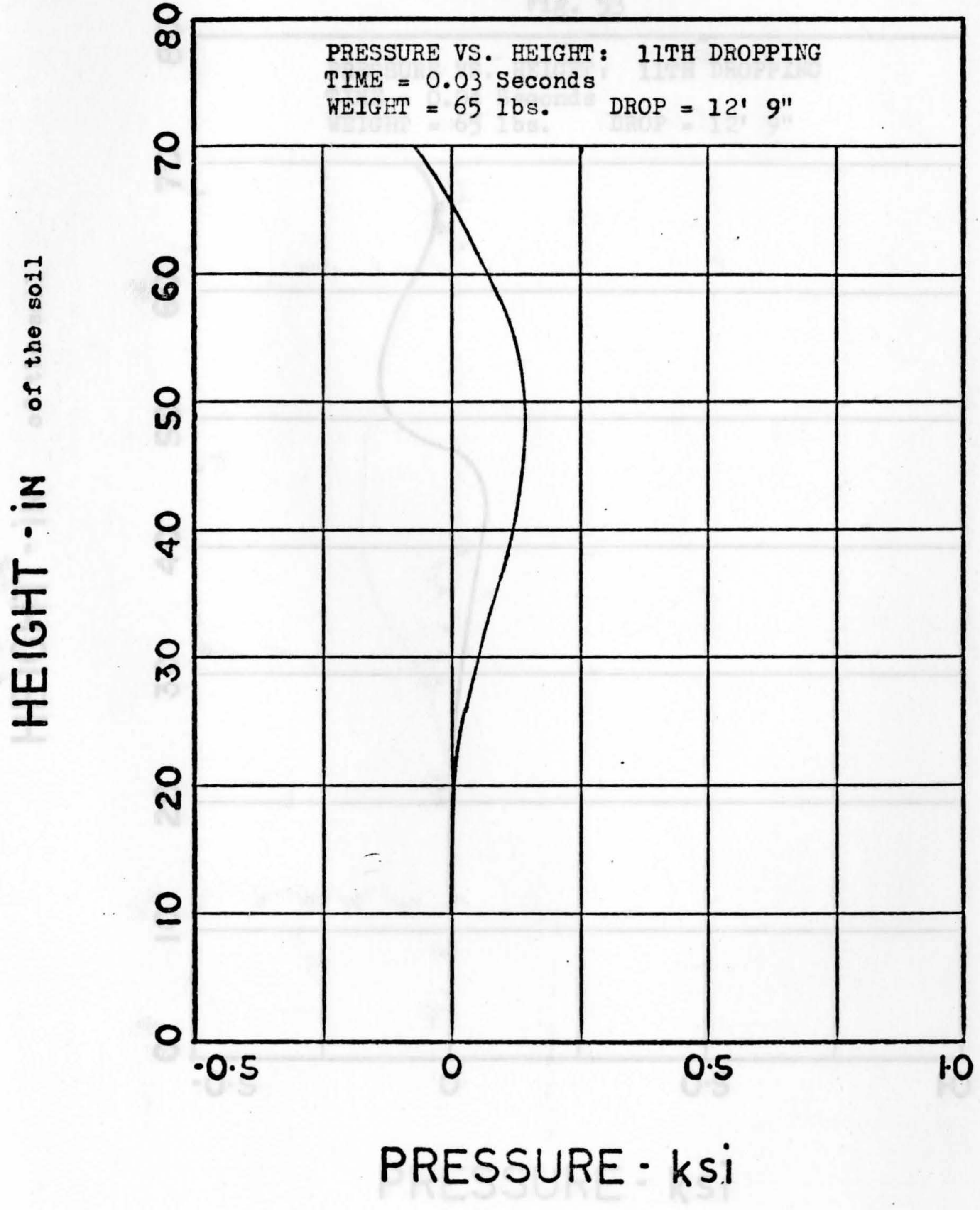
PRESSURE VS. HEIGHT: 11TH DROPPING
TIME = 0.03 Seconds
WEIGHT = 65 lbs. DROP = 12' 9"
HEIGHT - in of the soil
0
10
20
30
40
50
60
70
80
-0·5
0
0·5
1·0
PRESSURE - ksi

Fig. 53

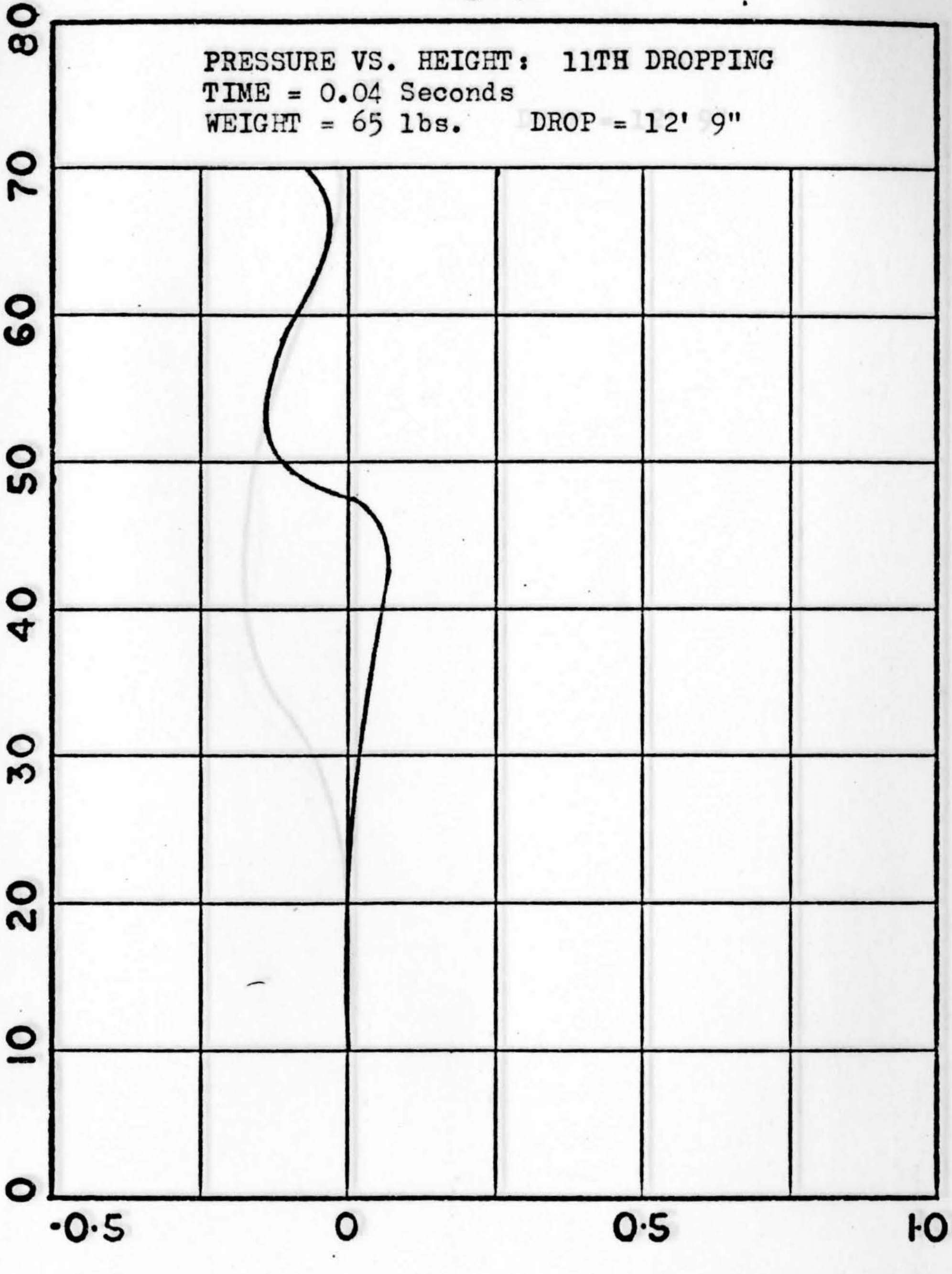
PRESSURE VS. HEIGHT: 11TH DROPPING
TIME = 0.04 Seconds
WEIGHT = 65 lbs. DROP = 12' 9"
HEIGHT - IN of the soil
0
10
20
30
40
50
60
70
80
-0·5
0
0·5
1·0
PRESSURE - ksi

Fig. 54

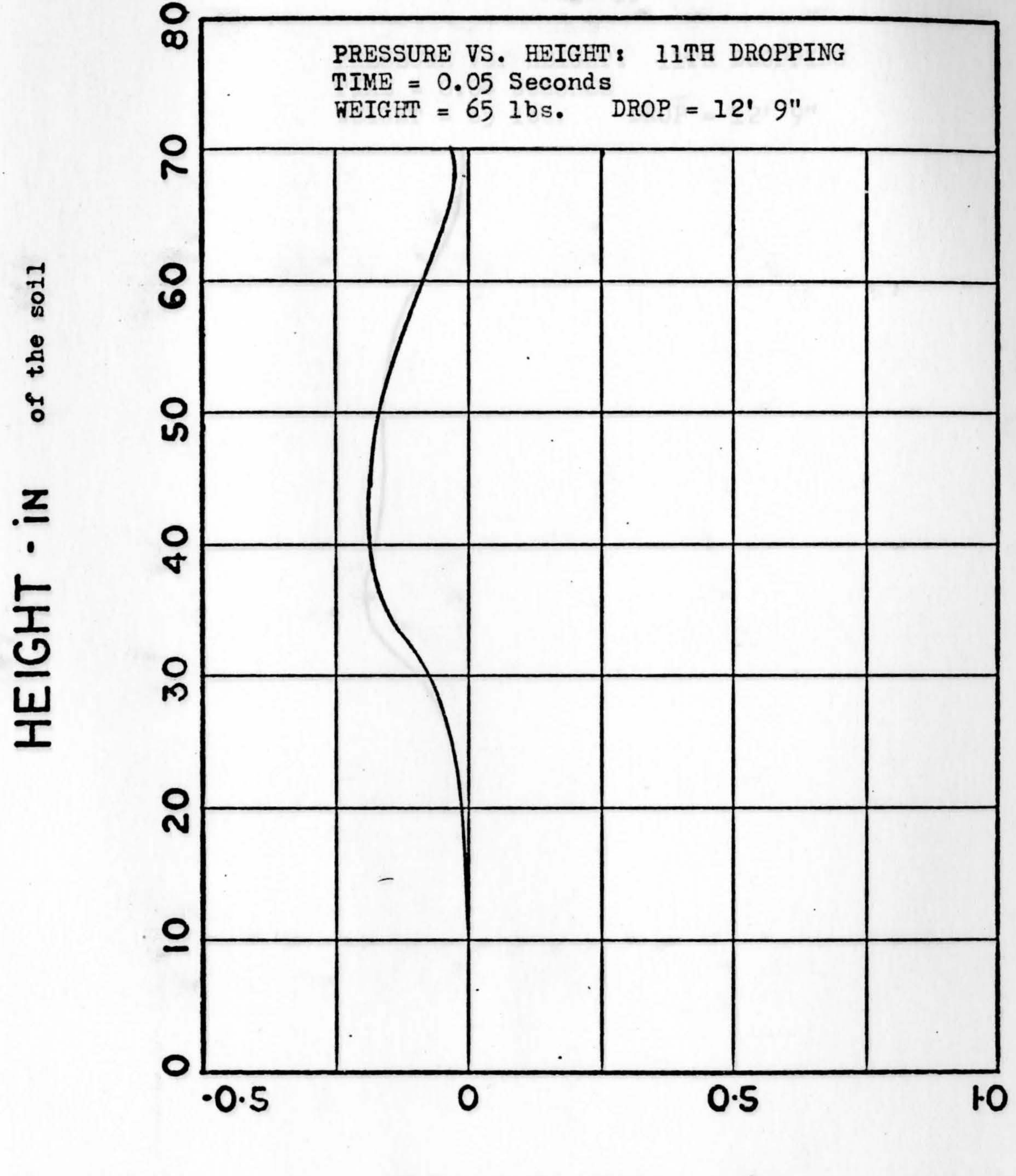
PRESSURE VS. HEIGHT: 11TH DROPPING
TIME = 0.05 Seconds
WEIGHT = 65 lbs. DROP = 12' 9"
HEIGHT - iN of the soil
0
10
20
30
40
50
60
70
80
-0·5
0
0·5
1·0
PRESSURE - ksi

Fig. 55

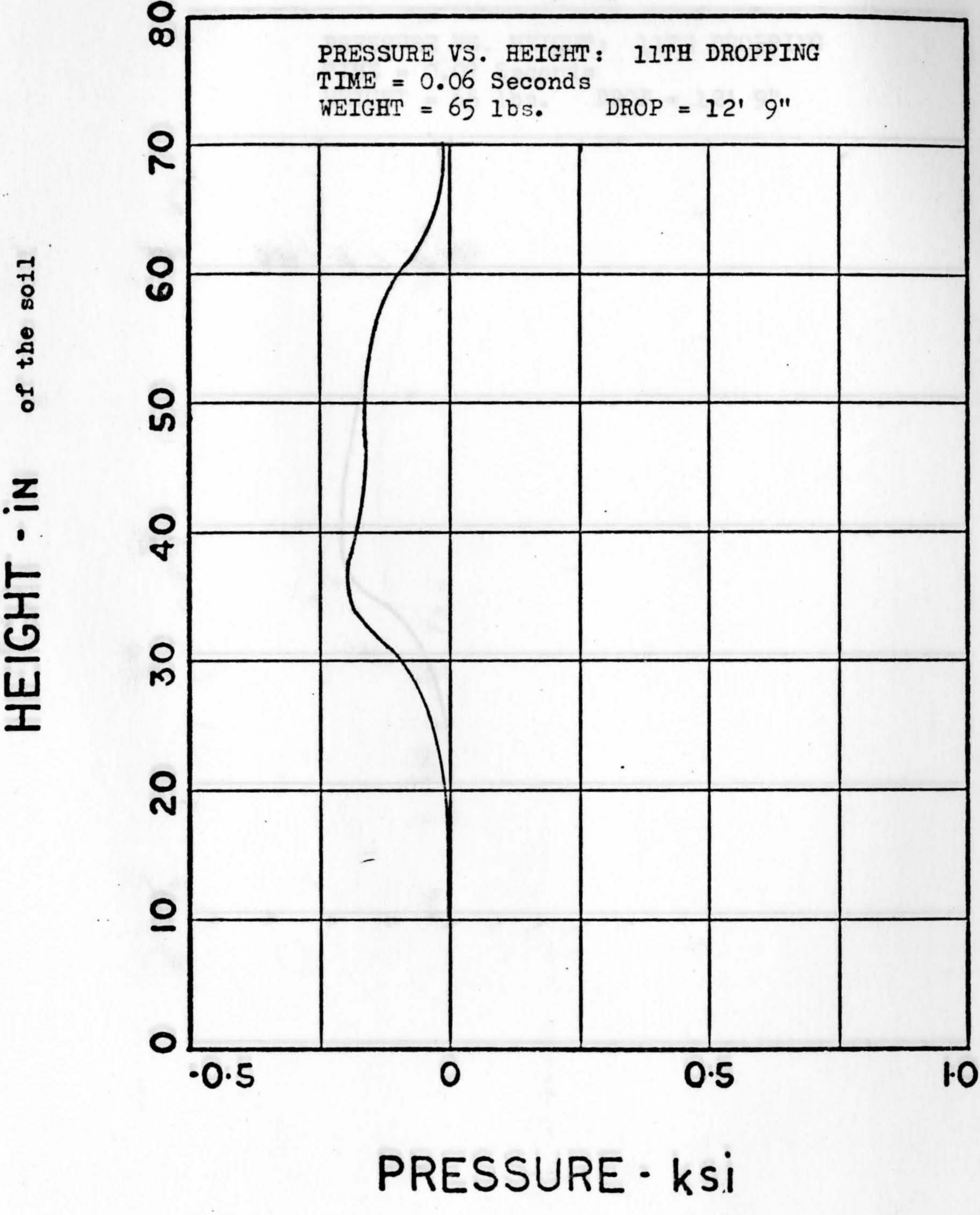
PRESSURE VS. HEIGHT: 11TH DROPPING
TIME = 0.06 Seconds
WEIGHT = 65 lbs. DROP = 12' 9"
HEIGHT - iN of the soil
0
10
20
30
40
50
60
70
80
-0·5
0
0·5
1·0
PRESSURE - ksi

Fig. 56

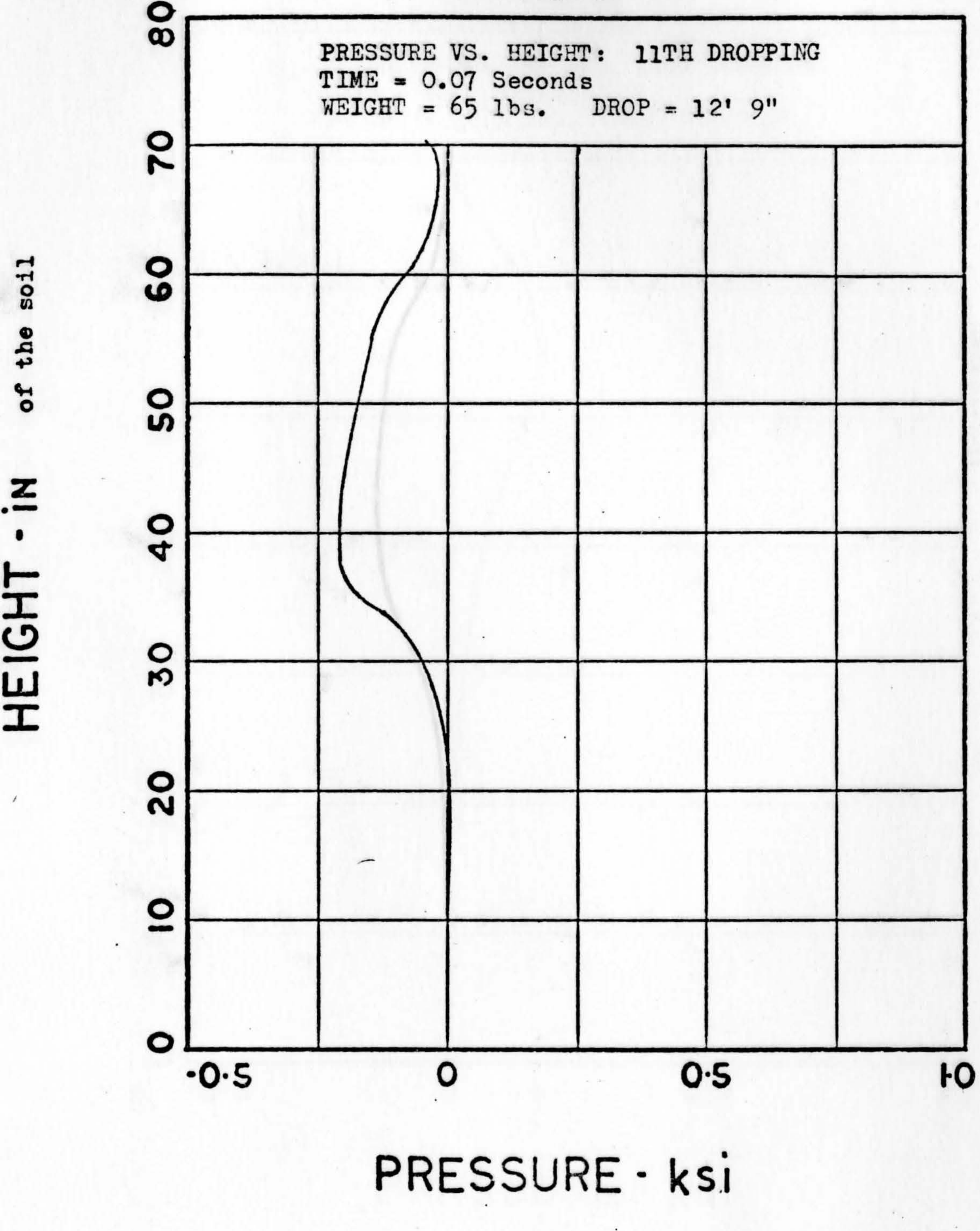
PRESSURE VS. HEIGHT: 11TH DROPPING
TIME = 0.07 Seconds
WEIGHT = 65 lbs. DROP = 12' 9"
HEIGHT - iN of the soil
0
10
20
30
40
50
60
70
80
-0·5
0
0·5
1·0
PRESSURE - ksi

Fig.57

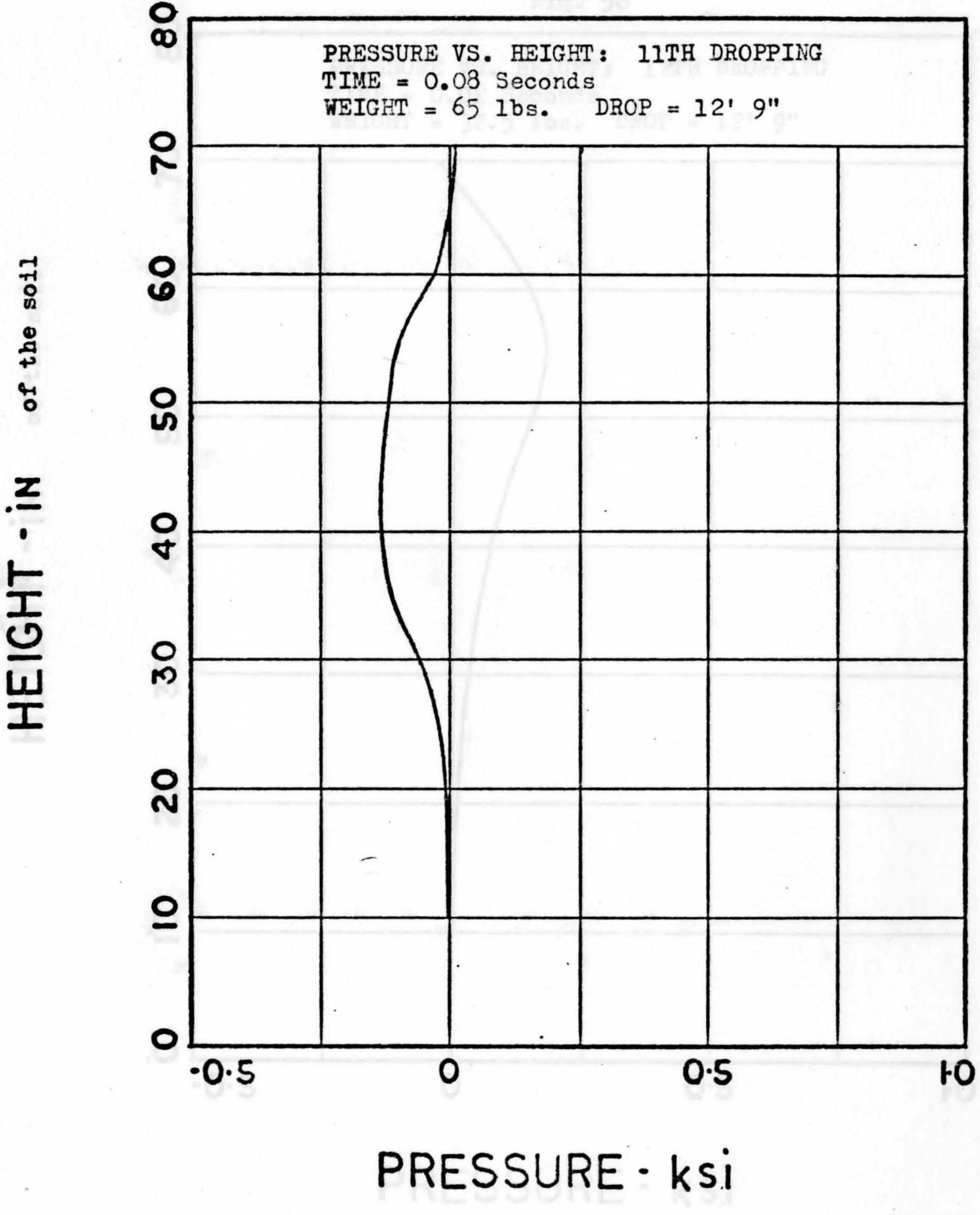
PRESSURE VS. HEIGHT: 11TH DROPPING
TIME = 0.08 Seconds
WEIGHT = 65 lbs. DROP = 12' 9"
HEIGHT - IN of the soil
80
70
60
50
40
30
20
10
0
-0.5
0
0.5
1.0
PRESSURE - ksi

Fig. 58

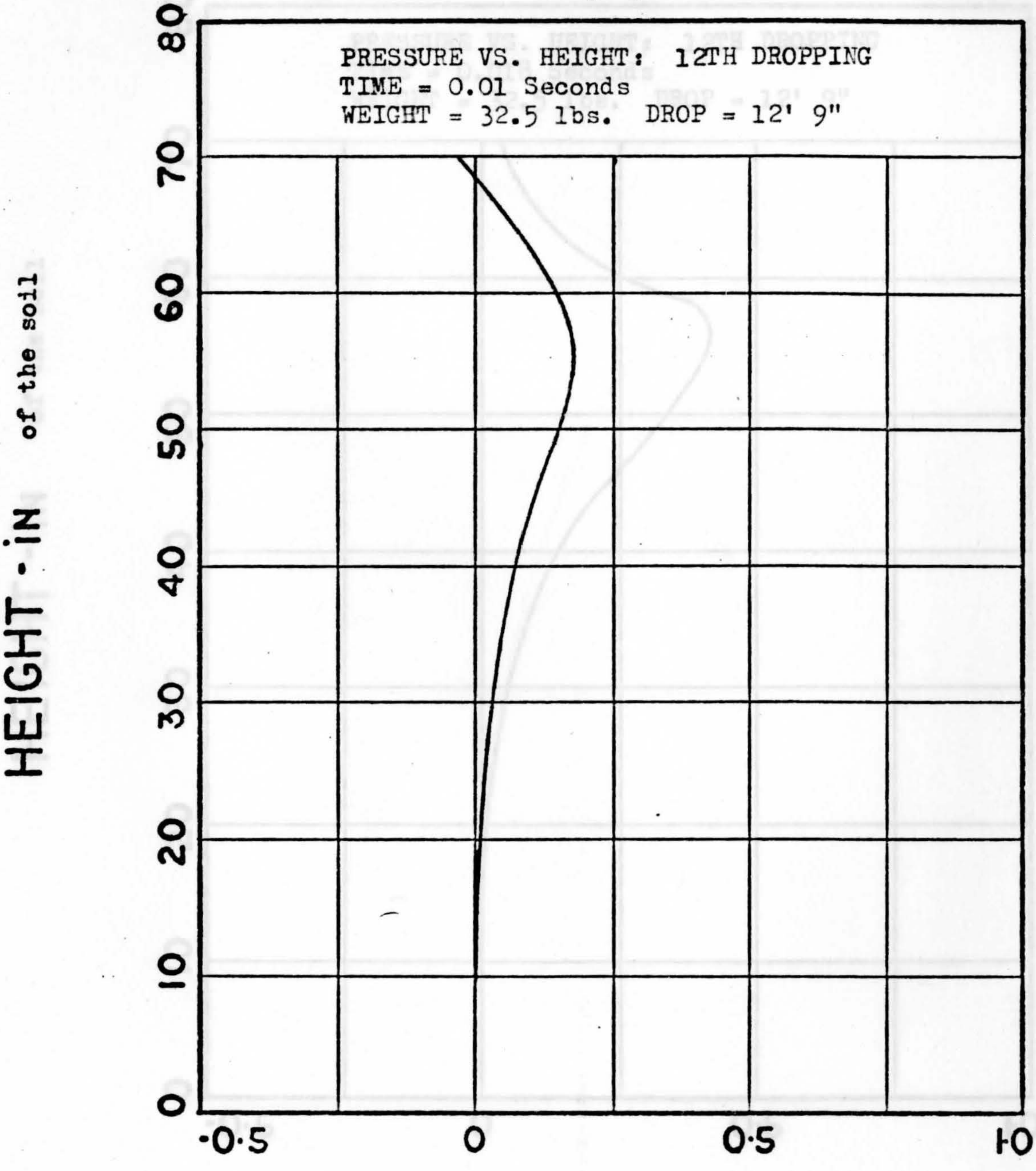
PRESSURE VS. HEIGHT: 12TH DROPPING
TIME = 0.01 Seconds
WEIGHT = 32.5 lbs. DROP = 12' 9"
HEIGHT - IN of the soil
80
70
60
50
40
30
20
10
0
-0.5
0
0.5
1.0
PRESSURE - ksi

Fig. 59

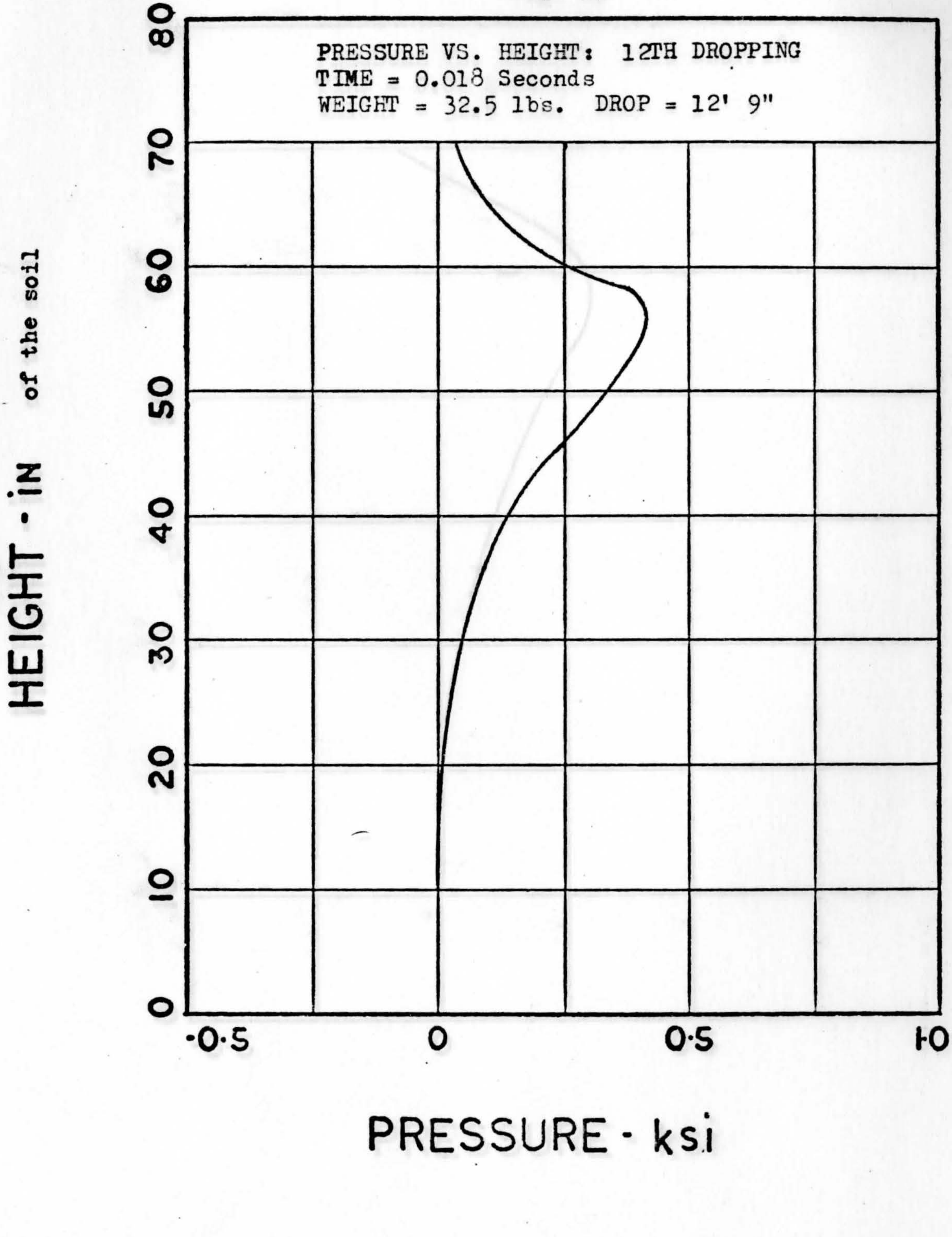
PRESSURE VS. HEIGHT: 12TH DROPPING
TIME = 0.018 Seconds
WEIGHT = 32.5 lbs. DROP = 12' 9"
HEIGHT - in of the soil
0
10
20
30
40
50
60
70
80
-0.5
0
0.5
1.0
PRESSURE - ksi

Fig. 60

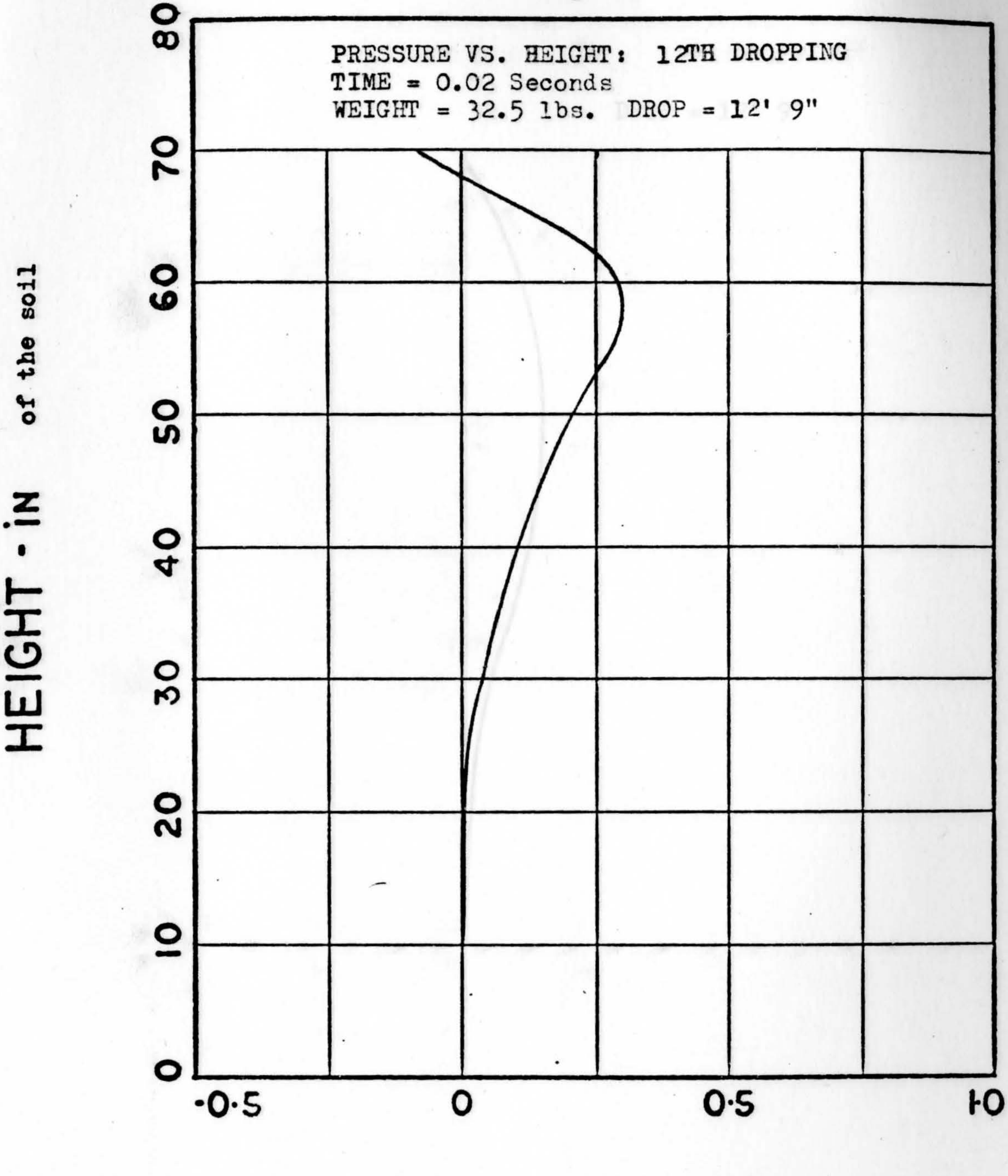
PRESSURE VS. HEIGHT: 12TH DROPPING
TIME = 0.02 Seconds
WEIGHT = 32.5 lbs. DROP = 12' 9"
HEIGHT - IN of the soil
80
70
60
50
40
30
20
10
0
-0·5
0
0·5
1·0
PRESSURE - ksi

Fig. 61

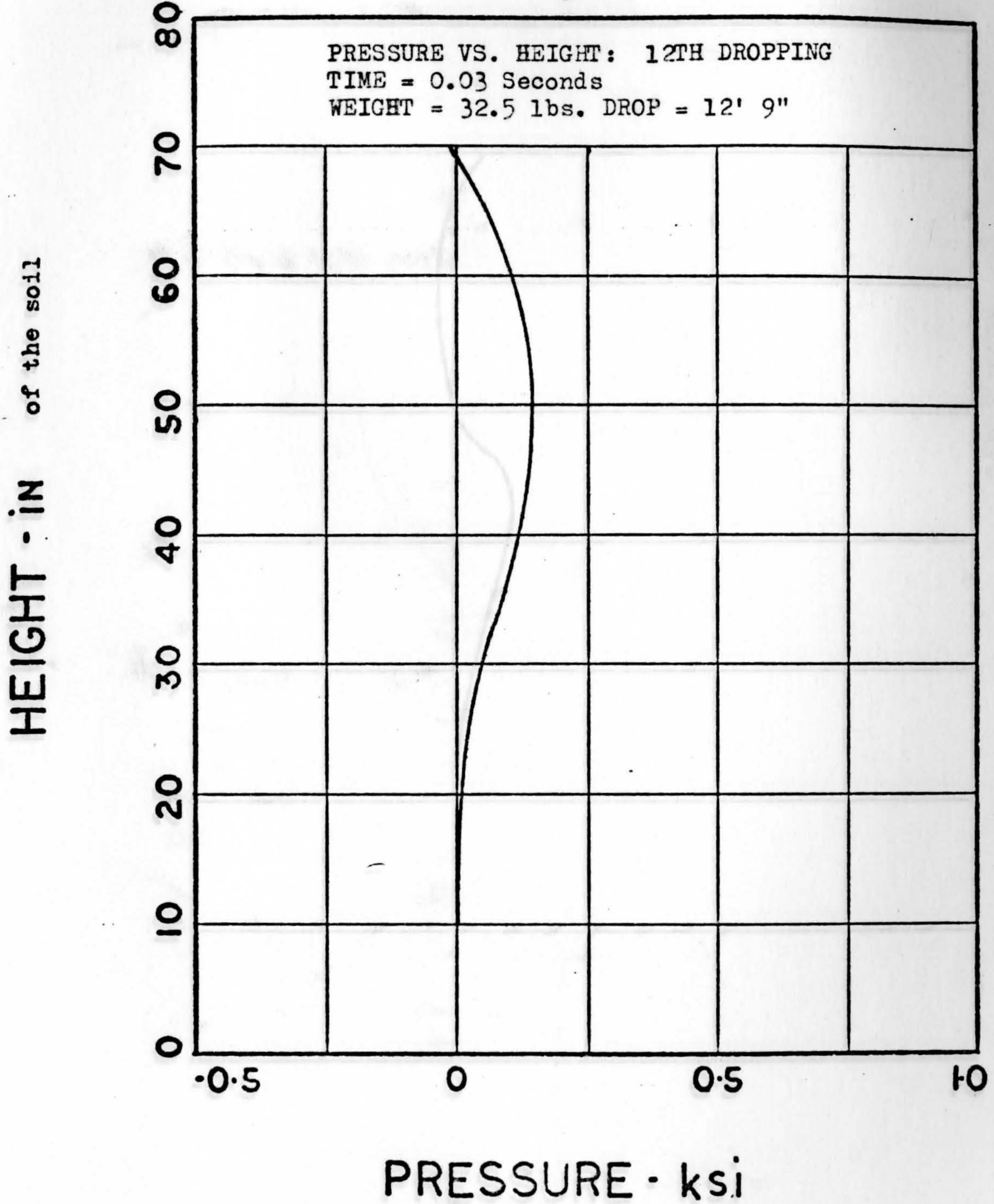
PRESSURE VS. HEIGHT: 12TH DROPPING
TIME = 0.03 Seconds
WEIGHT = 32.5 lbs. DROP = 12' 9"
HEIGHT · IN of the soil
0
10
20
30
40
50
60
70
80
-0·5
0
0·5
1·0
PRESSURE · ksi

Fig. 62

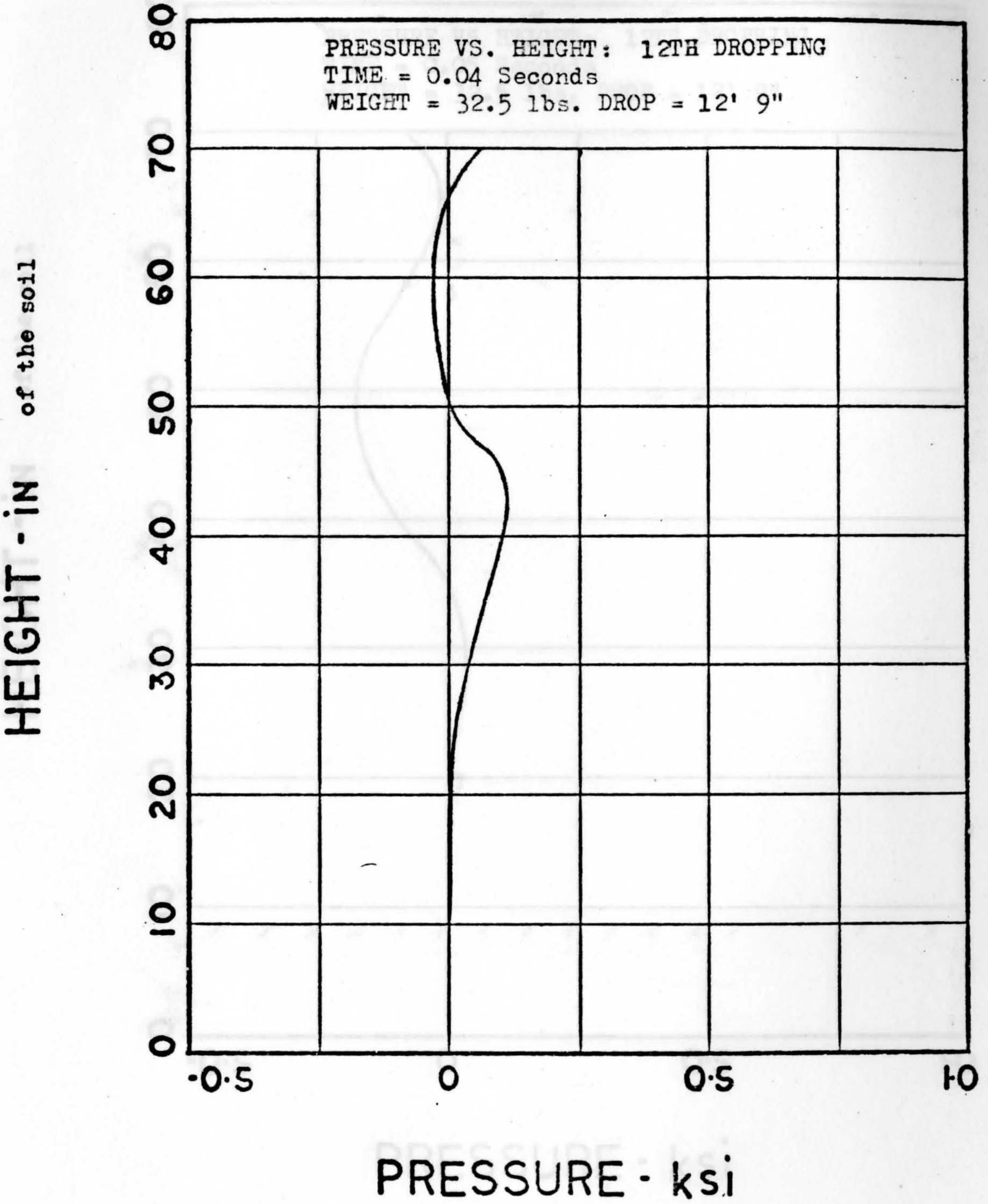
PRESSURE VS. HEIGHT: 12TH DROPPING
TIME = 0.04 Seconds
WEIGHT = 32.5 lbs. DROP = 12' 9"
HEIGHT - iN of the soil
0
10
20
30
40
50
60
70
80
-0·5
0
0·5
1·0
PRESSURE - ksi

Fig. 63

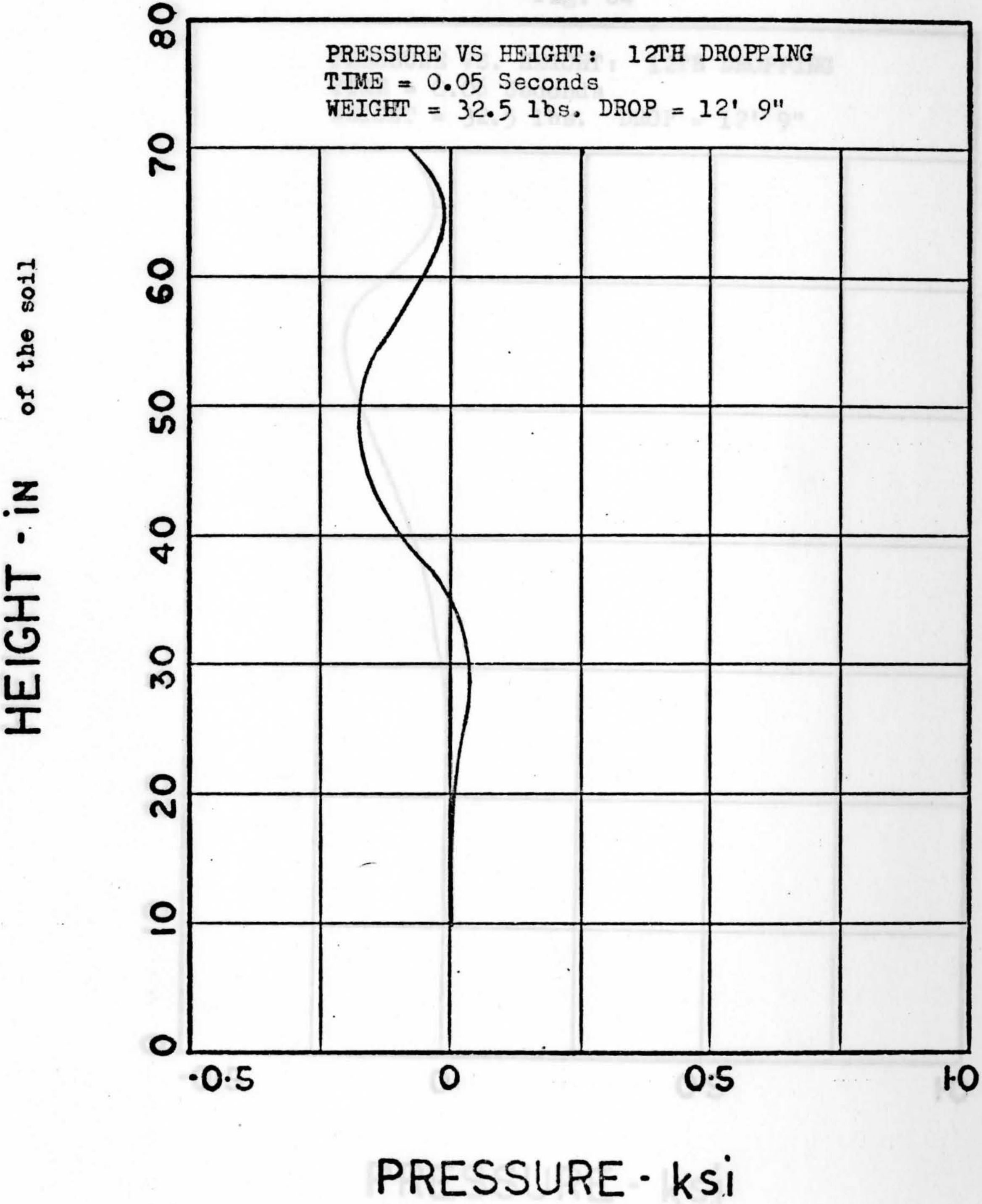
PRESSURE VS HEIGHT: 12TH DROPPING
TIME = 0.05 Seconds
WEIGHT = 32.5 lbs. DROP = 12' 9"
HEIGHT - IN of the soil
0
10
20
30
40
50
60
70
80
-0.5
0
0.5
1.0
PRESSURE - ksi

Fig. 64

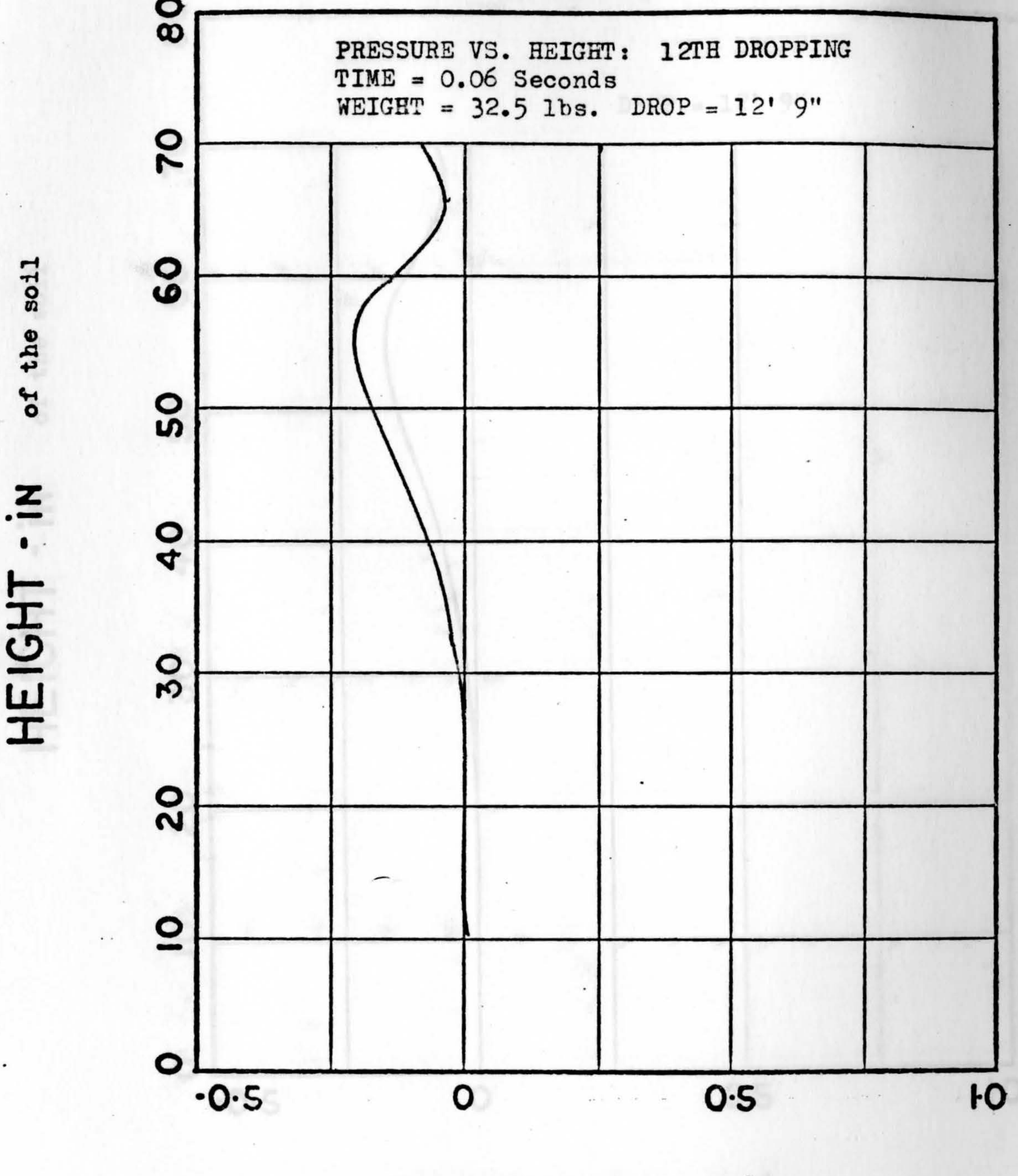
PRESSURE VS. HEIGHT: 12TH DROPPING
TIME = 0.06 Seconds
WEIGHT = 32.5 lbs. DROP = 12' 9"
HEIGHT - iN of the soil
80
70
60
50
40
30
20
10
0
-0·5
0
0·5
1·0
PRESSURE - ksi

Fig. 65

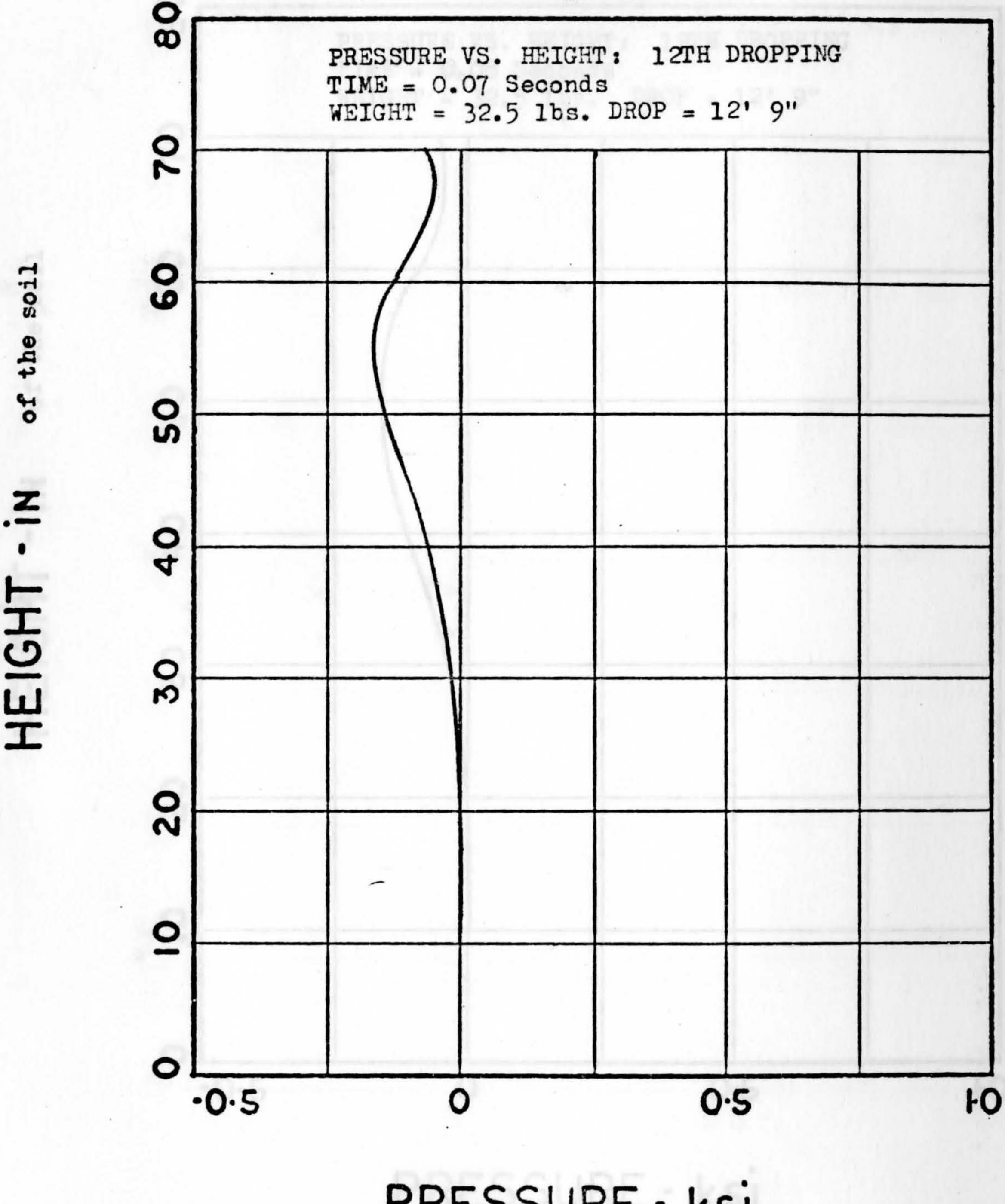
PRESSURE VS. HEIGHT: 12TH DROPPING
TIME = 0.07 Seconds
WEIGHT = 32.5 lbs. DROP = 12' 9"
HEIGHT - IN of the soil
80
70
60
50
40
30
20
10
0
-0·5
0
0·5
1·0
PRESSURE - ksi

Fig. 66

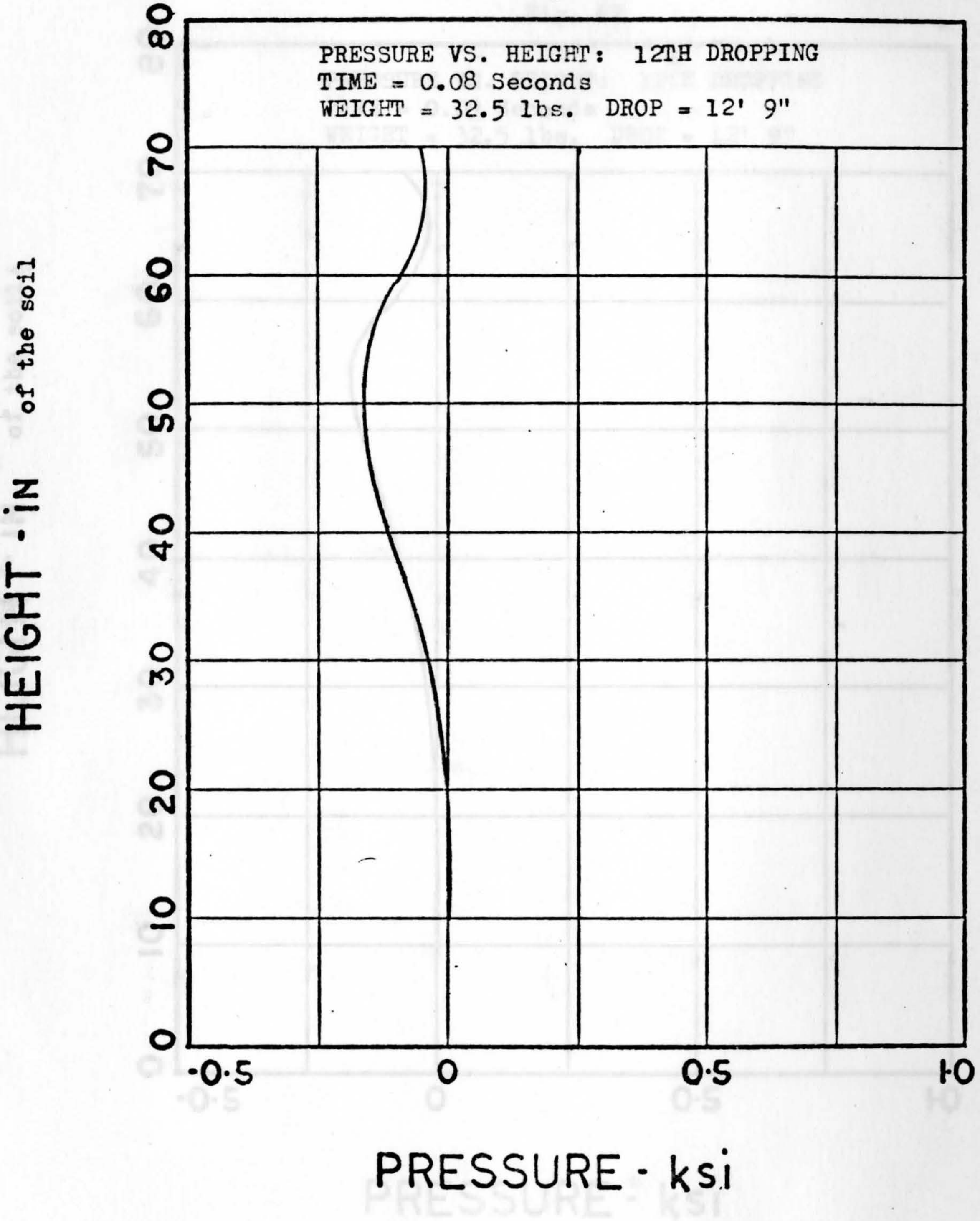
PRESSURE VS. HEIGHT: 12TH DROPPING
TIME = 0.08 Seconds
WEIGHT = 32.5 lbs. DROP = 12' 9"
HEIGHT - in of the soil
0
10
20
30
40
50
60
70
80
-0.5
0
0.5
1.0
PRESSURE - ksi

Fig. 67

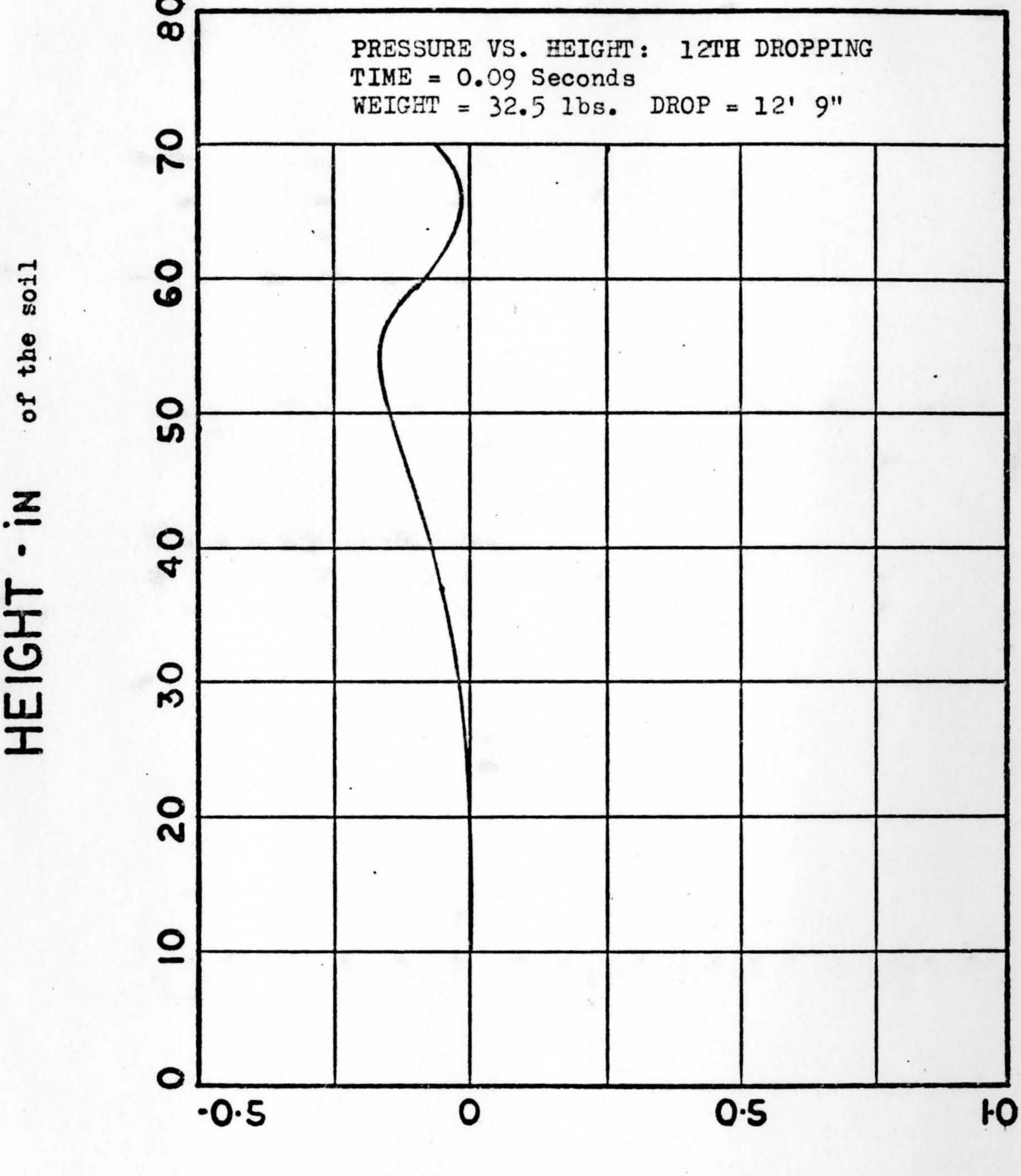
PRESSURE VS. HEIGHT: 12TH DROPPING
TIME = 0.09 Seconds
WEIGHT = 32.5 lbs. DROP = 12' 9"
HEIGHT - iN of the soil
0
10
20
30
40
50
60
70
80
-0·5
0
0·5
1·0
PRESSURE - ksi